THE
PHYSICAL REVIEW
A Journal of Experimental and Theoretical Physics Established by E. L. Nichols in 1893

VOL. 54, NO. 5 SEPTEMBER 1, 1938 SECOND SERIES

Transition Effects of Cosmic Rays in the Atmosphere

R. SERBER
University of California, Berkeley, California

(Received June 27, 1938)

The calculation of the multiplication of the soft component of the cosmic rays in the upper atmosphere is refined by use of the exact high energy radiative formulae of Bethe and Heitler, and the resulting diffusion equations are solved by the method of Snyder. Comparison with the vertical counter work of Pfotzer, and of Carmichael and Dymond, and with the ionization chamber data of Bowen, Millikan, and Neher, shows that the calculated position of the maximum of the multiplication curve is now in good agreement with that observed. The latter comparison also indicates that the penetrating component is at least largely of secondary origin.

I

THE general features of the variation of cosmic-ray intensity in the upper atmosphere have been explained by Carlson and Oppenheimer[1] and by Bhabha and Heitler[2] on the basis of the multiplication of high energy electrons and γ-rays in their passage through matter. Since the appearance of these papers, Bowen, Millikan, and Neher[3] have obtained ionization curves at different latitudes which give a fairly good picture of the energy distribution of incoming particles, as well as of the multiplication of particles in definite energy ranges, and Carmichael and Dymond[4] have extended the vertical counter work of Pfotzer.[5] On the other side, Snyder[6] and Landau and Rumer[7] have so far developed the solution of the multiplicative diffusion equations that one can now give quite accurately the theoretical multiplication curve. Since a comparison of the observed and calculated curves may be expected to give valuable information as to the source and production of the penetrating component of the cosmic rays, it seems worth while at the present time to give the results of the theoretical calculations in as precise a form as possible, and to make a preliminary comparison with experiment. The latter is necessarily rather rough, since a detailed interpretation of the ionization chamber work is limited by our lack of knowledge of the angular distribution of the incoming particles, while the counter experiments have so far been subject to such large statistical fluctuations that it has not been worth while to obtain latitude difference-curves.

II

Snyder, in his solution of the diffusion equations, followed Carlson and Oppenheimer in

[1] Carlson and Oppenheimer, Phys. Rev. **51**, 220 (1937).
[2] Bhabha and Heitler, Proc. Roy. Soc. **159**, 432 (1937).
[3] Bowen, Millikan and Neher, Phys. Rev. **52**, 80 (1937); **53**, 217, 855 (1938).
[4] Carmichael and Dymond, Nature **141**, 910 (1938).
[5] Pfotzer, Zeits. f. Physik **102**, 23, 41 (1936).
[6] Snyder, Phys. Rev. **53**, 960 (1938). See also Iwanenko and Sokolow, Phys. Rev. **53**, 910 (1938). An error in writing appeared in Snyder's formulae (the correct formulae were used in his calculations, however). The right-hand side of (23) and (24) should read $s\mu C(y, s-1)$.
[7] Landau and Rumer, Proc. Roy. Soc. **166**, 277 (1938).

using simplified formulae for the differential cross sections for the production of γ-rays and pairs. It has recently been pointed out by Landau and Rumer that the equations are not essentially complicated by introduction of the more exact cross sections given by Bethe and Heitler,[8] since these do not destroy the one feature of the diffusion equations which is exploited in obtaining a solution, namely that, except for ionization terms, they are homogeneous in the energy. The changes in Snyder's treatment entailed by use of the more exact expressions for the cross sections are of a purely formal nature, and it will only be necessary here to summarize the results. The physical basis of the calculation is in no way altered; for a more detailed discussion of the questions involved the reader is referred to Snyder's paper.

The screening constant which appears in the differential cross sections has been recalculated by Professor J. H. Bartlett and we are indebted to him for informing us of his results. He finds, for the probability an electron of energy E_0 will radiate a γ-ray of energy E in a distance dx,

$$P_\gamma dEdx=\frac{4\alpha Z^2r_0^2N}{EE_0^2}\left[\ln\left(\frac{191}{Z^{\frac{1}{3}}}\right)(E_0^2+E_1^2-\tfrac{2}{3}E_0E_1)+\frac{31}{90}E_0E_1\right]dEdx, \quad (1)$$

where $E_1=E_0-E$. The probability a γ-ray of energy E produces an electron of energy E_0 and a positron of energy $E_1=E-E_0$ is

$$P_\pi dE_0dx=\frac{4\alpha Z^2r_0^2N}{E^3}\left[\ln\left(\frac{191}{Z^{\frac{1}{3}}}\right)(E_0^2+E_1^2+\tfrac{2}{3}E_0E_1)-\frac{31}{90}E_0E_1\right]dE_0dx. \quad (2)$$

If we introduce a new unit of length,

$$t=4\alpha Z^2r_0^2N\ln(191/Z^{\frac{1}{3}})x,$$

(1) and (2) become, for air,

$$P_\gamma dEdt=(E_0^2+E_1^2-\tfrac{3}{5}E_0E_1)dEdt/EE_0^2, \quad (3)$$

$$P_\pi dE_0dt=(E_0^2+E_1^2+\tfrac{3}{5}E_0E_1)dE_0dt/E^3. \quad (4)$$

[8] See Heitler, *The Quantum Theory of Radiation*, pp. 170, 198.

The ionization energy loss per unit distance may be written

$$dE_{\text{ion}}/dt=\beta. \quad (5)$$

Following Snyder, we can obtain solutions of the diffusion equations which result from (3), (4), and (5) in terms of double contour integrals. Let $N(t, E)$ be the number of charged particles of energy *greater* than E at depth t, and $\gamma(t, E)$ the number of γ-rays of energy E per unit energy at t. The solution which represents an incident electron of energy E_0, accurate to order β/E_0, is

$$N(t, E)=e^{-\sigma t}\partial Z_1(t, E)/\partial t,$$

$$\gamma(t, E)=e^{-\sigma t}Z_2(t, E)/E,$$

$$Z_1(tE)=-\frac{1}{4\pi^2}\int_C\frac{dy}{y}\left(\frac{E}{E_0}\right)^{-y}\int_s ds\frac{\Gamma(-s)\Gamma(y+s)}{\Gamma(y)}\times\left(\frac{E}{\beta}\right)^{-s}\frac{K_\mu(y, s)e^{\mu(y)t}-K_\nu(y, s)e^{\nu(y)t}}{\mu(y)-\nu(y)}. \quad (6)$$

Here

$$\begin{matrix}\mu\\ \nu\end{matrix}=-\tfrac{1}{2}[A(y)-\sigma]\pm\tfrac{1}{2}\{[A(y)-\sigma]^2+4B(y)C(y)\}^{\frac{1}{2}},$$

$$\sigma=23/30,$$

$$A(y)=\frac{7}{5}[\psi(y)+\gamma]-\frac{1}{10}\left[9-\frac{4}{y+1}-\frac{10}{y+2}\right],$$

$$\psi(y)=d\ln\Gamma(y+1)/dy, \quad \gamma=0.577\cdots,$$

$$B(y)=\frac{2}{5}\left[\frac{5}{y+1}-\frac{7}{y+2}+\frac{7}{y+3}\right],$$

$$C(y)=\frac{1}{5}\left[\frac{7}{y}-\frac{7}{y+1}+\frac{5}{y+2}\right].$$

TABLE I.

y	a	k	b	H
0.2	1.916	2.29	2.62	0.290
0.4	1.496	1.138	2.01	0.362
0.6	1.265	0.584	1.74	0.388
0.8	1.122	0.236	1.64	0.399
1.0	1.000	0.000	1.60	0.399
1.2	0.881	−0.175	1.58	0.384
1.4	0.765	−0.301	1.54	0.362
1.6	0.672	−0.397	1.47	0.333
1.8	0.576	−0.470	1.39	0.302
2.0	0.492	−0.525	1.28	0.273
2.2	0.422	−0.567	1.17	0.252
2.4	0.358	−0.604	1.06	0.236
2.6	0.304	−0.629	0.95	0.220
3.0	0.223	−0.667	0.75	0.187

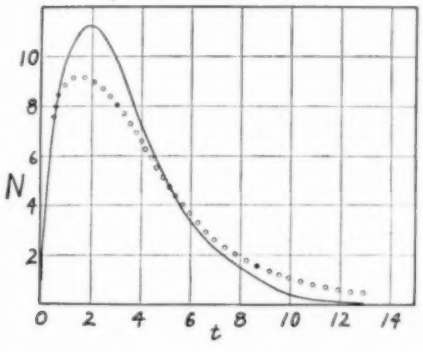

FIG. 1. Multiplication curve for an electron of 11×10^9 v, averaged over all directions of incidence. The circles give the San Antonio-Madras difference curve of Bowen, Millikan and Neher.

The difference equation satisfied by $K_\mu(y, s)$ is

$$\{\mu[A(y+s)-A(y)]-[B(s+y)C(s+y) -B(y)C(y)]\}K_\mu(y, s)=s\mu K_\mu(y, s-1),$$

and the normalization is such that $K_\mu(y, 0)=1$. The corresponding relations for $K_\nu(y, s)$ are obtained by replacing μ by ν.

The function $Z_2(t, E)$ differs from (6) by a factor $(s+y)C(s+y)$ in the integrand.

Snyder has shown that, for $t>\frac{1}{2}$, the total number of charged particles at thickness t is given by a relation of quite simple form:

$$N=He^{kt+\nu s}/(1+bt)^{\frac{1}{2}}, \quad t=(\epsilon y-1)/a, \qquad (7)$$

with $\epsilon=\ln(E_0/\beta)$. Here

$$H(y)=K_\mu(y, -y)\mu/(2\pi)^{\frac{1}{2}}(\mu-\nu),$$

$$k=\mu-\sigma, \quad a=-yd\mu/dy, \quad b=y^2d^2\mu/dy^2.$$

The values of k, a, b, and H are given in Table I. For air t is measured in units of 0.39 m water equivalent, $\beta=95$ Mev.

The depth at which the number of particles reaches a maximum is given quite well, for $\epsilon>3$, by

$$t_{\max}=\epsilon-\tfrac{1}{2}(1.6\epsilon+1)/(\epsilon-1). \qquad (8)$$

The maximum number is nearly equal to the number at $y=1$, so we may write

$$N_{\max}=0.4E_0/\beta[1+1.6(\epsilon-1)]^{\frac{1}{2}}. \qquad (9)$$

III

We shall first compare the theoretical multiplication curve with the San Antonio-Madras difference curve of Bowen, Millikan, and Neher. From the energy distribution determined by these authors, we estimate that the mean energy of the incoming particles in the relevant band is about 11×10^9 electron volts. Calculating the number of particles as a function of depth from (7), and averaging over all directions of incidence of the incoming particles, under the rough assumption that their intensity is independent of direction, we obtain the curve shown in Fig. 1. The circles represent the measurements of Bowen, Millikan, and Neher. The scale of the experimental curve is determined from Bowen, Millikan, and Neher's integration of the ionization curve; the areas under the calculated and observed curves are the same. It should be remarked that the ratio of the maximum heights of the two curves is approximately independent of the assumed initial energy, E_0, since the number of incident particles must be taken inversely proportional to the assumed E_0, while the number of particles at the maximum is approximately proportional to E_0, as one sees from (9).

The discrepancy in the curves at larger depths must be attributed to the penetrating component. At 5 m ($t=13$) this discrepancy is a factor 5, at 7 m ($t=18$) a factor 50. The fall of the observed curve below the calculated one in the neighborhood of the maximum is to be expected if γ-rays or electrons are in some part absorbed in the production of a nonmultiplying penetrating component. This interpretation is supported by the fact that at 5 m about 0.4 penetrating particles are present for each incident particle. If these were primary particles the electron multiplication curve would have to be reduced by a factor 0.6, which would lead to definite disagreement with the experimental multiplication factor of 9, This seems a strong argument that the penetrating component cannot be entirely of primary origin, that penetrating particles are produced in the atmosphere.

The vertical counter work of Pfotzer and of Carmichael and Dymond was carried out at high latitudes (Pfotzer, $\lambda=49°$; Carmichael and Dymond, $\lambda=88°$). At these latitudes the mean energy of the incident particles is about 7×10^9 v. In Fig 2 we give the multiplication curve calculated for this energy, and the experimental

curves of Pfotzer and Carmichael and Dymond. Because of the disagreement of the two experimental curves at intermediate depths, it has not seemed worth while to reduce them to an absolute scale, instead, their maxima have been made the same height as that of the calculated curve.

Snyder's multiplication curve differs from that of Carlson and Oppenheimer, and ours in turn from Snyder's, by a shift of the maximum towards smaller depths, the maximum becoming at the same time somewhat higher and narrower. It will be seen from Fig. 2 that the position calculated for the maximum now agrees very well with that observed.

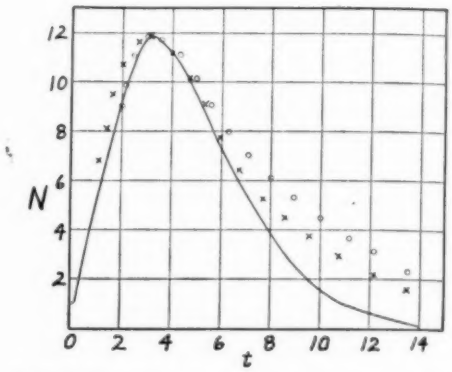

FIG. 2. Multiplication curve for an electron of 7×10^8 v. The circles represent the vertical counter data of Carmichael and Dymond, the crosses those of Pfotzer.

SEPTEMBER 1, 1938 PHYSICAL REVIEW VOLUME 54

Scattering and Loss of Energy of Fast Electrons and Positrons in Lead

W. A. FOWLER AND JACQUENETTE OPPENHEIMER
W. K. Kellogg Radiation Laboratory, California Institute of Technology, Pasadena, California

(Received June 1, 1938)

A cloud chamber investigation has been made of the scattering and loss of energy in a thin lead lamina (0.13 mm) of fast electrons and positrons (5.0 to 17.0 Mev) produced as secondaries by the gamma-radiation from Li^7+H^1. A comparison of the experimental scattering versus angle in the plane of the chamber with the Mott-Rutherford theory of single scattering shows good agreement above $\theta=13°$. Below this angle the experimental points behave in a manner reasonably consistent with multiple scattering. The dependence of the scattering on energy agrees with the relativistic term $(m_0c^2/W)^2$ in the theoretical scattering expression. Some evidence for an excess scattering at large angles of electrons over positrons has been found. The average loss of energy for two groups of tracks of mean energy 9.0 Mev and 13.5 Mev was found to be 35 Mev/cm and 54 Mev/cm, respectively. These values are roughly 1.5 times the theoretical values, a result in agreement with the findings of Crane and coworkers at Ann Arbor. From the observed scattering it does not seem possible to account completely for this excessive loss of energy on the basis of a longer effective path in the lamina. Two out of 97 tracks in the 9.0 Mev group and nine out of 179 tracks in the 13.5 Mev group lost more than 200 Mev/cm. The small excess over the large radiative losses to be expected theoretically is not statistically significant. No difference in the loss of energy of electrons and positrons was found.

IN connection with the experiments carried out to determine the energy spectrum of the gamma-radiation from lithium bombarded by protons,[1] numerous cloud chamber photographs were secured of the traversal of a thin lead lamina (0.13 mm) by high energy electrons and positrons. We have employed these photographs to investigate the scattering and loss of energy of electrons and positrons in lead; the actual measurements were made by one of us (J. O.).

The cloud chamber and high potential apparatus used in the original experiments have been described in the first reference. Although two stereoscopic photographs were originally taken only the one taken normal to the plane of the cloud chamber was analyzed in these measurements. This simplified the analysis considerably and did not detract significantly from the usefulness of the data in a comparison with theoretical expectations. The second view was employed mainly to check the identification of the incident and emergent portions of a given track.

The normal view was projected onto a screen to size and all those tracks extending from the

[1] Delsasso, Fowler and Lauritsen, Phys. Rev. **51**, 391 (1937).

wall of the chamber nearest the bombarded target to the lead lamina were measured. Thus only those incident tracks falling within 10° of the horizontal plane of the chamber were considered. As these photographs were taken with a magnetic field (2580 gauss) perpendicular to the plane of the chamber, it was possible to determine the energy of a track by a measurement of its radius of curvature. On a large sheet of glossy paper, arcs of circles differing by one-half centimeter radius of curvature were ruled. The paper was then cut along a line passing through the common center of these circles. One edge of each of the two resulting screens was thus normal to the circles drawn on it. These screens were employed to measure the radius of curvature of the incident track, the angle between the normal to the incident track and the lead lamina, the radius of curvature of the emergent track, and the angle in the plane of the cloud chamber between the normals to the incident and emergent tracks. The angles were measured to one degree with a small protractor. From these data the incident and emergent energy, the angle of scattering in the plane, and the length of path in the lead were computed.

Numerous tracks seemed to stop in the lead lamina in the normal view. It was possible to show by use of the other view that many of these merely passed out of the light beam near the lamina. For the stopping of the remainder there is at present no adequate explanation other than that the cloud chamber was not always equally sensitive on the two sides of the lead lamina. We do not feel that sufficient precautions have been taken in these experiments to show definitely the existence of any real stopping in the lead lamina and the results here reported are concerned only with those tracks which emerge from the lead lamina. The stopping if real is definitely not consistent with the observed scattering and loss of energy of the emergent tracks.

Theory of Scattering*

The theory of the scattering of electrons by charged nuclei has been developed on a relativistic quantum mechanical basis by Mott[2] and yields for the probability of scattering into a solid angle $d\Omega$ at the angle θ

$$P(\theta)d\Omega=\tfrac{1}{4}NtZ^2r_0^2((1-\beta^2)/\beta^4)\,f(\theta,\beta,Z)\csc^4\tfrac{1}{2}\theta d\Omega,$$

where N = number of scattering nuclei per cc
t = thickness of scattering lamina
Z = nuclear charge
$r_0=e^2/m_0c^2$
β = velocity of electron/velocity of light
$f(\theta,\beta,Z)=1-\beta^2\sin^2\tfrac{1}{2}\theta\pm\pi\beta Z\alpha\sin\tfrac{1}{2}\theta\cos^2\tfrac{1}{2}\theta+$terms in $(Z\alpha)^2$
$\alpha=e^2/\hbar c=1/137.$

The term in $Z\alpha$ is positive for electrons and negative for positrons. Champion[3] has found good agreement with this expression for the scattering in nitrogen between 20° and 180° of electrons with $0.83<\beta<0.95$. Neher[4] found the scattering in aluminum of electrons with energies up to 145 kv to be 32 percent greater than the value given by the above expression. For fast electrons passing through in lead, $\beta\to1$ and $Z=82$, so that

$$f(\theta)=1-\sin^2\tfrac{1}{2}\theta\pm1.88\sin\tfrac{1}{2}\theta\cos^2\tfrac{1}{2}\theta+\cdots$$

and $$P(\theta)d\Omega=4.4t\Psi\,f(\theta)\csc^4\tfrac{1}{2}\theta d\Omega,$$

where

$$\Psi=(1-\beta^2)/\beta^4=(1+\eta^2)/\eta^4=1/\beta^2\eta^2$$
$$=(w/(w^2-1))^2\approx(m_0c^2/W)^2\quad\text{for}\quad m_0c^2\ll W$$

and $\eta=H\rho e/m_0c^2=\dfrac{\text{electron momentum in units}}{m_0c}$

$W=wm_0c^2=$kinetic plus mass energy of electrons.

In the derivation of this expression the reaction of radiation on the scattering has not been taken into account. The radiation reaction will change the scattering only by an amount of the order of 1/137 and the experiments here described are not critical enough to detect such a small change. The theory of single scattering by a charged

* *Note added in proof:* In the following discussion only the theory of elastic single scattering is treated. In a private communication Professor E. J. Williams has kindly informed us of his most recent computations on plural and multiple scattering. His results make it possible to give a much more complete treatment of the experimental data presented in this paper. A comparison of the data with his results will be given in the near future. In addition, Dr. J. H. Bartlett has informed us that he is now investigating the possibilities of making accurate computations of single scattering by nuclei of large Z.

[2] Mott, Proc. Roy. Soc. **124**, 425 (1929).
[3] Champion, Proc. Roy. Soc. **153**, 353 (1935).
[4] Neher, Phys. Rev. **38**, 1321 (1931). Also see Klarmann and Bothe, Zeits. f. Physik. **101**, 489 (1936) and Skobeltzyn and Stepanowa, Nature **137**, 456 (1936).

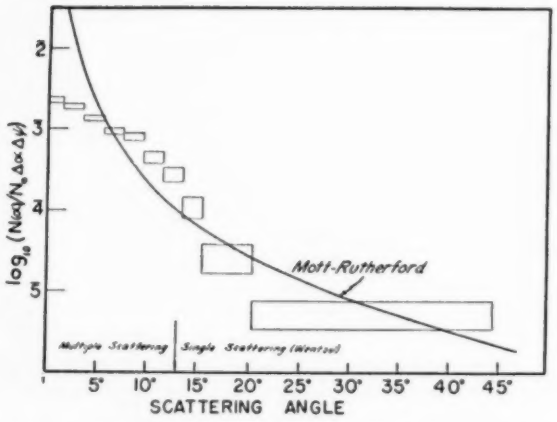

FIG. 1. The scattering in a lead lamina of thickness 0.015 cm of electrons and positrons of average kinetic energy 10.5 Mev as a function of the scattering angle. The vertical spread of the points represents the probable error in the original number of tracks measured in an angle interval denoted by the horizontal spread. The smooth curve represents the Mott-Rutherford theoretical scattering. The quantity $\Delta\alpha$ includes the equivalent angle intervals on both sides of $\alpha=0$.

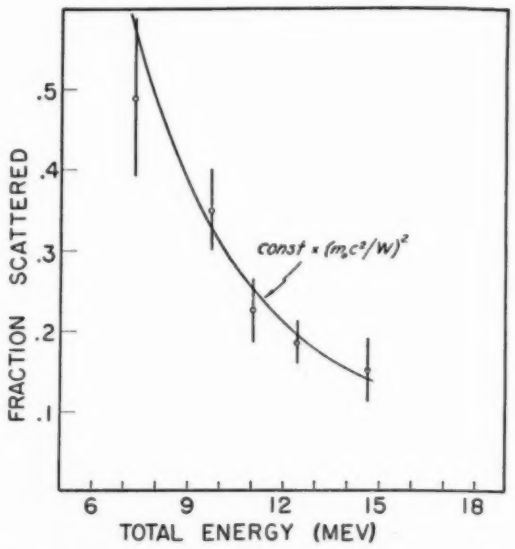

FIG. 2. The fraction of electrons and positrons scattered at an angle greater than 8.5° in the horizontal plane or scattered out of the cloud chamber light beam as a function of energy.

nucleus cannot be strictly compared to the observed scattering because of the screening and scattering by extranuclear electrons and especially because of multiple scattering. The screening effect is small except for very small scattering angles while the scattering by the extranuclear electrons of the lead atom is only 1/82 that due to the lead nucleus. The effect of multiple scattering will be discussed in the comparison with the observed scattering.

The first terms in $f(\theta)$ given above are certainly not accurate for a nucleus with $Z=82$. However, Mott[5] has calculated $f(90°)$ for fast electrons passing through gold and found it to be roughly 3. For angles less than 45°, $f(\theta)$ probably varies between 1.0 and 1.5 for electrons, and between 1.0 and 0.6 for positrons. This is insignificant compared to the variation in the $\csc^4 \frac{1}{2}\theta$ term. It is this essentially classical $\csc^4 \frac{1}{2}\theta$ term as well as the relativistic $(m_0c^2/W)^2$ term which can be tested by our experiments.

In comparing these terms with experiment we have chosen to use the data for electrons and positrons together in order to eliminate statistical fluctuations as much as possible. Although the number of electron tracks is greater than the number of positron tracks, the results should correspond very closely to those to be expected when $f(\theta)$ is assumed equal to unity. The small difference in the scattering of electrons and positrons will be discussed separately.

[5] Mott, Proc. Roy. Soc. **135**, 429 (1932).

THE EXPERIMENTAL SCATTERING

A total of 362 tracks (234 electrons, 128 positrons) with the average of their incident and emergent kinetic energy between 7.5 and 14.5 Mev were analyzed. The mean of this average energy for all the tracks was 10.5 Mev. All of these tracks had emergent lengths greater than 3 cm. An additional 29 tracks (21 electrons, 8 positrons) with incident energy in the same range had emergent track lengths less than 3 cm which precluded accurate scattering or loss of energy measurements. These tracks passed out of the light beam after being scattered in the lead. The light beam was 1.6 cm deep and thus the vertical plane angle of the solid angle in which the scattering was measured was approximately 2 arctan $(0.8/3.0)\approx 30°$. The fraction of tracks scattered into the solid angle bounded by this vertical plane angle and a horizontal plane angle of known interval was found from the measurements. The data so secured cannot immediately be compared with the theoretical expressions as the actual angle of scattering was not measured but only the projection on the

horizontal plane. However, the theoretical expression can be used to calculate $Q(\alpha)$, the probability of scattering per unit solid angle with a horizontal plane angle between α and $\alpha+\Delta\alpha$ and a vertical plane angle between $-\frac{1}{2}\Delta\psi$ and $+\frac{1}{2}\Delta\psi$. If $\gamma=\alpha/\Delta\psi$ then for all γ but for α and $\Delta\psi$ not too large we find approximately:

$$N(\alpha)/N_0=Q(\alpha)\Delta\alpha\Delta\psi$$
$$=P(\alpha)\{\gamma \arctan (1/2\gamma)+2\gamma^2/(1+4\gamma^2)\}\Delta\alpha\Delta\psi,$$

where $N(\alpha)$ is the number of particles scattered into the interval $\Delta\alpha\Delta\psi$ and N_0 is the number of incident particles. The function in γ is equal to zero for $\gamma=0$ and approaches unity for large γ. In Fig. 1 we have plotted $\log_{10}(N(\alpha)/N_0\Delta\alpha\Delta\psi)$ as a function of α as found experimentally. The vertical spread of the points represents the probable error in the original number of tracks measured in an angle interval denoted by the horizontal spread. The smooth curve represents the corrected Mott-Rutherford expression ($f(\theta)=1$) as given above in which we used the average straight line path length $t=0.015$ as found experimentally and the mean total energy 11.0 Mev. The effects of screening and radiative scattering are too small to be significant in this logarithmic plot.

According to Wentzel's criterion,[6] single scattering should hold for angles greater than 13°. The agreement between the experimental points and the theoretical curve above this angle does not constitute a decisive test of the theory but indicates that the order of magnitude and dependence with angle of Mott's theoretical expression is probably correct. The behavior for small angles is what is reasonably to be attributed to multiple scattering—a lack of tracks at very small angles and an excess before reaching the critical angle for single scattering.

TABLE I. *Comparison of electron and positron scattering.*

		Number Scattered		Ratio Electron/Positron Scattering			
				8.5° to 14.5°		>14.5°	
	N_0	8.5° to 14.5°	>14.5°	Obs.	Theor.	Obs.	Theor.
Electrons	255	36	27	1.2±0.3	1.3	1.6±0.4	>1.5
Positrons	136	16	9				

In order to compare the scattering with energy we have computed the fraction of tracks scattered at an angle greater than 8.5° in the horizontal plane or scattered out of the light beam as a function of energy. This is shown in Fig. 2. The influence of multiple scattering is small above this angle and the increased number of tracks over the number scattered at angles greater than 13° makes the results more reliable. For scattering outside a cone of angle θ, the Mott-Rutherford expression for $W\gg m_0c^2=0.51$ Mev gives

$$N(\theta)/N_0=55t(m_0c^2/W)^2 \cot^2 \tfrac{1}{2}\theta.$$

We have computed graphically the effective value for $\cot^2\frac{1}{2}\theta$ to be used in this case where the tracks counted lie outside a rectangle subtending 17° horizontally and 30° vertically at the point of scattering and found it to be ~100. A good fit to the experimental points can be secured by the use of the value 150 for $\cot^2\frac{1}{2}\theta$ as shown in Fig. 2. The excess can be quite reasonably attributed to multiple scattering. Fig. 2 indicates that those particles emerging from the lead obey the theoretical scattering dependence on energy (or more fundamentally on momentum) for particles of electronic mass and charge. The agreement is not as good if the particles are assumed to have an $H\rho$ or momentum value given by the curvature and field measurement but a rest mass so much larger than that of electrons that their velocity is appreciably less than that of light. The deviation of theory from experiment becomes marked if the rest mass is assumed to be as high as 5 Mev.

A comparison of the scattering of electrons and positrons should afford a very sensitive test of the quantum-mechanical term in $Z\alpha$ in $f(\theta)$. For not too large angles the ratio of fast electron to fast positron scattering in lead should be

$$f_-/f_+\approx 1+2\pi\beta Z\alpha \sin\tfrac{1}{2}\theta \cos^2\tfrac{1}{2}\theta\approx 1+1.88\theta.$$

TABLE II. *Loss of energy of electrons and positrons.*

Kinetic Energy (Mev)		Number of Tracks	Average Energy Loss (Mev/cm)		Number Losing More than 200 Mev/cm	
Interval	Mean		Exp.	Theor.	Exp.	Theor.
6–11	9.0	97	35	26.5	2	1.4
11–16	13.5	179	54	34.5	9	4

[6] Wentzel, Ann. d. Physik **69**, 333 (1922).

This expression will give a minimum value for the ratio of electron to positron scattering at an angle greater than θ and due to the rapid decrease with the $\csc^4 \frac{1}{2}\theta$ term in the scattering law this minimum will be a good approximation to the actual value. In Table I the experimental scattering of electrons and positrons (7.5 to 14.5 Mev) at angles between 8.5° and 14.5° and at angles greater than 14.5° is compared with the theoretical predictions. The existence of an excess electron scattering over positron scattering at large angles is indicated but it must be admitted that the observed numbers are subject to large statistical variations.

Loss of Energy

Because a very thin lead lamina was employed in these experiments the loss of energy of particles traversing the lead could not be accurately measured. In fact the measurements revealed on computation that numerous particles had apparently made small gains in energy. If one assumes the errors of measurement to be symmetrical as to gains and losses, the average loss will still be fairly reliable. The very few particles apparently gaining large amounts of energy were assumed to have actually originated in the far walls of the chamber and to be travelling in the opposite direction to the majority of particles and were not included in the average energy loss calculations. Results for two groups of particles of mean energy 9.0 and 13.5 Mev are given in Table II. The energy loss per cm for both groups is seen to be roughly 1.5 times the theoretical loss computed by adding the collision and radiation losses as given by Heitler.[7] This is in agreement with the original results of Turin and Crane[8] for beta-rays of approximately this energy and is further evidence that high energy beta-rays, Compton recoil electrons and electron or positron members of pairs behave in substantially the same manner in passing through matter. From the observed scattering it does not seem possible to account completely for the excessive loss of energy on the basis of a longer effective path in the lamina. We have also compared the number of tracks losing more than 200 Mev/cm² with the theoretical number expected as computed from

$$P(\delta) = \bar{\delta} E_i(\log \{1-\delta\}),$$

where $P(\delta)$ is the probability of an electron losing a portion of its energy greater than δ when $\bar{\delta}$ is the average fractional energy loss and E_i is the incomplete gamma function of $\log \{1-\delta\}$. This expression is shown to hold for small $\bar{\delta}$ and all δ by Heitler.[7] The theoretical expectations are certainly in agreement with the observed numbers within order of magnitude.

Conclusion

Although some experimental evidence[9] has been found for decided variations from the theoretical expectations for the behavior of fast electrons in passing through matter, the results here reported on the scattering and loss of energy by collisions and radiation certainly cannot be said to disagree with the present relativistic quantum mechanical calculations. It is especially to be emphasized that both scattering and radiation which are closely related even classically seem to be accounted for correctly by the theory. Again the theory of the behavior of fast electrons in passing through matter is fundamentally related to the Klein-Nishina expression[7] for the scattering of gamma-radiation and the Bethe-Heitler-Plesset-Oppenheimer expression[7] for the formation of pairs by gamma-radiation. It has previously been shown in this laboratory[1, 10] that the attenuation coefficients in lead and aluminum of gamma-rays of 6 and 17 Mev are correctly given theoretically. Our results then give no reason for questioning the applicability of calculations based on Dirac's fundamental theory to the behavior of electrons or photons of energies of the order of 10 Mev.

In conclusion we wish to thank Professor C. C. Lauritsen and Dr. L. A. Delsasso (now at Princeton University) in collaboration with whom the original pictures were taken, and Professor Robert Oppenheimer for discussions of the theoretical aspect of these problems, and especially for calling to our attention the possibility of a difference in the scattering of electrons and positrons.

[7] Heitler, *The Quantum Theory of Radiation*, pp. 173, 221.
[8] Turin and Crane, Phys. Rev. **52**, 63 (1937); Phys. Rev. **52**, 610 (1937). See also Ruhlig and Crane, Phys. Rev. **53**, 618 (1938).
[9] Skobeltzyn and Stepanowa, J. de phys. et rad. **6**, 1 (1935); Laslett and Hurst, Phys. Rev. **52**, 1035 (1937).
[10] Delsasso, Fowler and Lauritsen, Phys. Rev. **61**, 527 (1937).

X-Ray Diffraction of Substances under High Pressures

ROBERT B. JACOBS*
Research Laboratory of Physics, Harvard University, Cambridge, Massachusetts
(Received May 13, 1938)

An apparatus is described which may be used for x-ray diffraction work on substances under pressures up to 5000 atmospheres. The compressive medium is helium gas. A small (2.5 cm radius) Debye-Scherrer type camera is used. The camera, complete with film and specimen, was placed inside the high pressure chamber. The x-rays make their entrance through a beryllium window in the chamber wall. A general blackening of the film by scattering from helium is prevented by slits installed for this purpose, and the quality of the x-ray diffraction lines is quite good. Results are given for the transition AgI (II) to AgI (III). The crystal structure of AgI (II) is found to be cubic (NaCl type). The volume change in this transition is found to be greater when measured by x-ray methods than when measured by over-all methods. An interpretation of this is given. Some results on cadmium and RbCl are also described.

INTRODUCTION

THE importance of x-ray measurements on materials under high pressure has been recognized for some time. Several experimenters have worked in this field; each used a different method of approach. W. Cohn[1] used a conventional steel pressure bomb with two rather large beryllium windows, one to allow the entrance of the main beam and the other for the exit of the diffracted rays. This arrangement was not entirely satisfactory since the beryllium itself contributed too greatly to the diffracted beam and the desired diffraction from the specimen under observation was thus obscured. Another arrangement of this nature was that of L. Frevel,[2] who used a small Pyrex capillary as his pressure container. The substance to be examined filled this tube. Tube and sample were then mounted in the center of an ordinary Debye-Scherrer camera, and the exposure made. The results were quite satisfactory, but the pressure range was not sufficiently great for many uses since the strength of such a tube will not allow pressures much greater than 1000 atmospheres. McFarlan[3, 4] has been able to work out the crystal structure of some of the forms of ice stable at high pressures after securing them in metastable equilibrium at atmospheric pressure. He produced the desired polymorphic forms at high pressures, cooled them under pressure to liquid-air temperature, and then reduced the pressure to one atmosphere. At the low temperature at which he worked the ices do not revert to the form which is stable at one atmosphere pressure, and the exposure may be made in a low temperature camera.

Of the three methods described, McFarlan's has been the most fruitful, but it does not possess all the advantages of a method which will produce the diffraction pattern from a substance *while it is under pressure*. It is obvious that such an apparatus will give information which is entirely impossible to secure by other means. Such quantities as x-ray densities and compressibilities (as opposed to the over-all values) are examples. Likewise, the relation of new particle size to old in the case of a polymorphic transformation under pressure can be obtained only with this sort of apparatus. Finally, there is considerable importance in studying the nature of polymorphic transformations as regards completeness of reaction, etc., in addition to the crystal structures involved in the high pressure forms.

The apparatus described in this paper is considerably different from any used by others. It consists of a small Debye-Scherrer type camera which, complete with film and specimen, is placed inside a large steel pressure bomb. The bomb is filled with helium and the x-ray exposure is, of course, made with the gas at high pressure. The camera might be thought of as any normal camera which is subjected, not to the usual one atmosphere of air, but to 5000 atmospheres of

* This work undertaken while the author held a National Research Fellowship in Physics.
[1] W. Cohn, Proc. Am. Phys. Soc. **63**, June (1933).
[2] L. K. Frevel, R.S.I. **6**, 214 (1935).
[3] R. L. McFarlan, J. Chem. Phys. **4**, 60 (1936).
[4] R. L. McFarlan, J. Chem. Phys. **4**, 253 (1936).

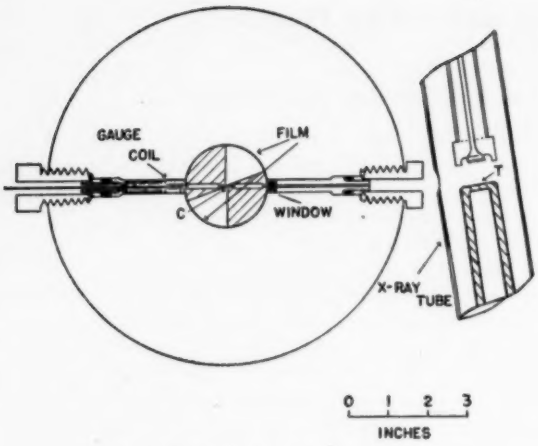

FIG. 1. Plan view of assembly.

helium gas. The beryllium window which allows the x-ray beam to enter the cylinder, lies *in front* of the camera slit system, and hence is unable to contribute undesirable scattering. Since at 5000 atmospheres the x-rays must traverse a great number of helium molecules, and the scattering from these would normally be large, an arrangement of slits is used which serves to reduce scattering to a minimum. Photographs quite comparable to those obtained at one atmosphere with the same camera have been taken at pressures over 4000 atmospheres.

GENERAL DESCRIPTION OF THE APPARATUS

The essential feature is that a small Debye-Scherrer type of camera is used inside a high pressure steel bomb,[5] which is provided with a beryllium window. Fig. 1 gives a general idea of this set-up. The x-ray beam coming from the target (T) enters the chamber through the beryllium window, passes through and is collimated by the slit, meets the crystalline specimen (C), and is diffracted to the film which is placed on the circumference of the camera. The x-ray tube (Philip's Metalix), is costly, and is therefore made readily demountable. It is placed in position after the pressure has been applied and, there is reasonable assurance that everything is "holding." A steel cylinder ($\frac{1}{2}$" wall thickness) concentric with the pressure cylinder serves as a support for the x-ray tube and as a shield for it against flying parts in case of accidents with the pressure cylinder. The camera is a separate, light-tight unit which may be loaded in the dark room, and then slipped into position in the high pressure cylinder. A complete description of it is given in the following section.

[5] The present bomb is a chrome-molybdenum steel cylinder used without heat treatment. Some stretching has been observed since the stresses do exceed the elastic limit by about 10 percent at maximum pressure.

THE CAMERA

The size of the camera was a most important consideration in the design of this apparatus.

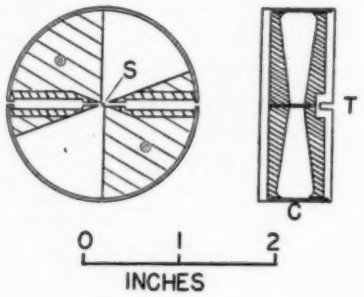

FIG. 2. Camera details.

The usual camera with about a 5 cm radius would be quite out of the question, since it would require a pressure cylinder of preposterous dimensions (for the equivalent strength of present apparatus: about 50 cm diameter). Furthermore, the free space within such a camera is much too large. It will be remembered that this space is eventually to be filled by the highly compressed helium. If an ordinary-sized camera were used, it would take about 1,000 liters of the gas at tank pressure to fill this space at a pressure of 5000 atmospheres. This would involve a potential energy of compression of the order of one million kilojoules, the danger of which cannot be overlooked.

Accordingly the camera was made as small as possible (5 cm diameter). Fig. 2 shows in plan and in cross section the essential details of the design. In the plan drawing, the x-ray beam travels from left to right. It is collimated by the slit system shown on the left. It there encounters the sample S, and is diffracted to the film placed around the circumference. After passing through the specimen the beam is immediately trapped by the slit arrangement on the right. The purpose

of this arrangement is to reduce the open path of the beam through the apparatus to a minimum, and thus avoid the possibility of an excessive general blackening of the film from helium scattering. It will also be noticed that only the first and third quadrants are used in this camera; the other two are filled in solid. By "filling in" all of the "free space" not actually traversed by the useful beams, as indicated in the cross section drawing of Fig. 2, a substantial reduction of free volume is possible. The present arrangement leaves a free space of 7.5 cc in the 5 cm diameter camera and does not seriously impair the accuracy of the measurements.

For absolutely pure helium the absorption in a 5 cm path is about 50 percent at 5000 atmospheres. However, the commercially available helium contains about 4 percent impurities (nitrogen, neon, etc.). *These by themselves* would absorb more than 90 percent of the incoming beam. Hence it is absolutely imperative that they be removed. In the present case a purity of 99.72 percent was obtained by running the gas at 100 atmospheres through charcoal at liquid-air temperature. With this gas the 0.28 percent of impurities still present do, nevertheless, absorb over $\frac{1}{3}$ as much as does the entire amount of helium.

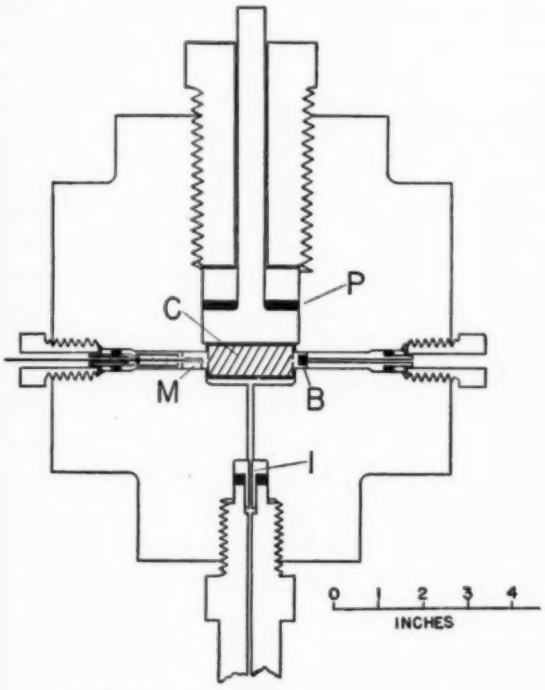

FIG. 3. Cross section of pressure bomb.

THE PRESSURE ARRANGEMENTS

The essential features of the high pressure arrangement are shown in Fig. 3, which is a cross section diagram of the main pressure cylinder. The camera (*C*) is shown in place. It is installed and removed through the large opening above it. After it is in position in the cylinder, the large mushroom packing (*P*) is brought into place and tightened down by the large following screw shown above it. This is the conventional "unsupported area" type of packing invented by Bridgman. To the right, the beryllium window unit is shown in position. It, too, is made tight in the cylinder by an "unsupported area" packing. The gauge coil is shown on the left. It is a manganin coil of about 100 ohms resistance, with electrical connection to the exterior by means of a packed insulated plug. Its resistance is a measure of the pressure. For purposes of lining up the x-ray beam, the gauge coil assembly can be removed, and the emerging beam observed through that opening.

The details of the beryllium window are shown somewhat more clearly in Fig. 4. The window

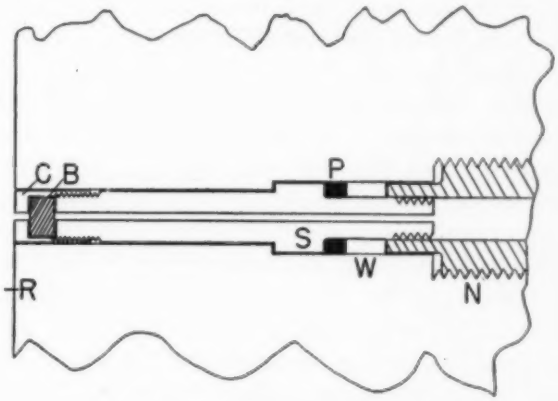

FIG. 4. Details of beryllium window packing.

proper is the small shaded block marked (*B*). It must be fastened in a perfectly gas-tight manner to the metal piece immediately to its right. A considerable number of different schemes were tried for this purpose, and finally the following one was adopted. The face of the beryllium block and, likewise, the face of the hardened steel block adjoining it were made approximately optically flat. A thin rubber gasket (about 0.004″) was cut to go between the two. The cap (*C*) was then

screwed down over the beryllium block forcing it against the rubber gasket with considerable pressure. This served as an original pressure seal. When the window is in operation the gas pressure behind it forces it against the gasket with sufficient force to keep it always tight. This window has been repeatedly used up to 5000 atmospheres without a detectable leak, which is most satisfactory in view of the fact that helium gas is the most difficult gas to handle at high pressures.

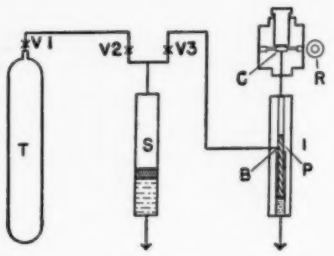

FIG. 5. High pressure helium supply.

The scheme used for supplying the helium to the main cylinder at the desired pressure is the conventional one illustrated in Fig. 5. The gas is normally stored in tank (T) at about 100 atmospheres pressure. When the apparatus is to be filled, it is first flushed to remove the air. Valves (V-1), (V-2), and (V-3) are then opened and the helium fills all parts of the system at tank pressure. Valves (V-1) and (V-2) are then closed, and liquid is pumped into the bottom of the separator cylinder (S), forcing the freely-moving piston upwards, and hence compressing the gas. This serves to compress the gas in all parts of the apparatus to the right of (V-2) to a pressure of about 1000 atmospheres. Now, valve (V-3) can be closed. Liquid is then pumped into the lower half of the intensifier cylinder (I), which pushes the piston (P) upward. This is a double-ended piston. The lower part has a greater area than the upper, consequently, it serves as a pressure multiplier. When the upper end of the piston passes the by-pass (B), it cuts off communication with all parts of the apparatus to the left, and the only gas to be compressed is now in the main cylinder and in the pumping cylinder immediately below it. When the desired pressure is attained, the valve in the liquid line behind the piston (not shown in Fig. 5) is closed, and the procedure is complete. If there are any leaks they will be made evident by the behavior of the manganin pressure gauge. Leaks, however, are not very frequent, and usually the pressure will remain steady for several days, allowing more than ample time for even the longest x-ray exposure which is about 10 hours.

BEHAVIOR OF PHOTOGRAPHIC FILM UNDER PRESSURE

The use of this apparatus of course entails the successful use of photographic film subjected to high gas pressures. Previously published work along this line,[6–8] was of little help because of the demands of this experiment. For one thing, the pressures used heretofore were 2000 atmospheres or less, and for another the exposures were either made before or after the pressure treatment, but never *during* it. In this laboratory Mr. Heilprin had subjected exposed film to 10,000 atmospheres pressure (liquid) and then developed it. He found only slight blurring of the image.

The present experiments have indicated that it is possible to use film under these conditions only if certain rules are rigidly adhered to. These are: First, that the reduction in pressure be *slow*, or else the gelatine will be violently blown from the celluloid backing by the outrush of the absorbed gas. Second, a time interval of several hours must be allowed between the complete reduction of pressure and the development of the film to enable *all* of the occluded gas to escape, since such gases will blow the softened gelatine into many small bubbles. Finally, a moist gas is more suitable than one which is absolutely dry, and it has been found advantageous to provide for the moistening of the helium in this work.

When these precautions are taken, the film is quite unharmed by the pressure. It is generally stretched about 2 percent in length, which makes fiducial markings necessary. No exact measurements have been taken as to the effect of pressure on the sensitivity of the emulsion, but the effect (if any) can be estimated to be not greater than 10 or 15 percent.

---

[6] Ny Tsi-Zé and Lü Ta-Yuan, J.O.S.A. **26**, 26 (1936).
[7] Poindexter, Reardon, DeFoe, Phys. Rev. **49**, 414 (1936).
[8] Lüppo Cramer, Kolloid Zeits. **81**, 222 (1937).

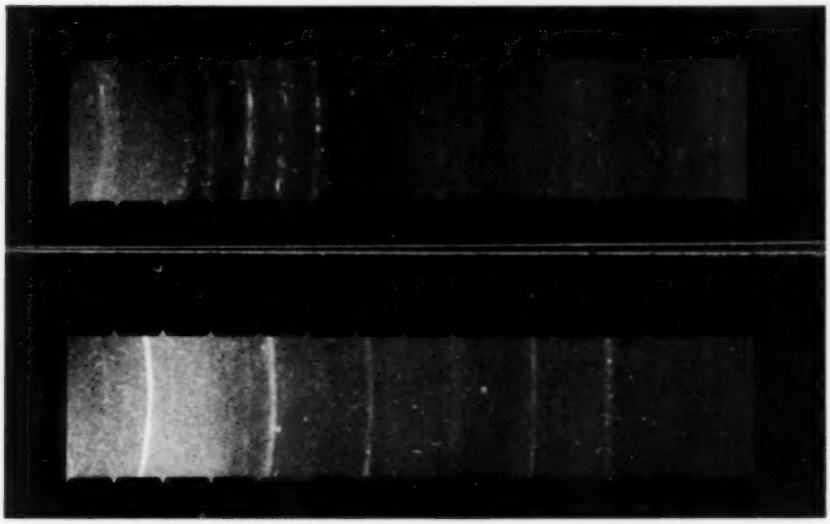

FIG. 7. Diffraction lines from AgI. Above: At atmospheric pressure (ZnS structure). Below: At 3550 atmospheres (NaCl structure).

THE CRYSTAL STRUCTURE OF SILVER IODIDE (III)

The phase diagram of AgI taken from the experimental data of P. W. Bridgman[9] is shown in Fig. 6. The crystal structures of AgI(I), AgI(II), and Ag(I′) (stable between 137 and 146°C at 1 atmos.) are given in the literature.[10–12]

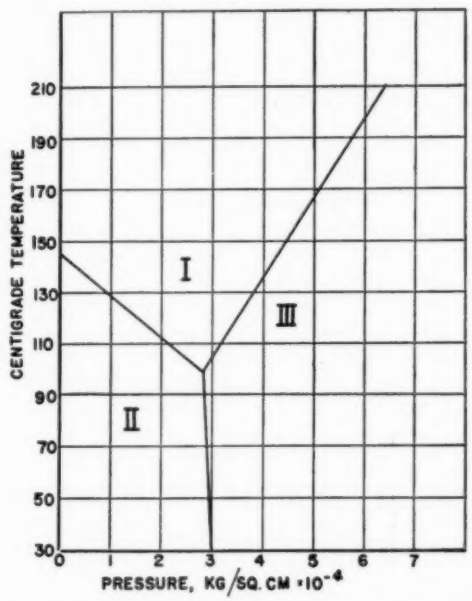

FIG. 6. Phase diagram of AgI (from P. W. Bridgman).

[9] P. W. Bridgman, Proc. Am. Acad. **51**, 47 (1915).
[10] R. B. Wilsey, Phil. Mag. **46**, 485 (1923).
[11] N. H. Kolkmeijer, J. W. A. van Henzel, Zeits. f. Krist. **88**, 317 (1934).
[12] L. W. Strock, Zeits. f. physik. Chemie **B25**, 441 (1934).

AgI(II) is cubic of the ZnS type, which has a coordination number of 4, hence AgI(III) could be anticipated to be either of the NaCl type (coordination number 6) or CsCl type with a coordination number of 8. The present investigation showed the former assumption to be the case. The material used was Eimer and Amend's c.p. It was first reduced largely to AgI(II), as indicated by x-ray analysis. The sample was then subjected to 3550 atmospheres pressure, and the picture taken. This allowed a 550 atmosphere *excess* of pressure over the equilibrium pressure of 3000 atmospheres. Fig. 7 shows the x-ray lines from the sample at the two pressures. Table I gives a summary of the measured lines. The indices as given here refer to a simple lattice rather than to a NaCl type of lattice. The averaged corrected lattice constant value referred to the former type of lattice is 3.03_5A.

THE VOLUME CHANGE FROM AgI(II) TO AgI(III)

It is interesting to compare the measurements of the volume change occurring in this transition when made by the over-all (piston-displacement) method with those obtained by the present x-ray method. The data given in Table I allow two separate and quite independent values to be given for the x-ray measurement. The one may be obtained by calculating the x-ray density of AgI(III) from the lattice constant, and com-

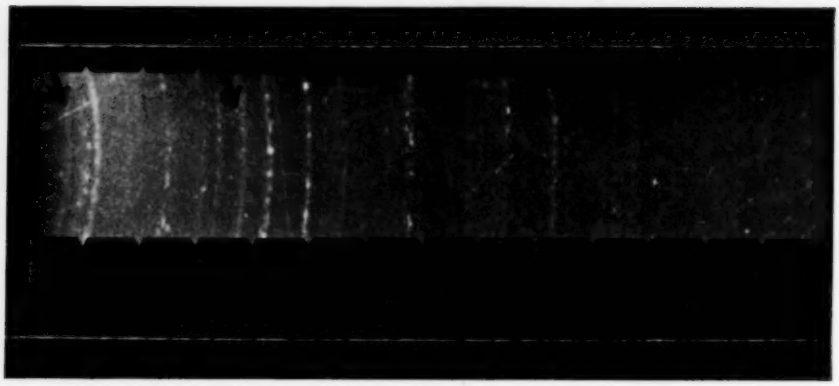

FIG. 8. Diffraction lines from $CsClO_4$ (2500 atmos.). Lines from the untransformed phase indicated by arrows. (Notice the difference in the character of the two sets of lines.)

paring this with the known x-ray density of AgI(II) corrected for the compression at 3550 atmospheres. The second method requires the use of only the *third* and *fourth* lines in Table I. They are both (110) lines, the one from AgI(II) and the other from AgI(III). Their separation then can be used as a *direct* measure of the volume change at 3550 atmospheres. The following equation is used:

$$\Delta V = V_{av}\, 3 \cot \theta_{av} \Delta\theta.$$

This follows directly from the Bragg equation. θ is the Bragg angle. $V_{av.}$ is the average specific volume of the two forms. $\Delta\theta$ is, of course, given by the separation of the two lines involved in the measurement. Table II gives in summary the results of the previous (piston-displacement) measurements, and those of the present investigation.

The difference between the x-ray and the over-all measurements of volume change seems too large to be attributed to experimental uncertainties. There is a greater likelihood that the transition does not run completely throughout the material even at pressures considerably beyond the equilibrium pressure. There is evidence for this conclusion in the present investigation of AgI, since lines belonging to each phase appear on the same film (Fig. 7) taken at a pressure of over 500 atmospheres beyond equilibrium between the two phases. If a small portion of the material remained unchanged in the case of the experiments of Tammann and Bridgman, this would account for the lower values of the volume change which they get. And if this actually is the case, it indicates the presence of a phenomenon not previously observed in high pressure transitions. This should not be confused with "sluggishness" which simply means that a transition point may be considerably overshot before the transition actually takes place. In such cases the transition is generally thought to take place quite completely once it begins, except for slight "rounding of corners" on the volume-pressure curve. $CsClO_4$ has exhibited the same phenomenon as AgI to even a more marked degree. In this case one may observe (Fig. 8) x-ray lines from the low pressure phase at a pressure of over 1000 atmospheres beyond the equilibrium line. In this particular exposure, the lines due to the

TABLE I. *Diffraction data for* AgI(III) Cu *k-α radiation. Temp.=25°C. Pressure=3550 atmospheres.*

INTENSITY	BRAGG ANGLE	INTERPLANAR DISTANCE	INDICES	LATTICE CONSTANT
wk.	12.08°	—Untransformed AgI(II)		
v.st.	14.41	3.089A	(100)	3.089A
wk.	19.48	Untransformed AgI(II)		
v.st.	20.73	2.173	(110)	3.073
m.	25.76	1.770	(111)	3.065
m-wk.	30.00	1.539	(200)	3.078
st.	34.23	1.366	(120)	3.065
m-st.	38.02	1.249	(112)	3.060
wk.	40.75	1.075	(220)	3.040
m-wk.	49.47	1.012	(122)	3.036
m-wk.	53.29	0.9601	(103)	3.036
m-wk.	57.32	0.9142	(113)	3.032
m.	71.42	0.8118	(123)	3.037

Averaged value (corrected) $=3.03_8 \pm 0.005$A

high pressure modification appear to be from the larger crystal grains; i.e., the smaller crystals appear to remain untransformed. Evidently, transitions are much more probable in the larger crystal grains, and crystals smaller than a certain size apparently fail to undergo transformations far into a region where they are unstable. For $CsClO_4$ it was impossible to compare the volume changes as a check, as with AgI, since the crystal form of the new phase has not yet been worked out from the x-ray data. In the case of RbI (to be described more completely in a later paper) no evidence of an untransformed phase was present at 400 atmospheres beyond the equilibrium pressure. Here the x-ray volume change is only slightly greater than the over-all measurements, and this difference may be within the limits of observational error.

How widespread this phenomenon is, and how important a role it plays in high pressure transitions can only be found from a far greater number of observations than have yet been made.

TABLE II. *Comparison of volume changes.*

MEASUREMENT	METHOD	ΔV CC/GRAM (3550 ATMOS. 20°C)
Tammann*	Piston Displacement	0.0204
Bridgman	" "	0.0239
Present	Density Difference	0.0288
"	Doublet Measurement	0.0285

*G. Tammann, Zeits. f. physik Chemie **75**, 733 (1921).

CADMIUM AND RUBIDIUM CHLORIDE

Cadmium has been found by Bridgman[13] to exhibit a transition at about 3000 atmospheres, which is detectable only when single crystals are used. The volume change is too small to be observed when the bulk metal is used, but a discontinuity in both size and electrical resistance may be observed in the case of a single crystal. Since cadmium is hexagonal close-packed, a change in crystal structure would undoubtedly mean a change to the face-centered cubic type, the other close-packed structure. This change would be readily detectable with the pressure camera used in this work. However, several samples of cadmium from different sources were tried, and no change in crystal structure was observed up to 4500 atmospheres. Evidently, the transition does not involve a change in crystal structure.

Rubidium chloride[14] has been shown to have a slight volume discontinuity in its pressure curve in the region of 1200 atmospheres, which suggested a transition of some type here. X-ray investigations up to 2000 atmospheres have failed to show this as a change in crystal structure. This is perhaps likewise a transition not involving a change in crystal structure.

In conclusion the author wishes to express his indebtedness to Professor Bridgman for many ideas on high pressure technique.

[13] P. W. Bridgman, Proc. Am. Acad. **60**, 342 (1925).
[14] P. W. Bridgman, unpublished work.

Optical Properties of the Alkali Metals

R. W. Wood and Charles Lukens
Johns Hopkins University, Baltimore, Maryland

(Received June 15, 1938)

The physical processes responsible for the unique optical properties of silver, in contrast to those of the alkali metals are briefly discussed from the standpoint of the zone theory of electron distribution in crystals. The results of experiments undertaken in the hope of finding a renewal of reflecting power in the remote ultraviolet in the case of the alkali metals, are recorded. Photographs of the spectra of the discharge of a condenser through a capillary tube after reflection from metal films condensed at liquid-air temperature showed no return of reflection in the region extending down to 500A.

THE high transparency of comparatively thick films of the alkali metals in the ultraviolet region was first observed and studied by one of us in 1919.[1] In this investigation only potassium and sodium were investigated; the former showed high reflecting power from the red down to $\lambda=3400$A, below which point the reflection fell off rapidly, and the metal became very transparent. Sodium, on the other hand, while exhibiting the high transparency in the ultraviolet below 3100A showed a reflecting power estimated at 50 percent between 2100A and 3000A, while in the visible spectrum it is of the order of 90 percent. In 1933[2] the behavior of the alkali metals was more thoroughly investigated and the region at which transparency commenced for all of these metals determined. Caesium showed high transmission beginning at wave-length 4400A, rubidium at 3600A, potassium at 3150A, sodium at 2100A, and lithium at a somewhat lower point, an uncertainty resulting from the presence of sodium as an impurity. In the region of transparency, which was investigated to wave-length 1850A, these metals have a Brewsterian angle and give plane polarized light by reflection. The transparency in the case of a potassium film was about 100,000 times as great in the ultraviolet as in the visible region; a film through which the sun's disk was barely visible transmitted 25 percent.

R. de L. Kronig[3] attempted to account for these results by his quantum theory of metallic dispersion, which is based on assumed quantum transitions of electrons from an energy level in one of the "zones" (formed by the widening of the atomic levels as the atoms approach one another) to a corresponding level in a zone of higher energy in the crystal lattice. While this treatment gives a qualitative picture of the narrow band of transparency of silver in the ultraviolet, it does not represent the behavior of the alkali metals. Zener[4] showed that good agreement with the observations of experiments resulted if the electrons were considered as free, and developed equations along the lines employed by Tonks and by Norton in their treatment of the action of the Kennelly-Heaviside layer on radio waves, in which case the dielectric constant is represented by $\epsilon=1-(Ne^2)/(\pi m\nu^2)$ in which N is the number of electrons in unit volume (or atoms in the case of the alkali metals since only the valence electron is concerned). Zener then shows that there is a critical frequency ν_0 (or wave-length λ_0) which gives the dielectric constant the value 0. That is

$$(Ne^2)/(\pi m\nu_0^2)=1 \quad \text{or} \quad \nu_0^2=C/\lambda_0=Ne^2/\pi m.$$

We then have total reflection when $\lambda>\lambda_0$ while for $\lambda<\lambda_0$ the proportion reflected is $R=(n-1)^2/(n+1)^2$ where $n=\sqrt{\epsilon}$.

The behavior of the alkali metals could thus be accounted for by free electrons in the crystal lattice; the energy states in the lower zone are incompletely filled. These electrons are considered as operating on radiant energy in the range of the visible spectrum in the same way that the electrons in the Heaviside layer operate on radio waves, reflecting them back to earth if

[1] R. W. Wood, Phil. Mag. July (1919).
[2] R. W. Wood, Phys. Rev. **44**, 353 (1933).
[3] Kronig, Nature **132**, 601 (1932).
[4] Zener, Nature **132**, 968 (1932).

the electron concentration is sufficiently high in comparison to the wave-length. It is known for example that, in certain states of the ionosphere radio waves are sometimes reflected from a lower stratum which they subsequently are able to penetrate, only to be reflected from a stratum at a much greater elevation. The wave-length at which reflection resulting from free, or Zener, electrons will cease, will be greatest for caesium (large atoms and least dense packing of the valence electrons) and least for lithium (smallest atoms and densest packing, i.e., N has its smallest value in the case of caesium).

The object of the present investigation was to see whether an extension of the study of the optical properties into the region of the shortest possible wave-length would show evidences of quantum absorption such as is shown in the case of silver on the short wave-length side of its band of transparency around $\lambda = 3100$A.

A clearer picture of the problem can be gathered perhaps by comparing the optical properties of silver with those of the alkali metals.

In the case of silver we have zones somewhat as shown in Fig. 1. The reflection (nearly 100 percent) in the visible region, and 50 percent on the long wave-length side of the narrow band of transparency can be attributed to the electrons in the uppermost filled band of the lower zone b, which act in the manner of Zener's "free electrons." This gives the high reflection on the long wave-length side of the region of transparency (where ϵ becomes 0) which corresponds to the similar region shown by the alkalis, but extends only to a very limited distance, for at and beyond its edge on the short wave-length side, the light photons have energy enough to effect transitions from levels in zone b to *corresponding* bands in zone a as shown by arrows. This is termed inner photoelectric (or quantum) absorption, and the reflecting power (which is very nearly zero in the region of transparency, acquires a considerable value, which is determined by the usual equation for semi-transparent media,

$$R=\frac{(n-1)^2+\kappa^2}{(n+1)^2+\kappa^2}.$$

It thus appears that the reflection on opposite sides of the band of transparency results from different physical processes.

In the case of the alkali metals the zones overlap, and form a continuum within which Zener's "free electrons" can operate, but in which quantum transitions can also occur. The quantum transitions are, however, of much smaller energy values than in the case of silver, and cause little or no absorption and reflection in the remoter ultraviolet. They do, however, introduce absorption on the long wave-length side of the point where $\epsilon = 0$ and consequently reduce the reflecting power as this point is approached from the visible region. Curves showing the reflection to be expected on Zener's treatment (free electrons only), and the same as modified by quantum absorption are shown in Fig. 2 for potassium.

It seemed possible however, that photons of sufficient energy might be able to effect quantum transitions for an electron in an inner closed shell,

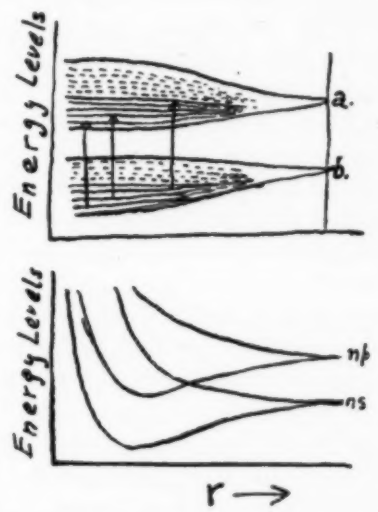

FIG. 1. Energy levels as a function of atomic distances. Upper curves for silver, lower curves for sodium.

and that such transitions would give rise to reflection as in the case of silver. In the case of caesium it seemed that such transitions could be brought about by light of wave-length not much shorter than 500A; this assumed value is based on the second ionization potential of caesium.

APPARATUS

The apparatus for the investigation was designed to operate as follows. The light from an

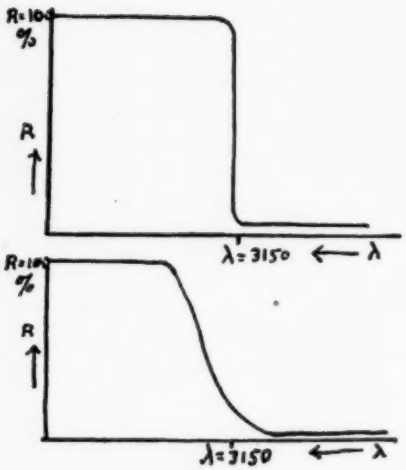

FIG. 2. Reflection coefficient. Upper curve for free electrons; lower shows modification by quantum absorption in potassium.

end-on capillary tube of Pyrex glass traversed by condenser discharges in helium fell on a hollow concave mirror which could be kept filled with liquid air. Below the mirror a small furnace was mounted from which the alkali metals were distilled onto the mirror, which then focused the light from the capillary on the slit of a small vacuum spectrograph. A diagram of the mirror and furnace chamber is shown in Fig. 3 (side view and not drawn to scale) and again in Fig. 4, in connection with the discharge tube (both viewed from above).

The hollow mirror was made by closing a fairly large Pyrex tube at the bottom, heating one side and pressing it in, until the flattened surface coincided with the axis of the tube. The flat surface was then ground concave and polished, with a radius of curvature of 13 cm and an area of 4 cm². The upper end was ground to a cone, and a thistle tube sealed in as shown. This construction was necessary to prevent the liquid air, (which was introduced through the thistle tube) from freezing the conical ground joint by which the mirror was rotated until the image of the capillary fell on the slit. The distance from the mirror to the ground joint was much longer than shown in the diagram.

The platinum furnace F was heated by an incandescent spiral of tungsten. The supply current came through wires sealed into the conical ground stopper G, which could be removed for charging or cleaning the furnace. The metals were evaporated from a shallow trough immediately above the spiral. The discharge tube, which was connected with the Y shaped furnace chamber by a ground joint is shown also in Fig. 4. (Side view immediately below the top view). It consisted of two large cylindrical tubes E_1 and E_2 containing the electrodes, joined by a short horizontal tube D with a sealed-in tube of smaller bore, into which the capillary discharge tube (surrounded by a glass sleeve), could be inserted by removing the window W. The insertion of a new capillary is necessary after every four or five hours of operation, as the bore is gradually enlarged by glass dust torn off from the surface by the heavy discharges. It is this dust, heated to a super-incandescence, which emits the continuum of short wave-lengths. Following Hopfield's technique we fitted the portion of the tube at H with another sealed-in tube into which a second capillary tube of 1 mm bore was inserted, to protect the mirror chamber and the attached spectrograph (where the lowest possible pressure was required) from the higher pressure necessary in the discharge tube to ensure its uniform operation. Helium, purified by passage through outgassed activated charcoal at liquid-air temperature, entered the discharge bulb E_1 through a long glass capillary thread; the rate of flow was about 100 cc per hour. In the capillary, L, which was 5 cm in length with a bore of one to three mm, brilliant flashes of light are produced about once a second by the dis-

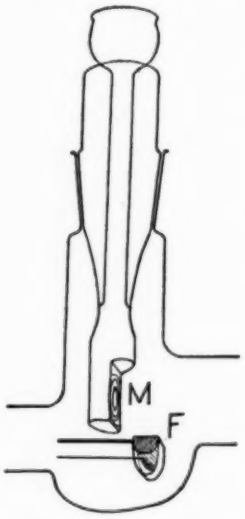

FIG. 3. Diagram of apparatus; side view.

charge of a condenser of 0.06 microfarad capacity charged to 50 kilovolts by a transformer and FP 84 thermionic rectifier. The impedance of the oscillatory circuit was made low by using heavy many stranded cable. The spark gap was between 5 inch brass spheres, one of which was swung to and fro by a constant speed motor. This gave better control of the exposures than with the irregular discharges which occurred with a fixed gap.

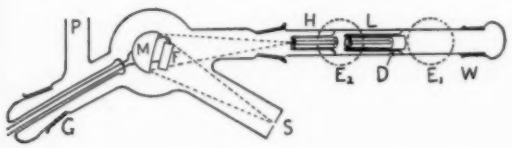

FIG. 4. Diagram of apparatus, as seen from above.

The light from the first capillary passed through the second, in part by multiple reflections, and fell upon the mirror. This second capillary was surrounded by a sheath of thin brass flared out at one end to a diameter equal to that of the tube connecting the two discharge bulbs. This blocked the passage of all light except that passing through the capillary, and facilitated the adjustment of the mirror to the position in which the image of the capillary was centered on the slit.

The spectrograph was equipped with a grating of 42 cm radius, 15,000 lines to the inch, etched on glass, and gave a nearly normal spectrum covering the wave-length range from 0 to 4100A on a 9 cm film. The film was Eastman process sensitized with one part Nujol in 30 parts benzene. Overlapping of the spectral orders was almost entirely eliminated by covering the fluorite region with a fluorite plate and the longer wave-length region with one of crystal quartz.

PREPARATION OF THE METALS

The metals, sodium and potassium were heated for an hour, with continual pumping in a Pyrex glass tube, one end of which had been drawn down to a thin walled "straw" about 3 mm in diameter and 50 cm in length. A plug of well-cleaned and heated steel wool had been previously packed into a constriction in the tube at the base of the tapering straw, and after outgassing the metal, the tube was sealed off from the pump, inverted and given a whip-like motion which projected the molten metal through the steel wool and down into the glass straw, in which it solidified, usually as short plugs with empty spaces between. In cases in which the tube filled solidly with metal, short bits were cut off as required and the open end sealed with a drop of molten Picein wax. The waxed end was cut off and rejected before using a second piece.

Lithium cannot be given this treatment, and was placed directly in the platinum trough of the furnace, after the surface was trimmed with a knife. Sodium and potassium were introduced by placing a short bit of the metal filled straw in the furnace, inserting the ground joint and starting the pump immediately.

Rubidium and caesium, sealed in short thin-walled tubes, were sent to us by Dr. H. E. Ives of the Bell Telephone Laboratories. Before attempting to introduce these tubes, the entire apparatus, including the spectrograph, was exhausted, and the "gate-valve" behind the slit closed. The rest of the apparatus was then filled with nitrogen, and a slow stream of the gas caused to flow out through the open joint, and past the furnace which was held just within the opening at *G*. The ends of the tube containing the metal were cut off as they were held (by gloved fingers) in the nitrogen stream issuing from *G*. This technique was imperative since caesium takes fire almost instantly on exposure to the air.

Photographs of the spectrum reflected from the glass mirror which were taken before any experiments with the metals were made showed that we were reaching a point a trifle short of 500 angstroms, but whether this limit was due to failure of the mirror to reflect or to the absence of shorter wave-lengths in the light, we did not determine.

PREPARATION OF THE METAL MIRRORS

The entire apparatus having been exhausted, the gate-valve to the spectroscope was closed, air (or nitrogen) admitted, and the metal placed in the furnace. Re-exhaustion was commenced immediately. The discharge tube was now operated for about an hour for outgassing. The helium was admitted after the vacuum had extinguished the

discharge. The mirror was then turned into such a position that it faced away from the furnace and the glass walls in its neighborhood well heated with a small torch. The tube was then allowed to cool and the current turned on to the furnace; the temperature was raised very gradually at first until the metal boiled out of the tube from the pressure of the occluded hydrogen. Usually there was a considerable evolution of metal vapor when this occurred but none reached the concave face of the mirror. The current was now considerably reduced, and a clear spot produced on the wall of the tube by local heating for the purpose of observing the mirror, which was now filled with liquid air and turned to a position such that it faced the furnace. After the vacuum had reached the point at which a "leak-tester" showed only a feeble fluorescence of the wall of the tube, the temperature was raised until evaporation of the metal commenced. The thickness of the film could be judged by its transmission of visible light.

If the evaporation was too rapid the mirror appeared grey or even black, probably because its surface was heated too rapidly for the heat to diffuse through the glass to the liquid air, or perhaps by too rapid a rise of pressure. Slow evaporation for about two hours invariably produced excellent mirrors.

The discharge was now started and the mirror turned until the image of the capillary appeared on the slit.

It will be readily understood that the assembling of the tubes and the spectroscope, so that this could be accomplished by simple rotation on a fixed axis, was a labor of some magnitude, as it involved local heating and slight bending of the glass on several occasions.

The exposure times for the spectrograms varied from 30 minutes to an hour or more.

Results

Taken as a whole the apparatus functioned very perfectly. The chief difficulty was with the source of the light; the ratio of the intensity of the continuum to that of the line spectrum was very variable. With a capillary of large bore the line spectrum predominated, and if we started with a small bore a progressive enlargement was always present owing to the stripping of the surface by the discharge.

Misleading results occur if the metal film is too thin, as in this case transmission in the ultraviolet occurs, and we have reflection from the glass.

The wave-length scale was determined approximately from the grating constant and the measured distance from the grating to the film, and checked by comparator measurements on several lines. Only a few lines due to helium were present; most of the others were ascribed to nitrogen, oxygen, hydrogen, carbon silicon, and boron.

The "central image" was reduced in intensity by a small strip of red Cellophane mounted in front of the plate, and appeared in the spectrograms as a sharp narrow line, on which accurate settings could be made.

With long exposures traces of tarnish appeared on the mirrors especially in the case of caesium, and it was usually found expedient to apply a second coat either from the furnace, or by driving off some of the deposit from the surrounding wall of the tube. A number of the spectrograms are reproduced in Fig. 5. The upper and lower, *a* and *i*, show the reflection spectrum from the glass mirror; the former, one of the first photographs taken, (with a discharge tube of 1 mm bore) was badly fogged in the short wave-length region but shows the continuum, with superposed lines, down to 500A, while the latter made with a discharge capillary of 3 mm bore, shows only the lines, but nothing beyond 500.

Spectrum *b* was made with a sodium mirror which was opaque to visible light, but sufficiently thin to permit the reflection from the glass to extend the spectrum to 1000A.

The next five spectrograms, *c* to *g*, show the reflection from all of the alkali metals in the order of their atomic numbers.

Spectrum *h*, taken with a thin film of rubidium shows strong reflection from the glass; the sharp breaks indicate the regions covered by the quartz and fluorite plates used for suppressing the second order spectrum of the shorter wave-lengths. Taken as a whole the spectra do not give a very satisfactory impression of a progressive shift of the limit of reflection. It must be remembered, however, that there is no sharply defined limit; the reflecting power decreases, in the case of

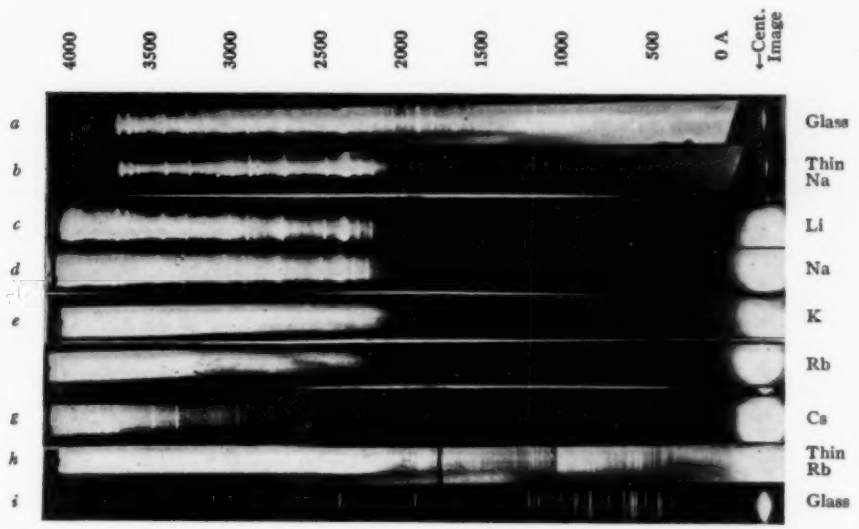

FIG. 5. Reflection spectra from various mirrors.

rubidium, from 60 percent to 10 percent in a range of 800A according to Ives.[5] Our spectrum *f* shows reflection down to 2300A, though Ives gives a value of about 1 percent at this point. The film in this case was evidently partially transparent and considerable reflection from the glass is evident. The oblique shadows are interference minima similar to those reproduced in the earlier paper.

From an inspection of all of our plates, and consideration of the reflection from the glass and the absorption of the gelatine and the oil film, we assigned the following values as the limits of reflection:

Li	Na	K	Rb	Cs
1550A	2100A	3150A	3400A	3800A

The limit cannot, however, be sharply defined as shown by the curves obtained by Ives, published in recent numbers of the *Journal of the Optical Society of America*, and the spectra reproduced would be very misleading in the absence of other data. They show, however, the complete absence (less than 1 percent) of reflection in the region of shorter wave-lengths as far down as 500A which was the limit of the spectrum of our discharge tube. To reach shorter wave-lengths it would have been necessary to employ a "capacity" many times greater than the one at our disposal. This would have given a higher temperature, and a consequent extension of the spectrum with a greatly reduced time of exposure. We made an attempt to secure this result with a vacuum spark, but the products of the discharge ruined the mirrors by corrosion in a few minutes.

An investigation is planned in which the simultaneous reflection and transmission spectra of a film will be photographed in coincidence from which the true absorption at various points of the spectrum can be computed.

[5] Herbert E. Ives, J. Opt. Soc. Am. **27**, 397 (1937).

Hyperfine Structure of Boron, Yttrium, Rhodium, and Palladium

D. T. WILLIAMS* AND L. P. GRANATH
Department of Physics, New York University, University Heights, New York, N. Y.

(Received June 27, 1938)

The spectra of boron, yttrium, rhodium, and palladium, excited in an uncooled Schuler lamp, were investigated in the region λλ2500–4000 with a 20-cm quartz Lummer-Gehrcke plate, in an attempt to find hyperfine structure. None was discovered that could be interpreted either as isotope shift, or as structure due to a nuclear magnetic moment.

INTRODUCTION

HYPERFINE structure may be due to nuclear magnetic moments or to the presence of isotopes. Structure from the former theoretically might be observed with any nucleus of nonvanishing spin and magnetic moment, and would be expected in elements whose nuclei are composed of an odd number of primary particles. That due to the isotope effect should from elementary considerations, be more apparent in the lighter elements. Experimentally, hyperfine structure is most easily observed in the heavier elements, because the lines are sharper, and because the separations are found to be fairly large. Spectral lines of the very light elements are so broad, because of the Doppler effect, that small h.f.s. is concealed; on the other hand, the elements in the middle of the periodic table have been found as a group to possess extremely small structure of any type.

The elements on which we report include boron, a very light element, and yttrium, rhodium, and palladium, in the central portion of the periodic table.

BORON

Boron consists of two isotopes, B^{10} and B^{11}, which occur in relative concentrations of 1 to 4. According to elementary theory, the spectral terms of the two isotopes should be separated by an energy difference proportional in the first approximation to the product of the term value for an infinitely heavy nucleus, and the difference of the reduced electron masses for the two nuclei. Similarly every spectral line will have two components of wave number separation approximately proportional to the product of the average wave number of the two, and the difference of the reduced electron masses. Thus each fine structure component of the boron resonance doublet at λ2496.73 and λ2497.93 should, under high dispersion and if sufficiently sharp, be doubled with separations of about 0.2 cm^{-1}.

A spin and nuclear moment have been predicted for the boron isotopes by Bethe and Rose;[1] these predictions suggest rather small magnetic splittings, so that each isotope should have a hyperfine structure pattern of about 0.02 cm^{-1} over-all breadth. The total pattern of each of the resonance lines would theoretically be a doublet of separation about 0.2 cm^{-1}, each component of which would be complex with breadth of about 0.02 cm^{-1}.

The boron resonance lines were excited in a Paschen-Schuler tube with an uncooled cathode. Attempts to excite the lines in water cooled and dry-ice cooled tubes were unsuccessful. Although for the estimated temperatures in the source the Doppler breadth is computed to be so large that the isotope doublets would probably not be resolved, we considered it quite possible that an asymmetry in the lines would be observable.

The lines were therefore photographed by use of the uncooled source. The spectrograph was a large Hilger 185 instrument, used with a 20-cm quartz Lummer plate, thickness 3.518 mm, in series with a Rochon prism and a quartz-fluorite achromat in front of the slit. The high dispersion apparatus was mounted on a lathe bed to reduce vibration, and enclosed in a box the temperature of which was controlled in the customary manner with a mercury thermostat and heater.

Exposures of 24 hours were sufficient to photograph the lines; the lines were not observ-

* Now at Carleton College, Northfield, Minnesota.

[1] Bethe and Rose, Phys. Rev. **51**, 205 (1937); **51**, 993 (1937).

TABLE I.

WAVE-LENGTH	TRANSITION	STRUCTURE
	Lines reported in yttrium II spectrum	
3982.59	$a^3D_2-z^1D_2'$	Single
3788.70	$a^3D_1-z^3F_2$	"
3776.56	$a^3D_2-z^1P_1$	"
3774.33	$a^3D_2-z^3F_3$	"
3747.55	$a^3D_1-z^1P_1$	"
3710.30	$a^3D_3-z^3F_4$	"
3664.62	$a^3D_3-z^3D_2'$	"
3633.13	$a^1S_0-z^1P_1$	"
3611.06	$a^3D_2-z^3D_2'$	"
3601.93	$a^3D_1-z^3D_1'$	"
3600.74	$a^3D_3-z^3D_3'$	Two components, intensities, 1 : 4
3549.02	$a^3D_2-z^3D_3'$	Single
3496.08	$a^1S_0-z^3D_1'$	"
3327.89	$a^1D_2-z^1F_3$	"
3242.30	$a^3D_3-y^3P_2$	"
3216.70	$a^3D_2-y^3P_1$	"
3195.62	$a^3D_1-y^3P_1$	Two components, one broad. 5 : 4
3173.07	$z^3F_4-a^3G_5$	Two components, one broad. 10 : 11
	Lines reported in yttrium III spectrum	
2945.92	$5^2S_1-5^2P_1$	Single
2817.03	$5^2S_1-5^2P_2$	"

ably asymmetrical. Rough measurement on λ2497.73 gave a half-breadth of 0.4 cm^{-1}.

YTTRIUM

Yttrium is an odd element consisting of a single isotope. Its visible spectrum has been found free of h.f.s. by Schuler and Schmidt[2] and by Kruger.[3]

In the ultraviolet, between λ3000 and λ4000, the stronger lines of the first spark spectrum are found. These were photographed by use of the same type of source and the same dispersing apparatus as in the investigation on boron. Although 17 of the 18 lines observed involve transitions of an *s* electron, no significant structure appeared. Table I is a list of the lines reported; they were examined and identified simultaneously with a comparator. The lines

[2] Schuler and Schmidt, Naturwiss. **22**, 839 (1934).
[3] Kruger, Phys. Rev. **47**, 509 (1935).

TABLE II. *Lines reported in the rhodium I spectrum.*

WAVE-LENGTH	TRANSITION	STRUCTURE	WAVE-LENGTH	TRANSITION	STRUCTURE
3975.32	$^2\bar{D}_3'-27_2$	Single	3498.74	$^4F_2-^2D_3$	Single
3958.86	$^2F_3-^2G_4$	"	3478.91	$^2\bar{D}_3-^2D_3$	"
3942.71	$^4P_2-^4\bar{P}_1$	"	3474.79	$^4F_2-^4G_2$	"
3934.23	$^2F_4-^4G_4$	"	3462.04	$^4F_2-^4\bar{F}_2$	"
3856.51	$^2F_4-^2G_5$	"	3440.68	Unclassified	2 comp., 3 : 2; heavier broadened
3833.87	$^2F_3-^2D_2$	"	3434.90	$^4F_5-^4G_6$	2 components, equal
3822.25	$^2F_3-^2\bar{F}_3$	"	3424.39	$^2F_3-^4D_3'$	2 components, 3 : 2
3806.77	$^4F_3-^4D_3$	"	3399.68	$^4F_2-^2\bar{F}_4$	Single
3805.92	$^2\bar{D}_3'-^2D_3^3$	"	3396.82	$^4F_5-^4\bar{F}_5$	2 components, equal
3799.32	$^2F_4-^2\bar{F}_4$	2 components, 20 : 1	3385.78	$^2D_3'-^2\bar{F}_4^2$	Single
3793.22	$^2F_4-^2D_3$	Single	3380.64	$^4F_4-^4G_4$	2 components, 10 : 2, dim.
3788.58	$^2\bar{D}_2-^2D_3$	"	3372.24	$^4F_3-^4G_3$	Single
3778.13	$^2\bar{D}_3'-34_3$	"	3369.68	$^2P_2-34_2$	"
3769.98	$^2\bar{D}_2'-40_2$	"	3368.38	$^4F_3-^4\bar{F}_2$	"
3765.08	$^2F_4-^4G_3$	"	3360.81	$^2\bar{D}_2-^4\bar{P}_2$	"
3748.23	$^4P_2-^4D_3^1$	"	3359.90	$^2P_1-44\frac{1}{2}_1$	"
3713.01	$^4F_2-^4D_2$	2 components, 3 : 1	3344.20	$^4P_1-40_2$	"
3700.90	$^4F_2-^4G_3$	Single	3342.90	$^4P_2-30_3$	"
3698.61	$^2\bar{G}_5-(^2\bar{F}_4^2)$	2 components, 3 : 1	3338.53	$^4F_4-^4\bar{F}_3$	"
3692.36	$^4F_5-^4D_4$	2 components, equal	3323.09	$^4F_4-^2G_5$	"
3690.72	$^2\bar{D}_3-^4D_2$	Single	3300.46	$^4P_2-38_2$	"
3681.06	$^2P_2-30_3$	"	3294.26	$^4D_2-\eta_3$	"
3658.00	$^4F_4-^4D_3$	"	3289.13	$^4F_2-^2D_2$	"
3626.61	$^4P_3-^4D_4'$	"	3286.38	$^2F_3-^2\bar{P}_2$	"
3612.47	$^4F_2-^4D_1$	"	3283.57	$^4F_3-^2G_4$	"
3597.15	$^2\bar{D}_3-^4G_4$	"	3280.54	$^4F_4-^2\bar{F}_4$	2 components, 4 : 3
3596.19	$^4F_3-^4D_2$	"	3271.61	$^2\bar{D}_3-^2D_2$	Single
3583.09	$^4P_2-^2\bar{P}_2$	"	3263.14	$^2\bar{D}_3-^2\bar{F}_3$	"
3549.53	$^2\bar{D}_3-^4\bar{F}_3$	"	3254.96	$^4\bar{F}_4-^4G_3$	"
3543.97	$^2\bar{D}_2-^2D_2$	"	3214.31	$^4F_4-^4G_4$	2 components, 5 : 4
3570.18	$^4F_2-^4\bar{F}_3$	3 components, 2 of them barely resolved	3211.37	$^4P_2-40\frac{1}{2}$	2 components, 1 : 4
3538.26	$^4F_4'-42\frac{1}{2}$	Single	3197.13	$^4F_3-^2D_2$	Single
3538.12	$^2F_4-^2\bar{F}_3$	"	3193.83	$^4G_2-\nu$	2 components, 3 : 2
3528.03	$^4F_4-^4\bar{F}_4$	"	3194.54	$^2F_4-^4D_3^1$	Single
3507.32	$^4F_3-^4G_4$	"	3191.31	$^2\bar{D}_2-^4D_2^1$	"
3502.54	$^4F_5-^4G_5$	2 components, equal	3189.16	$^4F_3-^2F_3$	"

λλ3600.74 and 3195.62, each of which was observed to be a doublet, are transitions between levels which are proven to be single by the presence of single lines ending on them. The line λ3173.07, which also appears doubled, is a transition not involving an *s* electron. It is impossible in this case, to be certain the doublet is true h.f.s. because no other transitions to the levels involved were photographed. We conclude the structure is not genuine in any case, but due to some impurity in the source.

In addition to the lines in the first spark spectrum, a pair in the second spark spectrum were barely visible on the plates. No complexity was observed.

Rhodium

Like yttrium, rhodium is an element of odd charge and mass number; it consists of the single isotope, number 103, except for a spectroscopically negligible concentration of rhodium 101. Its visible spectrum was observed by Schuler[2] who failed to find hyperfine structure. The ultraviolet region has been recently investigated by L. Sibaiya[4] who reports a spin of $\frac{1}{2}$ on the basis of h.f.s. doublets, of separation equal to 0.058 cm^{-1} in the two resonance lines λλ3434.90, and 3692.36. He rules out the possibility of absorption in the source as the origin of the structure on the basis of the following argument: The copper resonance lines appear unreversed under identical conditions of excitation; copper has a lower melting and boiling point than has rhodium.

Our investigation, first undertaken with the uncooled Schuler lamp in the ultraviolet region of the spectrum, revealed no significant structure in the lines listed in Table II. Doublet structure in the four resonance lines was proven to originate in absorption in the source. The resonance lines referred to are those ending on the level $^4F_5$, namely λλ3692.36, 3502.54, 3434.90, and 3396.82. The apparent complexity in the other lines cannot be considered evidence of true h.f.s., for the same reason as applied to the apparent structure in the yttrium spectrum.

In order to verify Sibaiya's results, if possible, we set up a Schuler tube with an aluminum water-cooled cathode, and photographed the spectrum again. No significant structure appeared; in particular, the lines reported as complex by Sibaiya, which we had previously found reversed, showed, in this case, a single component only.

Half-breadths for λλ3434.90 and 3692.36 were measured on two plates, the first plate taken with a current of 0.15 ampere and the second with 0.6 ampere through the source. The results appear in Table III. It can be seen that when the current was small, the half-breadths were just a little larger than the doublet separation reported by Sibaiya. Under these circumstances one would expect the two components, if they exist, to be more or less completely resolved. As a matter of fact, one should apparently expect such doublets to show up even on the plates taken with the larger current; for although in that case the half-breadths are large, they appear no larger than the half-breadth of the unresolved pattern whose microphotometer trace Sibaiya shows in his article.

We conclude that the rhodium arc spectrum has no hyperfine structure. We judge Sibaiya's results to have been the result of reversal due to absorption.

TABLE III. *Half-breadths in cm^{-1} of rhodium resonance lines photographed by use of water-cooled source.*

Current through Source	λ3434.90	λ3692.36
0.15 ampere	0.089 cm^{-1}	0.062 cm^{-1}
0.60 "	0.16 "	0.12 "

[4] L. Sibaiya, Proc. Ind. Acad. Sci. **6A**, 229 (1937).

Palladium

The element palladium is composed of six isotopes: 102, 104, 105, 106, 108, 110. Its spectrum has been investigated in the ultraviolet by L. Sibaiya,[5] who found no significant hyperfine structure.

The lines photographed and reported by us lie in the region λλ2700–4000, so that the anomalous term observed by Shenstone[6] was not involved in any transition. All the lines reported in Table IV are due to transitions of an *s* electron; no hyperfine structure was found. The slight broadening of the three lines which end on the resonance level, $^3D_3$, as well as of the line λ3718.91, is not considered by us to be of significance.

In the course of the research, we found that

[5] L. Sibaiya, Proc. Ind. Acad. Sci. **2A**, 313 (1935).
[6] Shenstone, Phys. Rev. **36**, 669 (1930).

TABLE IV. *Lines reported in the palladium I spectrum.*

WAVE-LENGTH	TRANSITION	STRUCTURE	WAVE-LENGTH	TRANSITION	STRUCTURE
3894.18	$5s^1D_2-5p^3D_3^0$	Single	3433.44	$5s^1D_2-5p^1P_1^0$	Single
3799.16	$5s^3D_2-5p^3P_2^0$	"	3421.24	$5s^3D_3-5p^3D_2^0$	"
3718.91	$5s^3D_1-5p^3P_2^0$	Broadened	3404.60	$5s^3D_3-5p^3F_4^0$	Broadened
3690.34	$5s^1D_2-5p^3F_3^0$	Single	3373.02	$5s^3D_3-5p^3D_3^0$	Single
3634.70	$5s^3D_3-5p^3P_2^0$	Broadened	3302.15	$5s^3D_1-5p^3D_1^0$	"
3609.56 –	$5s^3D_2-5p^3F_3^0$	Single	3287.26	$5s^3D_3-5p^3D_2^0$	"
3571.16	$5s^3D_1-5p^3P_0^0$	"	3258.78	$5s^3D_1-5p^1D_2^0$	"
3553.10	$5s^1D_2-5p^1F_3^0$	"	3251.64	$5s^3D_1-5p^1P_1^0$	"
3516.95	$5s^3D_2-5p^3P_1^0$	"	3242.71	$5s^3D_3-5p^3D_3^0$	Broadened
3489.79	$5s^1D_2-5p^3D_3^0$	"	3114.05	$5s^3D_2-5p^1F_3^0$	Single
3481.17	$5s^3D_1-5p^3F_2^0$	"	3065.31	$5s^3D_2-5p^3D_1^0$	"
3460.76	$5s^3D_3-5p^3F_3^0$	"	3027.92	$5s^3D_3-5p^1D_2^0$	"
3441.40	$5s^1D_2-5p^1D_2^0$	"	2763.08	$a^1S_0-5p^3P_1^0$	"

the iron lines were excited when the current was large. One might expect that such lines would be sharper when excited in the Schuler tube than when excited in the ordinary arc. We photographed and examined about 190 of them, but found no structure. The half-breadth of two of the stronger unreversed lines was about 0.11 cm^{-1}, which, if the broadening is due to the Doppler effect, would correspond to a temperature of about 1200°C.

This research was financed in part by a grant from the National Research Council.

SEPTEMBER 1, 1938 PHYSICAL REVIEW VOLUME 54

Ultraviolet Band Spectra of HgCl, CdCl, and ZnCl*

S. D. CORNELL
Sloane Physics Laboratory, Yale University, New Haven, Connecticut

(Received June 29, 1938)

The spectra of the chlorides of mercury, cadmium, and zinc, excited in a high frequency discharge, are examined at high dispersion in the region 3200–2000A. Vibrational analyses of several systems are presented. Included is a discussion of the electronic configurations involved in the systems analyzed.

INTRODUCTION

THE most extensive spectroscopic work on the halides of mercury, cadmium, and zinc appears to be that of Wieland[1, 2] in which he explored the wave-length region between 7000A and 2200A. This work was done in emission, a Geissler tube discharge serving as source, and at a relatively low dispersion, 10A per millimeter at best. A number of band systems were found; those of interest to the present discussion are as follows: for mercury chloride, a system between 2650A and 2400A, degraded to the violet, ascribed to HgCl, and a system from 2900A to 2700A, likewise degraded to the violet, but ascribed to $HgCl_2$; for cadmium chloride, nothing in the region of the present investigation; for zinc chloride, a system between 3100A and 2900A, degraded to the violet, and tentatively ascribed to ZnCl, although the author expresses some doubt concerning its true origin.

Of these systems, only the shorter wave-length one of HgCl appears well developed and for this system Wieland presents an extensive vibrational analysis. Detailed analyses are made for none of the other systems, although in a later paper[3] Wieland mentions the "poorly established" fundamental frequency of 290 cm^{-1} for the 2900A–2700A system.

Walter and Barratt,[4] working in absorption, at very low dispersion, list ten heads between 3000A

* Part of a dissertation presented to the faculty of the Graduate School of Yale University in candidacy for the degree of Doctor of Philosophy.

[1] K. Wieland, Helv. Phys. Acta **2**, 46 (1929).

[2] K. Wieland, Helv. Phys. Acta **2**, 77 (1929).

[3] K. Wieland, Zeits. f. Physik **77**, 157 (1932).

[4] J. M. Walter and S. Barratt, Proc. Roy. Soc. **122**, 201 (1929).

and 2900A which they attribute to "Zn+Cl." Nothing further is done with this system, but it is probably part of the system observed by Wieland in this region. In addition, a system between 3180A and 3018A ascribed to a chloride of cadmium is mentioned, but no further work was done on it.

More recently, Oeser[5] has reported this same 3180A to 3018A system as due to $CdCl_2$, and has mentioned the absence of absorption and fluorescence spectra of $ZnCl_2$ in both visible and ultraviolet regions.

In the present work the spectra of the chlorides of mercury, cadmium, and zinc have been investigated in the ultraviolet between about 3200A and 2000A. We have the advantages of very high dispersion.

Experimental

The spectra were excited by means of a high frequency power oscillator, of the tuned grid, tuned plate type described by Sloan, Thornton, and Jenkins.[6] The discharge tube was of vitreous silica, 12 inches in length and of $\frac{1}{2}$ inch bore, with external electrodes. Tapers were ground on the ends of the tube, one to receive the pump line, the other to recive a 5-inch glass tube of $1\frac{1}{4}$ inch diameter, narrowed at one end to fit the discharge tube, and ground flat at the other end to carry a quartz window. The tapered joints between discharge tube and glass fittings were waxed and water cooled.

In each case, the bichloride of maximum obtainable commercial purity was used. A small quantity of it was dried out in an evaporating dish and introduced into the discharge tube, which was then pumped out. It was found that in general favorable discharge conditions could be maintained by keeping a Meker burner constantly playing on the tube, and pumping on the system continuously with a Hyvac pump.

The aluminized 30,000 lines per inch 21-foot grating in an Eagle mounting was used, which gave a dispersion of 1.27A per millimeter in the first order. Exposure times were of the order of two hours, and during this time replenishment of the material in the discharge tube was in general necessary only once. Iron and copper arc lines were used for comparison purposes. Eastman type II-O plates were used throughout, sensitized with the usual ultraviolet sensitizer for wavelengths shorter than 2350A.

One exposure was made with zinc metal alone; for this purpose small strips of zinc were placed along the discharge tube, and the above technique then employed. Several exposures were made with the normal incidence 10-foot vacuum spectrograph on mercury chloride in the vacuum region. For these exposures, a metal cap with a hole carrying a small fluorite window was waxed over the slit-tube of the spectrograph, and the glass fitting of one end of the discharge tube was in turn waxed onto this metal cap. Ilford *Q*-plates were used in this region, and again exposures of roughly two hours were made.

For mercury chloride, the two systems reported by Wieland[1] were photographed at the present high dispersion, and remeasured. Wieland did little with the 2900–2700A system, which will be discussed below. A single brief CdCl system was found between 2240A and 2185A. For ZnCl a fragmentary system was photographed, at 2980–2905A. This evidently corresponds to the observations of Walter and Barratt.[4] Another emission region between 2095A and 2075A was observed.

Impurity spectra, in particular those of OH and N_2, were present on most of the plates. These came about as a result of the often troublesome property of a high frequency discharge which causes excitation of the spectra of vapors present at very low pressures. These impurities, however, in general caused little trouble, and extended efforts to eliminate them were not made. In the case of the longer wavelength ZnCl system, the entire region is overlaid by the $\Delta v = -2$ sequence of the second positive system of N_2, but these impurity lines were easily compared with those on a plate showing N_2 alone, and eliminated.

HgCl

It was deemed of value to remeasure the 2650–2400A HgCl system, shown in Fig. 1(a), because of the greatly increased dispersion in the present work as compared with that of

[5] E. Oeser, Zeits. f. Physik **95**, 699 (1935).
[6] D. H. Sloan, R. L. Thornton, and F. A. Jenkins, Rev. Sci. Inst. **6**, 75 (1935).

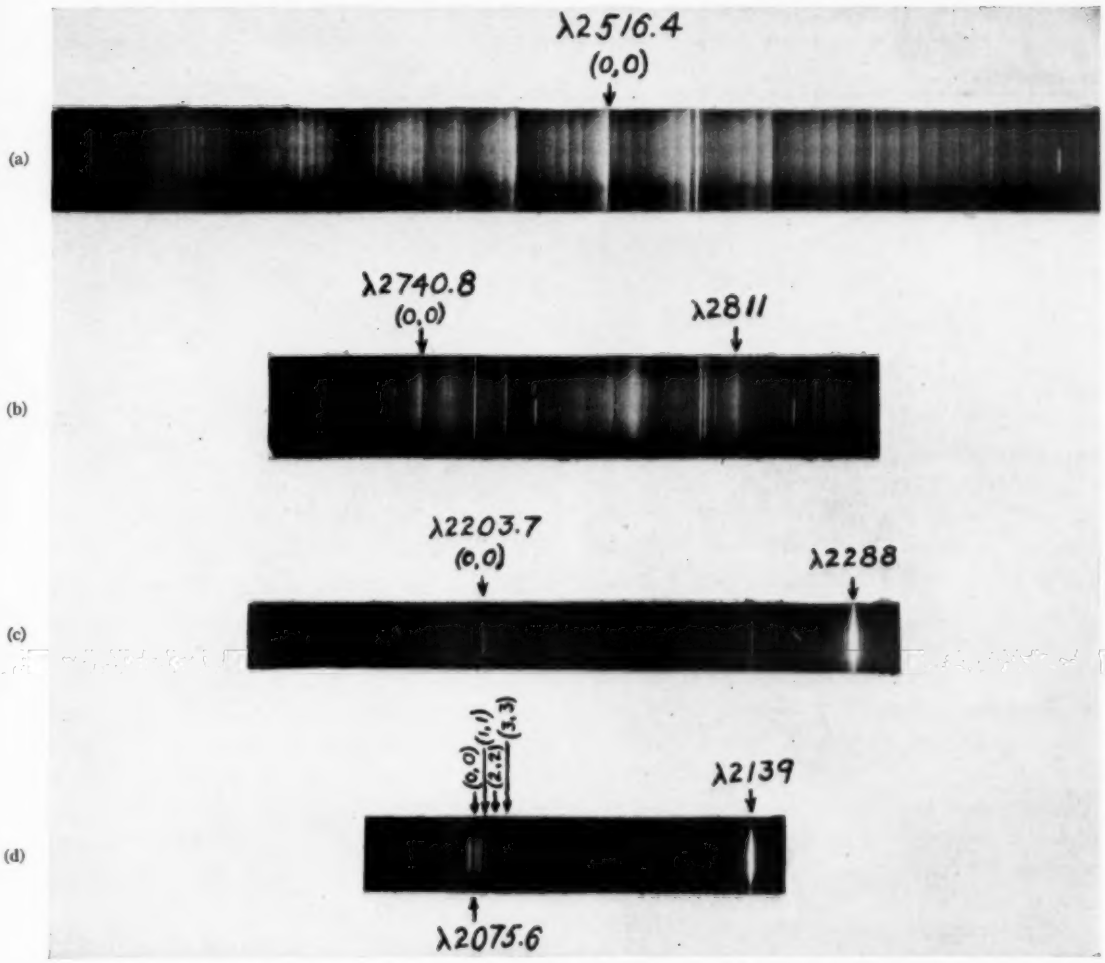

FIG. 1. (a) Mercury chloride system, 2650–2400A. (b) Mercury chloride system, 2900–2700A. The system starting at 2811A is due to OH. (c) Cadmium chloride system, 2240–2185A. The Cd resonance line is at 2288A. (d) Zinc chloride system, $\Delta v = 0$. The Zn resonance line is at 2139A.

Wieland.[1] The P and Q heads were easily resolvable throughout the system, which was not the case in Wieland's work, and hence far more accurate settings on the Q heads could be made than were before possible. The new vibrational constants calculated for the 2650–2400A HgCl system are as follows:

For $HgCl^{35}$

$$\omega_e'' = 293.4 \text{ cm}^{-1}, \quad x_e''\omega_e'' = 1.82 \text{ cm}^{-1},$$
$$\omega_e' = 341.8 \text{ cm}^{-1}, \quad x_e'\omega_e' = 1.87 \text{ cm}^{-1},$$
$$\nu_e = 39703.5 \text{ cm}^{-1}.$$

For $HgCl^{37}$

$$\omega_e'' = 283.9 \text{ cm}^{-1}, \quad x_e''\omega_e'' = 1.53 \text{ cm}^{-1},$$
$$\omega_e' = 333.4 \text{ cm}^{-1}, \quad x_e'\omega_e' = 1.60 \text{ cm}^{-1}.$$

The system is very well developed and entirely normal in appearance except for a striking intensity anomaly of some sort which causes the (1, 1) band to be missing, even on a heavily exposed plate. This anomaly is puzzling, for it cannot be attributed to a perturbation of either level involved, inasmuch as no similar anomaly is observed in the remainder of either the $v' = 1$ or the $v'' = 1$ progression. While the chlorine isotope effect is readily observable, and provides a valuable check on the vibrational analysis, the mercury isotope effect remains beyond the available resolving power, and manifests itself only in the broad and diffuse appearance of bands far from the system origin.

Figure 1(b) shows the 2900–2700A system,

TABLE I. *Mercury chloride system, 2900–2700A.*

v' \ v''	0	1	2	3	4	5	6	7	8
0	36475.3	36197.1	35920.2	35644.5					
1	36761.8	36482.7		35925.7	35653.5				
2		36767.2	36488.8			35663.7			
3			36772.2	36496.5			35674.7		
4				36780.3	36506.0			35687.0	
5					36789.0	36515.6			
6						36797.1	36524.6		
7							36804.8	36533.4	
8								36813.5	36542.5

attributed by Wieland to $HgCl_2$. That a system thus appearing in both a Geissler tube discharge and a high frequency discharge can be due to a triatomic molecule seems most improbable, in view of the highly disruptive nature of such spectroscopic sources. The system is therefore ascribed here to HgCl and discussed on this basis. An outstanding feature of the system is the presence of two well developed sequences, as can be clearly seen from the figure. These are apparently sequences of Q heads, and the weaker P heads are clearly visible, forming brief similar sequences. It is at first tempting to interpret these P heads as isotope heads, inasmuch as their spacing from the main Q heads is closely what one expects for the $HgCl^{35}-HgCl^{37}$ shift in successive sequences. However, on this basis, the calculated position of the system origin is near the extreme red limit of the system itself, and consequently the P head interpretation has been adopted. The longer wave-length of the two clearly distinguished sequences is the better developed, and is taken as the main diagonal of the vibrational array given in Table I. The vibrational constants are as follows:

$$\omega_e''=279.7\ \text{cm}^{-1},\quad x_e''\omega_e''=0.6\ \text{cm}^{-1},$$
$$\omega_e'=285.1\ \text{cm}^{-1},\quad x_e'\omega_e'=0.4\ \text{cm}^{-1},$$
$$\nu_e=36472.5\ \text{cm}^{-1}.$$

The Condon parabola is very narrow; its development is limited to a region very close to the main diagonal, as has been found in the case of other chloride systems which have the fundamental frequencies of the two states nearly equal. Furthermore, this near equality explains the broad, headless appearance of many of the bands, a characteristic which renders measurement difficult. Unfortunately, the entire long wave-length side of the system is very poorly developed; it would be of interest to photograph this in absorption if possible, to see what change in appearance is brought about. The fact that no chlorine isotope shift is observed is explained by the circumstance that the expected shift is in each case very nearly the same as the sequence spacing of the main bands, and because of the broad nature of these bands, resolution of the isotope bands is impossible. Beyond the short wave-length limit of each of the two principal sequences there are evidences of further bands showing similar spacings, which do not appear to belong to this system. A possible interpretation of these as part of a fragmentary system spaced about 80 cm^{-1} from the main system will be given below.

CdCl

Figure 1(c) shows the brief system between 2240 and 2185A, attributed to CdCl. The heads are sharply defined, but the unresolved rotational structure causes slight shading toward longer wave-length. Table II gives the vibrational array which appears best to fit the observed heads. Vibrational constants from this array are:

$$\omega_e''=330.5\ \text{cm}^{-1},\quad x_e''\omega_e''=1.2\ \text{cm}^{-1},$$
$$\Delta G'(\tfrac{1}{2})=247.9\ \text{cm}^{-1}.$$

Unfortunately no calculation of ω_e' or $x_e'\omega_e'$ is possible since no bands are observed involving v' greater than 1. This is in all probability ac-

TABLE II. *Cadmium chloride system, 2240–2185A.*

v' \ v''	0	1	2	3
0	45363.4	45033.9	44708.0	
1	45609.9	45282.9	44956.3	44632.8

counted for by predissociation occurring in the upper state for vibrational levels of higher quantum numbers.

The chlorine isotope effect is observed in the case of the (0,1) and (1,2) bands; the separations of -7.6 cm^{-1} and -8.9 cm^{-1} respectively agree satisfactorily with the expected splittings of -7.0 cm^{-1} and -8.5 cm^{-1}. In the (1,0) band the isotope head is weak and lost in the impurity lines in this region; the isotope heads for the (0,2) and (1,3) bands are too weak to measure accurately, but can be observed in the expected positions.

ZnCl

The system between 2980 and 2905A is apparently that observed at low dispersion by Walter and Barratt.[4] It consists of fairly strong heads appearing in groups, probably Q heads, with the heads of each group decreasing in intensity toward longer wave-length. A reproduction of the spectrogram is of little value because of the overlying $\Delta v=-2$ sequence of the second positive system of N_2. Two very strong groups of heads are in all probability the $\Delta v=0$ sequences of the two components of an electronic doublet, the doublet splitting being 383.5 cm^{-1}. Table III gives the two vibrational arrays for the doublet components. The vibrational constants are: For the shorter wave-length component,

$$\omega_e''=391.0\text{ cm}^{-1},\quad x_e''\omega_e''=1.8\text{ cm}^{-1},$$
$$\omega_e'=381.8\text{ cm}^{-1},\quad x_e'\omega_e'=1.0\text{ cm}^{-1},$$
$$\nu_e=33978.1\text{ cm}^{-1}.$$

For the longer wave-length component,

$$\omega_e''=390.0\text{ cm}^{-1},\quad x_e''\omega_e''=1.3\text{ cm}^{-1},$$
$$\omega_e'=384.0\text{ cm}^{-1},\quad x_e'\omega_e'=1.1\text{ cm}^{-1},$$
$$\nu_e=33593.2.$$

The chlorine isotope shift should again be observable, and several heads are observed in positions close to those calculated for $ZnCl^{37}$. Confusion of heads, however, is greatly increased by the happenstance of the near equality of the doublet splitting and the vibrational frequencies, and it appears impracticable to attempt to distinguish isotope heads from main heads and from N_2 lines.

Figure 1(d) shows the brief and unorthodox appearing ZnCl system which extends to longer wave-lengths from 2074.4A. The most satisfactory interpretation of this seems to be as a $\Delta v=0$ sequence; the flanking sequences are apparently too weak to observe on any of the plates obtained. In Figure 1(d) the arrows indicate the band origins measured. The first one, at 2075.6A, is shown by a null line gap, as are the second and third. Clearly, the R head is becoming progressively closer and closer to the origin, and the fourth band position is measured by setting on the head itself. Wave numbers of these four bands are as follows:

$$(0,0)\rightarrow 48163.0\text{ cm}^{-1},\quad (1,1)\rightarrow 48111.0\text{ cm}^{-1},$$
$$(2,2)\rightarrow 48052.1\text{ cm}^{-1},\quad (3,3)\rightarrow 47986.8\text{ cm}^{-1}.$$

The P branches in each case are cut off rather abruptly on the long wave-length side. This doubtless indicates a predissociation limit at a certain rotational energy.

Discussion

Because of the proximity of the origin of the shorter wave-length HgCl system to the 2537A intersystem combination line of Hg, the transitions involved in the two cases must in all probability bear a close relationship to one another. It can be inferred, then, that the lower state of the HgCl system is formed from a ^1S ground state Hg atom plus a $^2P_{3/2}$ ground state Cl atom, and is probably a $^2\Sigma$ state, the ground state of the HgCl molecule. The upper state involved is undoubtedly formed from a $^3P_1$ excited Hg atom plus a ^2P ground state Cl atom, and is a $^2\Pi$ upper state (accounting for the occurrence of Q branches) if the electronic coupling is of the case a type. It appears entirely possible that the upper state may represent a

Table III. *Zinc chloride electronic doublet system, 2980–2905A.*

v' \ v''	0	1	2
0	33973.7	33586.9	
1	34354.3	33966.1	33581.3
2		34343.3	33960.1
0	33590.2		
1	33971.9	33584.2	
2	34350.7	33963.7	33579.2
3		34341.1	33955.9

TABLE I. *Mercury chloride system, 2900–2700A.*

v' \ v''	0	1	2	3	4	5	6	7	8
0	36475.3	36197.1	35920.2	35644.5					
1	36761.8	36482.7		35925.7	35653.5				
2		36767.2	36488.8			35663.7			
3			36772.2	36496.5			35674.7		
4				36780.3	36506.0			35687.0	
5					36789.0	36515.6			
6						36797.1	36524.6		
7							36804.8	36533.4	
8								36813.5	36542.5

attributed by Wieland to $HgCl_2$. That a system thus appearing in both a Geissler tube discharge and a high frequency discharge can be due to a triatomic molecule seems most improbable, in view of the highly disruptive nature of such spectroscopic sources. The system is therefore ascribed here to HgCl and discussed on this basis. An outstanding feature of the system is the presence of two well developed sequences, as can be clearly seen from the figure. These are apparently sequences of Q heads, and the weaker P heads are clearly visible, forming brief similar sequences. It is at first tempting to interpret these P heads as isotope heads, inasmuch as their spacing from the main Q heads is closely what one expects for the $HgCl^{35}-HgCl^{37}$ shift in successive sequences. However, on this basis, the calculated position of the system origin is near the extreme red limit of the system itself, and consequently the P head interpretation has been adopted. The longer wave-length of the two clearly distinguished sequences is the better developed, and is taken as the main diagonal of the vibrational array given in Table I. The vibrational constants are as follows:

$$\omega_e''=279.7\ \text{cm}^{-1},\quad x_e''\omega_e''=0.6\ \text{cm}^{-1},$$
$$\omega_e'=285.1\ \text{cm}^{-1},\quad x_e'\omega_e'=0.4\ \text{cm}^{-1},$$
$$\nu_e=36472.5\ \text{cm}^{-1}.$$

The Condon parabola is very narrow; its development is limited to a region very close to the main diagonal, as has been found in the case of other chloride systems which have the fundamental frequencies of the two states nearly equal. Furthermore, this near equality explains the broad, headless appearance of many of the bands, a characteristic which renders measurement difficult. Unfortunately, the entire long wave-length side of the system is very poorly developed; it would be of interest to photograph this in absorption if possible, to see what change in appearance is brought about. The fact that no chlorine isotope shift is observed is explained by the circumstance that the expected shift is in each case very nearly the same as the sequence spacing of the main bands, and because of the broad nature of these bands, resolution of the isotope bands is impossible. Beyond the short wave-length limit of each of the two principal sequences there are evidences of further bands showing similar spacings, which do not appear to belong to this system. A possible interpretation of these as part of a fragmentary system spaced about 80 cm^{-1} from the main system will be given below.

CdCl

Figure 1(c) shows the brief system between 2240 and 2185A, attributed to CdCl. The heads are sharply defined, but the unresolved rotational structure causes slight shading toward longer wave-length. Table II gives the vibrational array which appears best to fit the observed heads. Vibrational constants from this array are:

$$\omega_e''=330.5\ \text{cm}^{-1},\quad x_e''\omega_e''=1.2\ \text{cm}^{-1},$$
$$\Delta G'(\tfrac{1}{2})=247.9\ \text{cm}^{-1}.$$

Unfortunately no calculation of ω_e' or $x_e'\omega_e'$ is possible since no bands are observed involving v' greater than 1. This is in all probability ac-

TABLE II. *Cadmium chloride system, 2240–2185A.*

v' \ v''	0	1	2	3
0	45363.4	45033.9	44708.0	
1	45609.9	45282.9	44956.3	44632.8

counted for by predissociation occurring in the upper state for vibrational levels of higher quantum numbers.

The chlorine isotope effect is observed in the case of the (0,1) and (1,2) bands; the separations of -7.6 cm^{-1} and -8.9 cm^{-1} respectively agree satisfactorily with the expected splittings of -7.0 cm^{-1} and -8.5 cm^{-1}. In the (1,0) band the isotope head is weak and lost in the impurity lines in this region; the isotope heads for the (0,2) and (1,3) bands are too weak to measure accurately, but can be observed in the expected positions.

ZnCl

The system between 2980 and 2905A is apparently that observed at low dispersion by Walter and Barratt.[4] It consists of fairly strong heads appearing in groups, probably Q heads, with the heads of each group decreasing in intensity toward longer wave-length. A reproduction of the spectrogram is of little value because of the overlying $\Delta v=-2$ sequence of the second positive system of N_2. Two very strong groups of heads are in all probability the $\Delta v=0$ sequences of the two components of an electronic doublet, the doublet splitting being 383.5 cm^{-1}. Table III gives the two vibrational arrays for the doublet components. The vibrational constants are: For the shorter wave-length component,

$$\omega_e''=391.0 \text{ cm}^{-1}, \quad x_e''\omega_e''=1.8 \text{ cm}^{-1},$$
$$\omega_e'=381.8 \text{ cm}^{-1}, \quad x_e'\omega_e'=1.0 \text{ cm}^{-1},$$
$$\nu_e=33978.1 \text{ cm}^{-1}.$$

For the longer wave-length component,

$$\omega_e''=390.0 \text{ cm}^{-1}, \quad x_e''\omega_e''=1.3 \text{ cm}^{-1},$$
$$\omega_e'=384.0 \text{ cm}^{-1}, \quad x_e'\omega_e'=1.1 \text{ cm}^{-1},$$
$$\nu_e=33593.2.$$

The chlorine isotope shift should again be observable, and several heads are observed in positions close to those calculated for $ZnCl^{37}$. Confusion of heads, however, is greatly increased by the happenstance of the near equality of the doublet splitting and the vibrational frequencies, and it appears impracticable to attempt to distinguish isotope heads from main heads and from N_2 lines.

Figure 1(d) shows the brief and unorthodox appearing ZnCl system which extends to longer wave-lengths from 2074.4A. The most satisfactory interpretation of this seems to be as a $\Delta v=0$ sequence; the flanking sequences are apparently too weak to observe on any of the plates obtained. In Figure 1(d) the arrows indicate the band origins measured. The first one, at 2075.6A, is shown by a null line gap, as are the second and third. Clearly, the R head is becoming progressively closer and closer to the origin, and the fourth band position is measured by setting on the head itself. Wave numbers of these four bands are as follows:

(0,0)→48163.0 cm^{-1}, (1,1)→48111.0 cm^{-1},
(2,2)→48052.1 cm^{-1}, (3,3)→47986.8 cm^{-1}.

The P branches in each case are cut off rather abruptly on the long wave-length side. This doubtless indicates a predissociation limit at a certain rotational energy.

Discussion

Because of the proximity of the origin of the shorter wave-length HgCl system to the 2537A intersystem combination line of Hg, the transitions involved in the two cases must in all probability bear a close relationship to one another. It can be inferred, then, that the lower state of the HgCl system is formed from a ^1S ground state Hg atom plus a $^2P_{3/2}$ ground state Cl atom, and is probably a $^2\Sigma$ state, the ground state of the HgCl molecule. The upper state involved is undoubtedly formed from a $^3P_1$ excited Hg atom plus a ^2P ground state Cl atom, and is a $^2\Pi$ upper state (accounting for the occurrence of Q branches) if the electronic coupling is of the case a type. It appears entirely possible that the upper state may represent a

Table III. *Zinc chloride electronic doublet system, 2980–2905A.*

v' \ v''	0	1	2
0	33973.7	33586.9	
1	34354.3	33966.1	33581.3
2		34343.3	33960.1
0	33590.2		
1	33971.9	33584.2	
2	34350.7	33963.7	33579.2
3		34341.1	33955.9

situation tending markedly toward case c, as has been discussed by Mulliken[7] for HgH, and by Howell[8] for TlF, and if so, then the upper state is to be designated by its Ω value alone, and accordingly is probably a $\frac{1}{2}$ or $\frac{3}{2}$ state. The other component of the expected electronic doublet is not present, in all likelihood because of predissociation.

The longer wave-length HgCl system cannot involve the same $^2\Sigma$ lower state as that mentioned above, because of the different ω_e'' observed. However, another $^2\Sigma$ state is to be expected from the ^1S Hg atom plus a $^2P_{1/2}$ Cl atom, and this is assumed to be the lower state of this system, inasmuch as configuration theory indicates that the Π states possible from $^1S+^2P$ combinations are in this case of little or no stability. The upper state is probably formed from a $^3P_0$ Hg atom plus a ^2P ground state Cl atom, and is again in case c notation, a $\frac{1}{2}$ or $\frac{3}{2}$ molecular level. The fragmentary system mentioned above, 80 cm^{-1} further toward shorter wave-lengths, may be assumed to involve the same $^2\Sigma$ ground state, and an upper $\frac{3}{2}$ state which is considerably less stable than the $\frac{1}{2}$ state which may be taken as the upper level of the main 2900–2700A system.

The CdCl system, showing no electronic doublet characteristics, probably represents a $^2\Sigma-^2\Sigma$ transition. Proximity of this system to the Cd resonance line at 2288A suggests that the lower $^2\Sigma$ arises from a ^1S ground state Cd atom plus a ^2P ground state Cl atom, while the upper state derives from a ^1P Cd atom plus a ^2P ground state Cl atom.

The ZnCl system, 2980–2905A, is fairly close to the 3076A $^3P_1-^1S$ combination line of Zn, and shows characteristics of an electronic doublet. It can, then, be assigned to a $^2\Pi-^2\Sigma$ transition; the $^2\Pi$ arising from a $^3P_1$ excited Zn atom plus a ^2P ground state Cl atom, and the $^2\Sigma$ coming from the $^1S+^2P$ combination exactly analogous to that observed in HgCl and CdCl.

The shorter wave-length sequence at 2075A is not far from the 2139A resonance line of Zn, and, because it shows only P and R branches, may therefore be considered to arise in the $^2\Sigma—^2\Sigma$ transition analogous to that observed in CdCl.

An attempt was made to find a HgCl system of shorter wave-length than the 1850A resonance line of Hg, similar to the systems found for CdCl and ZnCl, but exposures of several hours' duration failed to bring out any such system.

The author gratefully acknowledges the many suggestions and extensive assistance of Professor W. W. Watson, and likewise expresses his thanks to Professor F. A. Jenkins for interesting discussions of several of the points covered.

[7] R. S. Mulliken, Phys. Rev. **36**, 1440 (1930).
[8] H. G. Howell, Proc. Roy. Soc. **160**, 242 (1937).

New Terms in the Spectrum of Na III

D. H. TOMBOULIAN
Department of Physics, Cornell University, Ithaca, New York
(Received June 30, 1938)

The spectrum of doubly ionized sodium has been excited by an electrodeless discharge. Wave-length measurements have been made in the region from 500 to 2600A. On the basis of these determiniations it has been possible to establish 30 new levels arising from the $2s^22p^43p$, $2s^22p^43d$, and $2s^22p^44s$ configurations.

THE spectrum of Na III has been investigated by Edlén and Ericson,[1] Mack and Sawyer,[2] Vance,[3] and more recently by Söderqvist.[4] The identifications made by these authors are based primarily on data obtained in the extreme ultraviolet region. In the present paper the analysis of this spectrum has been extended to the classification of transitions involving radiations of somewhat longer wave-lengths.

Experimental Details

The spectrum was excited by an electrodeless discharge in sodium vapor and was photographed from 350 to 2600A by means of a 1.5 meter vacuum spectrograph. The dispersion of the instrument was 11.3A per mm. In the reduction of the plates, impurity lines were employed as standards. In the region from 500 to 1900A, the oxygen and carbon lines measured by Edlén[5] and the wave-lengths computed by Paschen[6] for hydrogen were used. From 1900 to 2600A the second orders of the above-mentioned lines were taken as standards. The error in the measurements is believed to be less than 0.05A (1.3 cm^{-1} at 2000A, to 5 cm^{-1} at 1000A).

Exposures made with a discharge at different vapor pressures served to distinguish between various stages of ionization. In all cases the lines belonging to the spectrum of Na II[7] were excited very strongly. The resonance lines in the spectrum of Na IV (a group around 410A) served as a convenient indicator in estimating the excitation of a particular exposure.

Term Values and Classifications

In his study[4] of the spectra of sodium in the extreme ultraviolet, Söderqvist has identified transitions into the $2s^22p^5\ ^2P^0$ levels of Na III from even levels arising from the $2s^22p^53s$ and $2s^22p^43d$ configurations. In addition he has reported several odd multiplets associated with the $2s^22p^43p$ configuration. This investigation, which was undertaken previous to the publication of Söderqvist's work, has yielded a number of additional terms arising from the $3p$, $3d$, and $4s$ configurations, and has offered confirmatory evidence for most of the previously assigned terms.

Table I gives the new terms of Na III as well as those reported by Söderqvist. For the sake of uniformity the author has adopted Söderqvist's scale of approximate absolute term values by choosing the $2s^22p^4(^3P)3s\ ^2P_{3/2}$ as a reference level. The term value of this level is assumed to be 204,400.0, cm^{-1} with respect to $^3P_2$ limit. On the basis of the present data a slight adjustment has been made in the values of some of the terms reported by Söderqvist.

The analysis offered here differs from that of Söderqvist in the following respects:

(1) The term values provisionally assigned by Söderqvist to the $2s^22p^4(^3P)3d\ ^4D$ levels are not in agreement with the classification presented here. Söderqvist's determination of these levels is based only on transitions to the ground levels. Because of the J selection rule only the $^4D_{1/2}$, $^4D_{3/2}$, and $^4D_{5/2}$ levels could be thus determined. He has listed the last two of these levels, only one of which involves two transitions. In the

[1] Edlén and Ericson, Comptes rendus **190**, 173 (1930).
[2] Mack and Sawyer, Phys. Rev. **35**, 299 (1930).
[3] Vance, Phys. Rev. **41**, 480 (1932).
[4] Söderqvist, Nova Acta Reg. Soc. Sci. Upsaliensis, ser. IV **9**, No. 7 (1934).
[5] Edlén, Zeits. f. Physik **85**, 85 (1933).
[6] Paschen, Ber. Preuss. Akad. d. Wiss. Phys. Math. Klasse **30**, 662 (1929).
[7] Frisch, Zeits. f. Physik **70**, 498 (1931).

TABLE I. *Term values* Na III.

Term Symbol	Term Value (cm^{-1})	Term Symbol	Term Value (cm^{-1})	Term Symbol	Term Value (cm^{-1})
$2s^2 2p^5\ ^2P^0_{3/2}$	578,033 *	$2s^2 2p^4(^1D)3p\ ^2F^0_{5/2}$	137,561.0	$2s^2 2p^4(^3P)3d\ ^4P_{5/2}$	114,775.6
" $^2P^0_{1/2}$	576,669 *	" $^2F^0_{7/2}$	137,480.6	" $^2F_{7/2}$	114,064.2
$2s\ 2p^6\ ^2S_{1/2}$	313,584 *	" $^2P^0_{3/2}$	135,322.5	" $^2F_{5/2}$	112,264.2
$2s^2 2p^4(^3P)3s\ ^4P_{5/2}$	211,867.7**	" $^2P^0_{1/2}$	134,771.4	" $^2D_{5/2}$	113,640.9(a)
" $^4P_{3/2}$	210,980.7**	" $^2D^0_{3/2}$	133,284.9	" $^2D_{3/2}$	113,005.1**
" $^4P_{1/2}$	210,471.1**	" $^2D^0_{5/2}$	133,208.0	" $^2P_{1/2}$	112,045.0**
" $^2P_{3/2}$	204,400.0**			" $^2P_{3/2}$	111,260.0**
" $^2P_{1/2}$	203,351.6**	$2s^2 2p^4(^3P)4s\ ^4P_{5/2}$	110,259.2	$2s^2 2p^4(^1D)3d\ ^2G_{7/2}$	86,104.8
$2s^2 2p^4(^1D)3s\ ^2D_{5/2}$	178,853.6**	" $^4P_{3/2}$	109,504.5		
" $^2D_{3/2}$	178,850.3**	" $^4P_{1/2}$	109,083.5	" $^2P_{1/2}$	84,841.7**
$2s^2 2p^4(^1S)3s\ ^2S_{1/2}$	143,002 *	" $^2P_{3/2}$	106,586.4	" $^2P_{3/2}$	84,743.7**
$2s^2 2p^4(^3P)3p\ ^4P^0_{5/2}$	171,832.1**	" $^2P_{1/2}$	105,782.4	" $^2D_{3/2}$	84,179.8**
" $^4P^0_{3/2}$	171,471.0**	$2s^2 2p^4(^1D)4s\ ^2D_{5/2}$	66,623 *	" $^2D_{5/2}$	83,434.0**
" $^4P^0_{1/2}$	171,157.0**			" $^2F_{7/2}$	82,586.2
" $^4D^0_{7/2}$	167,045.1**	$2s^2 2p^4(^3P)3d\ ^4D_{7/2}$	117,765.2	" $^2F_{5/2}$	82,364.4
" $^4D^0_{5/2}$	166,484.8**	" $^4D_{5/2}$	117,612.0	" $^2S_{1/2}$	80,281.8
" $^4D^0_{3/2}$	166,069.1**	" $^4D_{3/2}$	117,427.4	$2s^2 2p^4(^1S)3d\ ^2D_{3/2}$	48,568 *
" $^4D^0_{1/2}$	165,831.5**	" $^4D_{1/2}$	117,273.7	" $^2D_{3/2}$	48,535 *
" $^2D^0_{5/2}$	163,752.0**	" $^4F_{9/2}$	116,155.6?	$2s^2 2p^4(^3P)4d\ ^2D_{5/2}$	63,381 *
" $^2D^0_{3/2}$	162,859.8**	" $^4F_{7/2}$	114,920.2	" $^2P_{3/2}$	62,654 *
" $^2S^0_{1/2}$	161,122.8	" $^4F_{5/2}$	114,404.9	" $^2P_{1/2}$	63,010 *
" $^4S^0_{3/2}$	160,617.5**	" $^4F_{3/2}$	114,570.8	$2s^2 2p^4(^1D)4d\ ^2D_{5/2}$	33,297 *
" $^2P^0_{3/2}$	159,614.9	" $^4P_{1/2}$	115,641.8	" ^2P	33,806 *
" $^2P^0_{1/2}$	159,476.1	" $^4P_{3/2}$	115,069.4		

* Established by Söderqvist (reference 4).
** Established by Söderqvist (reference 4) and by the author independently.
(a) Söderqvist gives 113,651 for this term.

TABLE II. *Classified lines of* Na III.

Int.	λ (vac.)	ν cm^{-1}	Classification	Int.	λ (vac.)	ν cm^{-1}	Classification
25	*2564.09	39,000.2	$2s^2 2p^4(^2P)3s\ ^4P_{1/2} - 2s^2 2p^4(^2P)3p\ ^4P^0_{3/2}$	0	2181.32	45,843.8	$2s^2 2p^4(^3P)3p\ ^4S^0_{3/2} - 2s^2 2p^4(^3P)3d\ ^4P_{5/2}$
25	* 54.38	148.4	" $(^3P)3s\ ^4P_{3/2}$ — " $(^3P)3p\ ^4P^0_{5/2}$	3	75.12	974.5	" $(^3P)3p\ ^2P^0_{3/2}$ — " $(^3P)3d\ ^2D_{5/2}$
10	* 43.66	313.4	" $(^3P)3s\ ^4P_{1/2}$ — " $(^2P)3p\ ^4P^0_{1/2}$	1	74.53	986.9	" $(^3P)3p\ ^2D^0_{5/2}$ — " $(^3P)3d\ ^4D_{7/2}$
15	* 30.97	510.5	" $(^3P)3s\ ^4P_{3/2}$ — " $(^3P)3p\ ^4P^0_{3/2}$	0	71.32	46,054.9	" $(^3P)3p\ ^2S^0_{1/2}$ — " $(^3P)3d\ ^4P_{3/2}$
20	* 11.13	822.7	" $(^3P)3s\ ^4P_{3/2}$ — " $(^3P)3p\ ^4P^0_{1/2}$	3	67.35	139.3	" $(^3P)3p\ ^2D^0_{5/2}$ — " $(^3P)3d\ ^4D_{5/2}$
50	*2497.80	40,035.3	" $(^3P)3s\ ^4P_{5/2}$ — " $(^3P)3p\ ^4P^0_{5/2}$	1	64.00	210.7	" $(^3P)3p\ ^4S^0_{3/2}$ — " $(^3P)3d\ ^4F_{5/2}$
40	* 75.44	396.8	" $(^3P)3s\ ^4P_{5/2}$ — " $(^3P)3p\ ^4P^0_{3/2}$	1	48.06	553.6	" $(^3P)3p\ ^2S^0_{1/2}$ — " $(^3P)3d\ ^4F_{3/2}$
30	* 69.62	492.1	" $(^3P)3s\ ^4P_{1/2}$ — " $(^3P)3p\ ^2D^0_{3/2}$	0	17.76	47,219.7	" $(^3P)3p\ ^2D^0_{3/2}$ — " $(^3P)3d\ ^4P_{1/2}$
45	* 60.14	648.1	" $(^3P)3s\ ^2P_{3/2}$ — " $(^3P)3p\ ^2D^0_{5/2}$	8	17.38	228.2	" $(^3P)3s\ ^4P_{3/2}$ — " $(^3P)3p\ ^2D^0_{5/2}$
8	21.74	41,292.6	" $(^1D)3s\ ^2D_{5/2}$ — " $(^1D)3p\ ^2F^0_{5/2}$	d1	08.30	431.5	" $(^3P)3p\ ^2P^0_{1/2}$ — " $(^3P)3d\ ^2P_{1/2}$
18	* 07.32	539.9	" $(^3P)3s\ ^2P_{3/2}$ — " $(^3P)3p\ ^2D^0_{3/2}$	1	00.27	612.9	" $(^3P)3s\ ^4P_{1/2}$ — " $(^3P)3p\ ^2D^0_{3/2}$
4	2368.05	42,228.8	" $(^3P)3s\ ^2P_{1/2}$ — " $(^3P)3p\ ^2S^0_{1/2}$				" $(^3P)3p\ ^4S^0_{3/2}$ — " $(^3P)3d\ ^2D_{3/2}$
3	15.38	43,189.4	" $(^3P)3p\ ^4S^0_{3/2}$ — " $(^3P)3d\ ^4D_{3/2}$	0	2079.73	48,083.1	" $(^3P)3p\ ^2D^0_{3/2}$ — " $(^3P)3d\ ^4P_{5/2}$
30	10.68	277.3	" $(^3P)3s\ ^2P_{3/2}$ — " $(^3P)3p\ ^2S^0_{1/2}$	10	74.04	215.1	" $(^3P)3p\ ^2P^0_{1/2}$ — " $(^3P)3d\ ^2P_{3/2}$
25	2297.85	518.9	" $(^3P)3s\ ^2P_{1/2}$ — " $(^3P)3p\ ^4D^0_{1/2}$	18	68.07	354.2	" $(^3P)3p\ ^2P^0_{3/2}$ — " $(^3P)3d\ ^2P_{3/2}$
25	97.35	528.4	" $(^1D)3s\ ^2D_{3/2}$ — " $(^1D)3p\ ^2P^0_{3/2}$	10	65.89	405.2	" $(^3P)3p\ ^4D^0_{1/2}$ — " $(^3P)3d\ ^4D_{3/2}$
35	86.43	736.3	" $(^3P)3s\ ^2P_{1/2}$ — " $(^3P)3p\ ^2P^0_{3/2}$	8	63.63	458.3	" $(^3P)3p\ ^4D^0_{3/2}$ — " $(^3P)3d\ ^4D_{5/2}$
3	80.56	848.8	" $(^3P)3p\ ^2S^0_{1/2}$ — " $(^3P)3d\ ^4D_{1/2}$	8	59.38	558.3	" $(^3P)3p\ ^4D^0_{1/2}$ — " $(^3P)3d\ ^4D_{1/2}$
40	79.19	875.2	" $(^3P)3s\ ^2P_{1/2}$ — " $(^3P)3p\ ^2P^0_{1/2}$	10	55.83	642.1	" $(^3P)3p\ ^4D^0_{3/2}$ — " $(^3P)3d\ ^4D_{3/2}$
8	68.66	44,078.9	" $(^1D)3s\ ^2D_{3/2}$ — " $(^1D)3p\ ^2P^0_{1/2}$	8	52.56	719.6	" $(^3P)3p\ ^4D^0_{5/2}$ — " $(^3P)3d\ ^4D_{1/2}$
45	* 52.14	402.2	" $(^3P)3s\ ^4P_{1/2}$ — " $(^3P)3p\ ^4D^0_{1/2}$	8	49.34	796.2	" $(^3P)3p\ ^4D^0_{3/2}$ — " $(^3P)3d\ ^4D_{1/2}$
20	51.87	407.5	" $(^2P)3p\ ^2P^0_{1/2}$ — " $(^2P)3d\ ^4P_{3/2}$	18	46.08	873.9	" $(^3P)3p\ ^4D^0_{5/2}$ — " $(^3P)3d\ ^4D_{3/2}$
40	47.37	496.4	" $(^3P)3s\ ^4P_{3/2}$ — " $(^3P)3p\ ^4D^0_{5/2}$	0	41.75	977.6	" $(^3P)3p\ ^2D^0_{5/2}$ — " $(^3P)3d\ ^4P_{5/2}$
3	44.88	545.8	" $(^3P)3p\ ^2P^0_{3/2}$ — " $(^3P)3d\ ^4P_{3/2}$	10	38.36	49,059.0	" $(^3P)3p\ ^4D^0_{5/2}$ — " $(^3P)3d\ ^4D_{3/2}$
45	* 40.14	640.1	" $(^3P)3s\ ^4P_{1/2}$ — " $(^3P)3p\ ^4D^0_{1/2}$	3	36.50	103.8	" $(^1D)3p\ ^2D^0_{3/2}$ — " $(^1D)3d\ ^2D_{3/2}$
40	32.87	785.4	" $(^3P)3s\ ^2P_{3/2}$ — " $(^3P)3p\ ^2P^0_{3/2}$	0	33.31	180.9	" $(^3P)3p\ ^2D^0_{3/2}$ — " $(^3P)3d\ ^4F_{3/2}$
d50	* 31.00	822.9	" $(^3P)3s\ ^4P_{5/2}$ — " $(^3P)3p\ ^4D^0_{7/2}$	10	31.76	218.4	" $(^3P)3p\ ^2D^0_{3/2}$ — " $(^3P)3d\ ^2D_{3/2}$
15	30.26	837.8	" $(^3P)3p\ ^2P^0_{3/2}$ — " $(^3P)3d\ ^4P_{5/2}$	25	29.21	280.3	" $(^3P)3p\ ^4D^0_{7/2}$ — " $(^3P)3d\ ^4D_{7/2}$
8	26.89	905.6	" $(^3P)3p\ ^2P^0_{1/2}$ — " $(^3P)3d\ ^4F_{3/2}$	8	26.10	355.9	" $(^3P)3p\ ^4S^0_{3/2}$ — " $(^3P)3d\ ^2P_{3/2}$
45	* 26.60	911.5	" $(^3P)3s\ ^4P_{3/2}$ — " $(^3P)3p\ ^4D^0_{3/2}$	10	22.93	433.2	" $(^3P)3p\ ^2P^0_{3/2}$ — " $(^3P)4s\ ^4P_{5/2}$
12	25.99	923.8	" $(^3P)3s\ ^2P_{3/2}$ — " $(^3P)3p\ ^2P^0_{1/2}$				" $(^3P)3p\ ^4D^0_{7/2}$ — " $(^3P)3d\ ^4D_{5/2}$
0	23.49	974.3	" $(^3P)3p\ ^4S^0_{3/2}$ — " $(^3P)3d\ ^4P_{1/2}$	30	12.53	688.7	" $(^3P)3p\ ^2D^0_{5/2}$ — " $(^3P)3d\ ^2F_{7/2}$
25	14.87	45,149.4	" $(^3P)3s\ ^4P_{3/2}$ — " $(^3P)3p\ ^4D^0_{1/2}$	8	09.08	774.0	" $(^1D)3p\ ^2D^0_{5/2}$ — " $(^1D)3d\ ^2D_{5/2}$
1	11.86	210.8	" $(^3P)3p\ ^2P^0_{3/2}$ — " $(^3P)3d\ ^4F_{5/2}$	6	05.98	850.9	" $(^1D)3p\ ^2D^0_{3/2}$ — " $(^1D)3d\ ^2D_{3/2}$
40	* 03.48	382.7	" $(^3P)3s\ ^4P_{5/2}$ — " $(^3P)3p\ ^4D^0_{5/2}$	30	05.89	853.2	" $(^3P)3s\ ^4P_{1/2}$ — " $(^2P)3p\ ^4S^0_{3/2}$
2	01.06	432.6	" $(^3P)3p\ ^2D^0_{3/2}$ — " $(^3P)3d\ ^4D_{3/2}$				" $(^3P)3p\ ^2D^0_{3/2}$ — " $(^3P)3d\ ^2D_{3/2}$
2	2198.70	481.4	" $(^3P)3p\ ^2S^0_{1/2}$ — " $(^3P)3d\ ^4P_{1/2}$	0	05.45	864.1	" $(^3P)3p\ ^2S^0_{1/2}$ — " $(^3P)3d\ ^2P_{3/2}$
1	95.54	546.8	" $(^3P)3p\ ^4S^0_{3/2}$ — " $(^3P)3d\ ^4P_{3/2}$	3	1995.62	50,109.7	" $(^3P)3p\ ^2D^0_{5/2}$ — " $(^3P)3d\ ^2D_{5/2}$
1	93.77	583.7	" $(^3P)3p\ ^2D^0_{3/2}$ — " $(^3P)3d\ ^4D_{1/2}$				" $(^2P)3p\ ^2P^0_{3/2}$ — " $(^3P)4s\ ^4P_{3/2}$
d5	90.87	643.9	" $(^1D)3s\ ^2D_{3/2}$ — " $(^1D)3p\ ^2D^0_{5/2}$	30	* 85.58	363.1	" $(^3P)3s\ ^4P_{3/2}$ — " $(^3P)3p\ ^4S^0_{3/2}$
15	83.43	799.5	" $(^3P)3s\ ^4P_{5/2}$ — " $(^3P)3p\ ^4D^0_{3/2}$	0	80.95	480.8	" $(^1D)3p\ ^2P^0_{3/2}$ — " $(^1D)3d\ ^2P_{1/2}$

TABLE II.—*Continued.*

INT.	λ (VAC.)	ν CM^{-1}	CLASSIFICATION	INT.	λ (VAC.)	ν CM^{-1}	CLASSIFICATION
1	1977.14	50,578.1	$2s^22p^4(^1D)3p\ ^2P^0_{3/2} - 2s^22p^4(^1D)3d\ ^2P_{3/2}$	2	1816.83	55.040.9	$2s^22p^4(^1D)3p\ ^2P^0_{3/2} - 2s^22p^4(^1D)3d\ ^2S_{1/2}$
1	76.62	591.4	" $(^1D)3p\ ^2P^0_{1/2}$ — " $(^1D)3d\ ^2D_{3/2}$	3	14.35	116.1	" $(^1D)3p\ ^2F^0_{7/2}$ — " $(^1D)3d\ ^2F_{5/2}$
0	75.58	618.0	" $(^1D)3p\ ^2D^0_{3/2}$ — " $(^1D)3d\ ^2F_{7/2}$	5	11.70	196.8	" $(^1D)3p\ ^2F^0_{5/2}$ — " $(^1D)3d\ ^2F_{5/2}$
18	65.04	889.5	" $(^3P)3p\ ^4D^0_{7/2}$ — " $(^3P)3d\ ^4F_{9/2}$	4	10.74	226.0	" $(^3P)3p\ ^4D^0_{3/2}$ — " $(^3P)3d\ ^2P_{3/2}$
20	60.76	51,000.6	" $(^3P)3p\ ^4D^0_{3/2}$ — " $(^3P)3d\ ^4P_{3/2}$	7	01.27	516.4	" $(^3P)3p\ ^4P^0_{1/2}$ — " $(^3P)3d\ ^4P_{1/2}$
0	56.48	112.2	" $(^3P)3p\ ^4S^0_{3/2}$ — " $(^3P)4s\ ^4P_{3/2}$	8	1791.80	809.9	" $(^3P)3p\ ^4D^0_{3/2}$ — " $(^3P)4s\ ^4P_{3/2}$
8	55.31	142.8	" $(^1D)3p\ ^2P^0_{3/2}$ — " $(^1D)3d\ ^2D_{3/2}$	10	91.23	827.6	" $(^3P)3p\ ^4P^0_{3/2}$ — " $(^3P)3d\ ^4P_{1/2}$
40 *	51.21	250.2	" $(^3P)3s\ ^4P_{5/2}$ — " $(^3P)3p\ ^4S^0_{3/2}$	12	82.92	56,087.8	" $(^3P)3p\ ^4P^0_{1/2}$ — " $(^3P)3d\ ^4P_{3/2}$
15	50.79	261.2	" $(^3P)3p\ ^4D^0_{1/2}$ — " $(^3P)3d\ ^4F_{3/2}$	0	75.32	327.9	" $(^3P)3p\ ^4D^0_{1/2}$ — " $(^3P)4s\ ^4P_{3/2}$
0	46.70	368.9	" $(^3P)3s\ ^4P_{3/2}$ — " $(^3P)3p\ ^2P^0_{3/2}$	0	73.00	401.5	" $(^3P)3p\ ^4P^0_{3/2}$ — " $(^3P)3d\ ^4P_{3/2}$
d20	46.43	376.1	" $(^1D)3p\ ^2F^0_{7/2}$ — " $(^1D)3d\ ^2G_{7/2}$	0	67.21	586.4	" $(^3P)3p\ ^4P^0_{1/2}$ — " $(^3P)3d\ ^4F_{3/2}$
d3	44.99	414.1	" $(^3P)3p\ ^4D^0_{5/2}$ — " $(^3P)3d\ ^4P_{3/2}$	3	63.84	694.5	" $(^3P)3p\ ^4P^0_{3/2}$ — " $(^3P)3d\ ^4P_{5/2}$
6	43.40	456.2	" $(^1D)3p\ ^2F^0_{5/2}$ — " $(^1D)3d\ ^2G_{7/2}$	0	62.13	749.5	" $(^3P)3p\ ^4D^0_{1/2}$ — " $(^3P)4s\ ^4P_{1/2}$
6	42.19	488.3	" $(^3P)3p\ ^2D^0_{5/2}$ — " $(^3P)3d\ ^2F_{5/2}$	1	61.05	784.3	" $(^3P)3p\ ^4D^0_{7/2}$ — " $(^3P)4s\ ^4P_{5/2}$
0	41.77	499.4	" $(^3P)3p\ ^4D^0_{3/2}$ — " $(^3P)3d\ ^4F_{5/2}$	0	54.97	981.0	" $(^3P)3p\ ^4D^0_{5/2}$ — " $(^3P)4s\ ^4P_{3/2}$
0	41.61	503.6	" $(^3P)3s\ ^4P_{3/2}$ — " $(^3P)3p\ ^2P^0_{1/2}$	3	52.65	57,056.5	" $(^3P)3p\ ^4P^0_{5/2}$ — " $(^3P)3d\ ^4P_{5/2}$
0	39.32	564.4	" $(^3P)3p\ ^4D^0_{5/2}$ — " $(^3P)3d\ ^4F_{7/2}$	1	52.06	075.6	" $(^3P)3p\ ^2D^0_{3/2}$ — " $(^3P)4s\ ^2P_{1/2}$
0	35.54	665.2	" $(^3P)3p\ ^4D^0_{3/2}$ — " $(^3P)3d\ ^4F_{5/2}$	0	46.39	260.9	" $(^3P)3p\ ^4P^0_{5/2}$ — " $(^3P)3d\ ^4F_{3/2}$
30	33.87	709.8	" $(^3P)3p\ ^4D^0_{1/2}$ — " $(^3P)3d\ ^4P_{3/2}$	1	41.33	427.3	" $(^3P)3p\ ^4P^0_{3/2}$ — " $(^3P)3d\ ^4F_{5/2}$
15	27.21	888.5	" $(^1D)3p\ ^2P^0_{3/2}$ — " $(^1D)3d\ ^2D_{5/2}$	0	31.08	767.4	" $(^3P)3p\ ^4P^0_{3/2}$ — " $(^3P)3d\ ^2F_{7/2}$
45	26.27	913.8	" $(^3P)3p\ ^4D^0_{3/2}$ — " $(^3P)3d\ ^4F_{3/2}$	0	19.60	58,153.0	" $(^3P)3p\ ^4P^0_{1/2}$ — " $(^3P)3d\ ^2D_{3/2}$
6	20.12	52,080.1	" $(^3P)3p\ ^4D^0_{5/2}$ — " $(^3P)3d\ ^4F_{5/2}$	0	18.48	190.9	" $(^3P)3p\ ^4P^0_{5/2}$ — " $(^3P)3d\ ^2D_{5/2}$
6	18.46	125.1	" $(^3P)3p\ ^4D^0_{7/2}$ — " $(^3P)3d\ ^4F_{7/2}$	1	1691.70	59,112.1	" $(^3P)3p\ ^4P^0_{1/2}$ — " $(^3P)3d\ ^2P_{3/2}$
8	13.17	269.3	" $(^3P)3p\ ^4D^0_{7/2}$ — " $(^3P)3d\ ^4P_{5/2}$	1	78.74	568.4	" $(^3P)3p\ ^4P^0_{3/2}$ — " $(^3P)3d\ ^2F_{5/2}$
3	1899.70	639.9	" $(^3P)3p\ ^4D^0_{7/2}$ — " $(^3P)3d\ ^4F_{9/2}$	d3	69.52	897.4	" $(^3P)3p\ ^4D^0_{5/2}$ — " $(^3P)4s\ ^2P_{3/2}$
12	90.75	889.1	" $(^3P)3p\ ^2P^0_{1/2}$ — " $(^3P)4s\ ^2P_{3/2}$				" $(^3P)3p\ ^4P^0_{1/2}$ — " $(^3P)3d\ ^2P_{1/2}$
15	87.48	980.7	" $(^3P)3p\ ^4D^0_{7/2}$ — " $(^3P)3d\ ^2F_{7/2}$	2	58.71	60,287.8	" $(^3P)3p\ ^4D^0_{3/2}$ — " $(^3P)4s\ ^2P_{1/2}$
4	85.75	53,029.3	" $(^3P)3p\ ^2P^0_{3/2}$ — " $(^3P)4s\ ^2P_{3/2}$	1	50.91	572.6	" $(^3P)3p\ ^4P^0_{3/2}$ — " $(^3P)3d\ ^2P_{3/2}$
0	74.22	355.5	" $(^3P)3p\ ^2D^0_{3/2}$ — " $(^3P)4s\ ^4P_{3/2}$	4	33.64	61,213.0	" $(^3P)3p\ ^4P^0_{5/2}$ — " $(^3P)4s\ ^4P_{5/2}$
4	73.32	381.2	" $(^1D)3p\ ^2F^0_{5/2}$ — " $(^1D)3d\ ^2D_{3/2}$	12	24.07	573.7	" $(^3P)3p\ ^4P^0_{5/2}$ — " $(^3P)4s\ ^4P_{5/2}$
1	72.45	405.9	" $(^3P)3p\ ^4D^0_{7/2}$ — " $(^3P)3d\ ^2D_{5/2}$	5	21.94	654.6	" $(^3P)3p\ ^4P^0_{1/2}$ — " $(^3P)4s\ ^4P_{3/2}$
1	69.43	492.3	" $(^3P)3p\ ^2D^0_{5/2}$ — " $(^3P)4s\ ^4P_{5/2}$	8	13.77	966.7	" $(^3P)3p\ ^4P^0_{3/2}$ — " $(^3P)4s\ ^4P_{3/2}$
6	62.40	694.2	" $(^3P)3p\ ^2P^0_{1/2}$ — " $(^3P)4s\ ^2P_{1/2}$	4	10.97	62,074.4	" $(^3P)3p\ ^4P^0_{1/2}$ — " $(^3P)4s\ ^4P_{1/2}$
15	61.19	729.1	" $(^3P)3p\ ^4P^0_{1/2}$ — " $(^3P)3d\ ^4D_{3/2}$	6	04.47	325.9	" $(^3P)3p\ ^4P^0_{5/2}$ — " $(^3P)4s\ ^4P_{3/2}$
0	59.61	774.7	" $(^3P)3p\ ^2D^0_{3/2}$ — " $(^3P)4s\ ^4P_{1/2}$	5	02.91	386.5	" $(^3P)3p\ ^4P^0_{3/2}$ — " $(^3P)4s\ ^4P_{1/2}$
0	59.20	786.5	" $(^3P)3p\ ^4D^0_{1/2}$ — " $(^3P)3d\ ^2P_{1/2}$	8	1548.68	64,571.1	" $(^3P)3p\ ^4P^0_{1/2}$ — " $(^3P)4s\ ^2P_{3/2}$
5	57.57	833.8	" $(^3P)3p\ ^2P^0_{3/2}$ — " $(^3P)4s\ ^2P_{1/2}$	1	41.19	884.9	" $(^3P)3p\ ^4P^0_{3/2}$ — " $(^3P)4s\ ^2P_{3/2}$
20	56.73	858.1	" $(^3P)3p\ ^4P^0_{3/2}$ — " $(^3P)3d\ ^4D_{5/2}$	1	29.67	65,373.5	" $(^3P)3p\ ^4P^0_{1/2}$ — " $(^3P)4s\ ^2P_{1/2}$
15	55.91	881.9	" $(^3P)3p\ ^4P^0_{1/2}$ — " $(^3P)3d\ ^4D_{1/2}$	3	1458.15	68,580.0	" $(^3P)3s\ ^2P_{1/2}$ — " $(^1D)3p\ ^2P^0_{1/2}$
18	50.39	54,042.7	" $(^3P)3p\ ^4P^0_{3/2}$ — " $(^3P)3d\ ^4D_{3/2}$	12	36.21	69,627.7	" $(^3P)3s\ ^2P_{3/2}$ — " $(^1D)3p\ ^2P^0_{1/2}$
20	50.24	047.0	" $(^1D)3p\ ^2F^0_{7/2}$ — " $(^1D)3d\ ^2D_{5/2}$	0	27.27	70,063.8	" $(^3P)3s\ ^2P_{1/2}$ — " $(^1D)3p\ ^2D^0_{3/2}$
35	49.58	066.3	" $(^3P)3p\ ^4P^0_{5/2}$ — " $(^3P)3d\ ^4D_{7/2}$	d6	1337.39	74,772.5	" $(^3P)3p\ ^2P^0_{3/2}$ — " $(^1D)3d\ ^2P_{3/2}$
10	47.54	126.0	" $(^1D)3p\ ^2F^0_{5/2}$ — " $(^1D)3d\ ^2D_{3/2}$	2	1265.66	79,010.2	" $(^3P)3p\ ^2D^0_{3/2}$ — " $(^1D)3d\ ^2P_{3/2}$
12	45.10	197.6	" $(^3P)3p\ ^4P^0_{3/2}$ — " $(^3P)3d\ ^4D_{1/2}$	1	56.68	574.7	" $(^3P)3p\ ^2D^0_{3/2}$ — " $(^1D)3d\ ^2D_{3/2}$
20	44.36	219.3	" $(^3P)3p\ ^4P^0_{3/2}$ — " $(^3P)3d\ ^4D_{5/2}$	d4	35.40	80,945.4	" $(^3P)3p\ ^4D^0_{7/2}$ — " $(^1D)3d\ ^2G_{7/2}$
			" $(^3P)3p\ ^4D^0_{5/2}$ — " $(^3P)3d\ ^2F_{5/2}$	4	24.73	81,650.6	" $(^3P)3p\ ^4D^0_{1/2}$ — " $(^1D)3d\ ^2D_{3/2}$
2	43.43	246.7	" $(^3P)3p\ ^2D^0_{3/2}$ — " $(^3P)4s\ ^2P_{3/2}$	d4	23.44	736.7	" $(^3P)3p\ ^4D^0_{3/2}$ — " $(^1D)3d\ ^2P_{3/2}$
6	38.11	403.7	" $(^3P)3p\ ^4P^0_{5/2}$ — " $(^3P)3d\ ^4D_{3/2}$	5	21.12	892.0	" $(^3P)3p\ ^4D^0_{5/2}$ — " $(^1D)3d\ ^2D_{5/2}$
15	35.22	489.4	" $(^1D)3p\ ^2P^0_{1/2}$ — " $(^1D)3d\ ^2S_{1/2}$	8	1180.40	84,717.0	" $(^1D)3p\ ^2D^0_{5/2}$ — " $(^3S)3d\ ^2D_{5/2}$
10	25.44	781.3	" $(^3P)3p\ ^4D^0_{7/2}$ — " $(^3P)3d\ ^2F_{5/2}$	2	53.04	86,727.3	" $(^3P)3p\ ^4P^0_{3/2}$ — " $(^1D)3d\ ^2P_{3/2}$
0	24.52	808.9	" $(^3P)3p\ ^4D^0_{3/2}$ — " $(^3P)3d\ ^2P_{3/2}$	0	22.30	89,102.7	" $(^3P)3p\ ^4P^0_{3/2}$ — " $(^1D)3d\ ^2F_{5/2}$
12	21.68	894.4	" $(^1D)3p\ ^2F^0_{7/2}$ — " $(^1D)3d\ ^2F_{7/2}$	5	00.49	90,868.6	" $(^3P)3p\ ^4P^0_{1/2}$ — " $(^1D)3d\ ^2S_{1/2}$
2	19.01	974.9	" $(^1D)3p\ ^2F^0_{5/2}$ — " $(^1D)3d\ ^2F_{7/2}$				

* Classified by Söderqvist also.
d Denotes a diffuse line.

present investigation all four levels belonging to this multiplet have been located on the basis of combinations with $2s^22p^4(^3P)3p\ ^4D^0$ and $2s^22p^4(^3P)3p\ ^4P^0$ levels, and all possible transitions have been observed.

(2) The $2s^22p^4(^3P)4s\ ^2P_{1/2}$ level given by Söderqvist has not been confirmed by the present observations. In the classification of the author the $2s^22p^4(^3P)4s\ ^2P$ levels are established on the basis of half a dozen or more combinations with various $3p$ levels. Furthermore the position of this doublet level relative to the $2s^22p^4(^3P)4s\ ^4P$ multiplet is consistent with any reasonable estimate of the relative position of the ^2P and ^4P states arrived at from the corresponding states of Ne II. The quartet levels were not reported by Söderqvist.

None of the allowed tansitions between the $4d$ levels listed by Söderqvist and the $3p$ levels which were determined by him and the author independently have been found, although their computed wave-lengths would have placed them within the spectral region studied.

Combinations between states built on the ^1S level of Na IV are few and probably extremely faint. It has not been possible to locate the $2s^22p^4(^1S)3p\ ^2P^0$ levels and confirm the term values assigned by Söderqvist to the $2s^22p^4(^1S)$-$3s\ ^2S$ and $2s^22p^4(^1S)3d\ ^2D$ levels. Of the $3d$ levels based on the ^3P limit, the $2s^22p^4(^3P)3d\ ^4F_{9/2}$ state is open to question. Due to the J selection rule this level would combine only with $2s^22p^4(^3P)3p\ ^4D^0_{7/2}$ level. The line listed for this transition yields an unexpectedly large $^4F_{9/2-7/2}$

separation. The $2s^22p^4(^1D)3d\ ^2G_{9/2}$ level has been omitted because the transition between it and the $2s^22p^4(^1D)3p\ ^2F^0_{7/2}$ level could not be identified uniquely.

The classified lines by which the new levels were established are included in Table II. The intensities are visual estimates and are comparable only over short regions of the spectrum. Numerous intercombination lines between the doublet and quartet levels (limit ^3P) have been observed.

The author acknowledges with pleasure the advice and criticism of Professor R. C. Gibbs during the course of this investigation.

SEPTEMBER 1, 1938 PHYSICAL REVIEW VOLUME 54

The Spectra of Rb III and Sr IV

D. H. TOMBOULIAN
Department of Physics, Cornell University, Ithaca, New York
(Received June 30, 1938)

By applying Shortley's equations to the $4s^24p^5(^3P^0)5p$ levels of Rb II, the separation of the ground levels $4s^24p^5\ ^2P^0$ of Rb III has been computed, and experimentally observed to be 7380 cm^{-1}. In the case of Sr IV, the $^2P^0$ separation has been predicted from the regular doublet law and identified from the data as 9731 cm^{-1}. On the basis of transitions into the ground doublet certain $4s^24p^44d$ and $4s^24p^45s$ levels have been located.

AN analysis of the spectrum of Br I has been given by Kiess and de Bruin,[1] and the spectrum of Kr II has been investigated by de Bruin, Humphreys and Meggers.[2] The present investigation was undertaken to extend the Br I like sequence to Rb III and Sr IV. The essential features of the study presented here consist in predicting and locating the separation of the lowest levels and identifying certain transitions into the ground doublet.

EXPERIMENTAL

The condensed spark in vacuum was used to excite the spectra of Rb III and Sr IV. The region from 250 to 1200A was photographed with a vacuum spectrograph which was equipped with a grating having 30,000 lines per inch. The dispersion of the instrument was about 5.3A/mm. A kenetron rectifier (output potential 45 kv) supplied the high potential. The condenser had a capacitance of 0.18μf. In procuring the data for rubidium, aluminum electrodes cored with Rb_2SO_4 were employed. The rubidium lines were duplicated when the discharge occurred between electrodes cored with Rb I. As a further aid in isolating the lines due to rubidium, a comparison spectrum of Rb_2SO_4 and Rb I was obtained. After eliminating the usual impurity lines of carbon, oxygen and aluminum, the remaining lines common to both spectra were regarded as belonging to rubidium. A similar procedure was followed in exciting the strontium spectrum, metallic strontium and strontium oxide serving as sources of strontium. Aluminum, carbon, and oxygen lines were used as standards in the reduction of the plates. The wave-lengths of the aluminum lines were taken from Ekefors,[3] those of carbon and oxygen from Edlén's list.[4]

THE ANALYSIS OF THE SPECTRA

The normal $4s^24p^5$ electron configuration of Rb III and Sr IV gives rise to inverted $^2P^0$ terms. The terms which arise when one of the $4p$ electrons is raised to the $4d$, $5s$, $5p\cdots$ states are given in Table I.

The starting point for the search of Rb III doublets was the prediction of the separation of

[1] Kiess and de Bruin, Nat. Bur. Stand. J. Research **4**, 667 (1930).
[2] de Bruin, Humphreys and Meggers, Nat. Bur. Stand. J. Research **11**, 409 (1933).
[3] Ekefors, Zeits. f. Physik **51**, 471 (1928).
[4] Edlén, Zeits. f. Physik, **85**, 85 (1933).

the ground levels. This separation was computed by the use of Shortley's[5] equations. These relations apply to the ten s^2p^5p levels of a rare gas type spectrum and express the values of the levels involved in terms of a set of parameters one of which is related to the doublet separation of the next higher ion. Utilizing the term values for the $4s^24p^55p$ levels of Rb II, determined by Laporte, Miller and Sawyer[6] one obtains 7550 cm^{-1} for the separation of the lowest doublet of Rb III. With this value as a guide, a careful examination of the Rb data yielded a score of pairs of lines having $\Delta\nu=7380$ cm^{-1}. This difference occurred more frequently than any other and included some of the strongest lines.

The next step was the determination of the separation of the lowest levels of Sr IV. Since no classification of Sr III has been carried out the previous procedure could not be used here. Recourse was therefore made to the regular doublet law given by

$$\Delta\nu=R\alpha^2(Z-s)^4/n^3(l+1)l.$$

The values of the screening constant s were calculated on the assumption $\Delta\nu=7380$ cm^{-1} for Rb III and by the use of the known separations of the ground levels of Br I and Kr II. It is known that the screening constant plotted against the atomic number Z results in a smooth curve with diminishing slope as one passes on to the higher members in an isoelectronic sequence. There is also a progressive diminution in the values of s. Guided by these facts an extrapolated value of $\Delta\nu=9825$ cm^{-1} was obtained for the $4s^24p^5\ {}^2P^0$ separation of Sr IV.

A search for recurring differences of about this magnitude resulted in the location of pairs of lines having the separation $\Delta\nu=9731$ cm^{-1}. This was in good agreement with the predicted value and was assumed to be the separation of the ground doublet of Sr IV. The value of s for Sr IV was calculated by using this value of $\Delta\nu$. The results for the sequence are shown in Table II and the graph of the screening constant against the atomic number is given in Fig. 1.

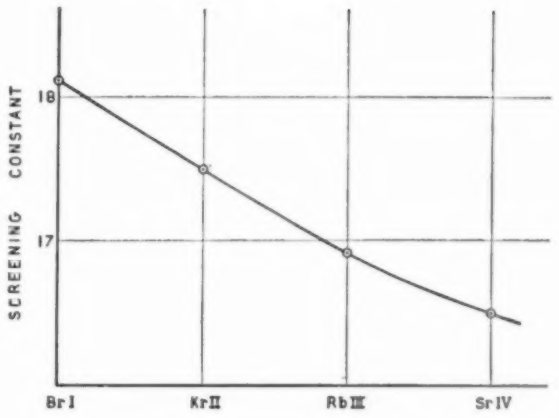

FIG. 1. Screening constant, configuration $4s^24p^5$.

TABLE I. *Term table for* Br I *like spectra.*

CONFIGURATION	TERMS			
$4s^24p^5$ $4s\ 4p^6$	$^2P^0$ ^2S			
	Limit $4s^24p^4\ ^3P$		Limit $4s^24p^4\ ^1D$	Limit $4s^24p^4\ ^1S$
$4s^24p^4ns$ $(n\geq 5)$	^4P	^2P	^2D	^2S
$4s^24p^4np$ $(n\geq 5)$	$^4D^0\ ^4P^0\ ^4S^0$	$^2D^0\ ^2P^0\ ^2S^0$	$^2F^0\ ^2D^0\ ^2P^0$	$^2P^0$
$4s^24p^4nd$ $(n\geq 4)$	$^4F\ ^4D\ ^4P$	$^2F\ ^2D\ ^2P$	$^2G\ ^2F\ ^2D\ ^2P\ ^2S$	^2D

ASSIGNMENT OF TERMS

The first lines to be identified were the transitions

$$4s^24p^5\ {}^2P^0-4s^24p^4(^3P)5s\ {}^2P$$
$$\text{“}\quad {}^2P^0-\quad\text{“}\quad {}^4P_{3/2,\ 1/2}.$$

TABLE II. *Configuration $4s^24p^5$. Separation of $^2P^0$ levels and values of the screening constant.*

SPECTRUM	$\Delta\nu$	$(Z-s)$	Z	s	Δs
Br I	3685	16.87	35	18.13	
					0.67
Kr II	5371	18.54	36	17.46	
					0.53
Rb III	7380	20.07	37	16.93	
					0.43
Sr IV	9731	21.50	38	16.50	

These four pairs of lines have their origin in the lowest levels belonging to the 5s electron configuration. Consequently they form a characteristic group of lines of high intensity. Their approximate positions had been predicted by the use of a Moseley diagram. The location of the observed lines agreed well with prediction. The $4s^24p^4(^1D)5s\ {}^2D_{3/2}$ and $4s^24p^4(^1S)5s\ {}^2S_{1/2}$ levels were also identified by extrapolations on a Moseley graph. These levels are well separated

[5] Shortley, Phys. Rev. **44**, 666 (1933).
[6] Laporte, Miller and Sawyer, Phys. Rev. **38**, 843 (1931).

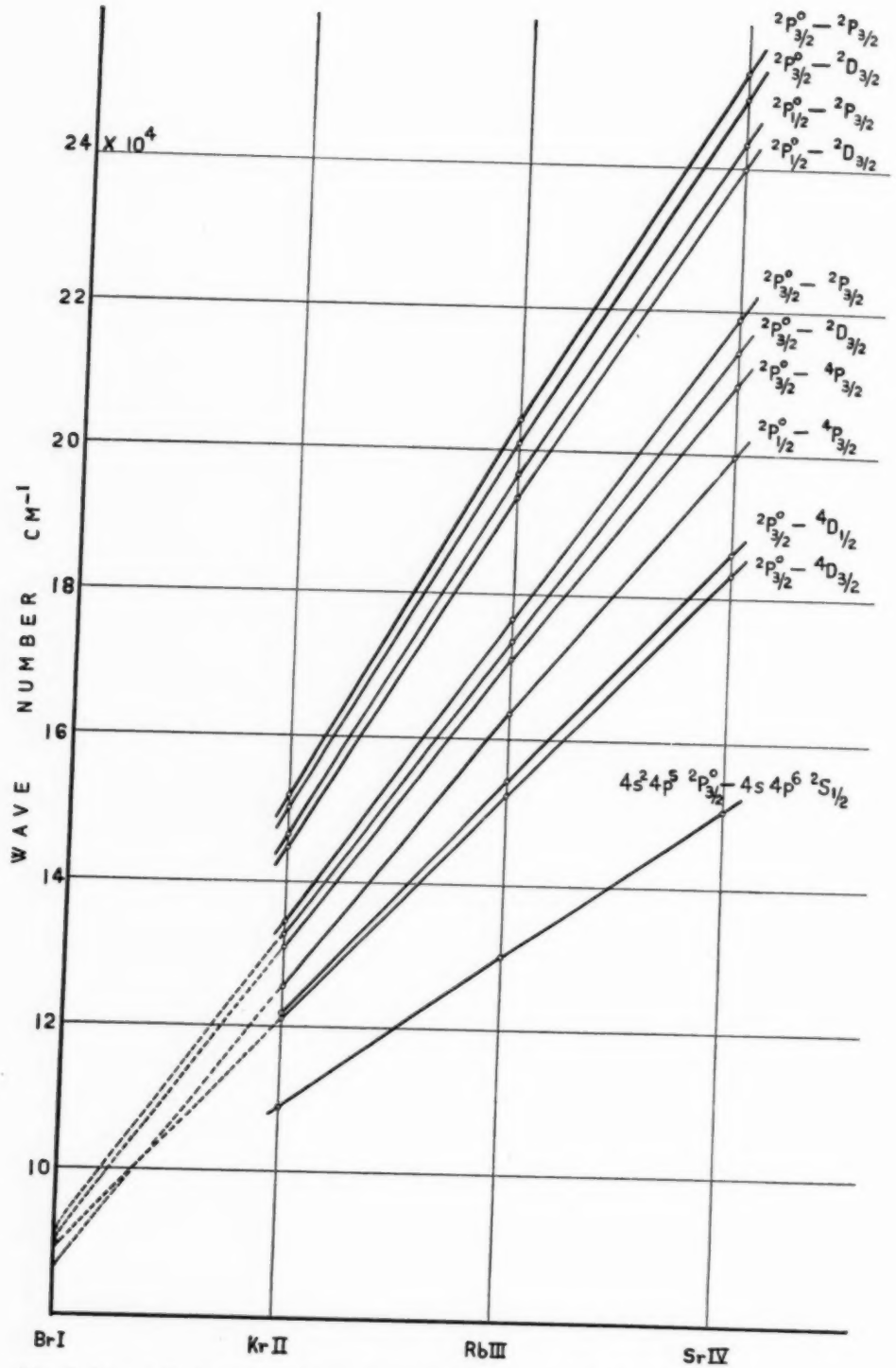

FIG. 2. Linear displacement of wave number. Transitions $4p^5-4p^4 4d$ and $4p^5-4s4p^6$.

and lie much higher than the $5s$ states built on the ^3P limit. The remaining $5s$ levels, namely $4s^24p^4(^1D)5s\ ^2D_{5/2}$ and $4s^24p^4(^3P)5s\ ^4P_{5/2}$ could not be identified with certainty since they combine only with the $4s^24p^5\ ^2P^0{}_{3/2}$ level.

The $4p-4d$ transitions do not involve a

TABLE III. *Square roots of certain terms.*

CONFIGURATION	TERM	Br I	$\Delta(T)^{\frac{1}{2}}$	Kr II	$\Delta(T)^{\frac{1}{2}}$	Rb III	$\Delta(T)^{\frac{1}{2}}$	Sr IV
$4s^24p^5$	$^2P^0_{3/2}$	309.1	136.1	445.2	119.8	565.0*	113.2	678.2*
$4s4p^6$	$^2S_{1/2}$	—		298.6	137.2	435.8	120.5	556.3
$4s^24p^4(^2P)5s$	$^4P_{3/2}$	175.1	113.1	288.2	106.1	394.3	94.4	488.7
"	$^2P_{3/2}$	168.4	113.9	282.3	102.4	384.7	91.8	476.5
$4s^24p^4(^1D)5s$	$^2D_{3/2}$	135.1	130.6	265.7	104.5	370.2	90.6	460.8
$4s^24p^4(^3P)4d$	$^4D_{3/2}$	75.4	202.4	277.8	131.6	409.4*	116.6	526.0*
"	$^2P_{3/2}$	—		252.1	125.9	378.0	112.9	490.9
$4s^24p^4(^1D)4d$	$^2D_{3/2}$	—		219.0	126.1	345.1	113.5	458.6
$4s^24p^4(^1S)5s$	$^2S_{1/2}$	140.2	88.6	228.8	106.9	335.7	98.1	433.8

* Used in determining the approximate absolute term values.

change in the total quantum number. Hence a plot of the wave numbers of analogous transitions against the atomic number should result in nearly straight lines. Accordingly several $4d$ levels which combine with the ground doublet were established on the basis of the irregular doublet law. Fig. 2 represents certain $4p-4d$ transitions for Br I like spectra.

In an isoelectronic sequence when the square roots of corresponding term values are plotted against the atomic number, smooth curves are obtained. Such curves tend to become approximately linear as one progresses to higher members of a sequence. Furthermore, as a consequence of the irregular doublet law, the difference between the square roots of the term values of levels approaching the same limit and having the same total quantum number should be independent of the atomic number, i.e., $\Delta\sqrt{T}$ = const. The absolute term values were approximated by the application of these two regularities. On a Moseley diagram (see Fig. 3 and Table III) the lines representing the $4s^24p^5\ ^2P^0_{3/2}$ and $4s^24p^4(^3P)4d\ ^4D_{3/2}$ levels were extended to Rb III and Sr IV so as to keep $\Delta\sqrt{T}$ nearly constant and at the same time the ordinates were chosen so that the difference between their squares was equal to the wave number of the $4s^24p^5\ ^2P^0_{3/2}-4s^24p^4(^3P)4d\ ^4D_{3/2}$ transition. In this manner the approximate absolute term value of the $4s^24p^5\ ^2P^0_{3/2}$ level in Rb III was found to be 320,000 cm^{-1} below the ^3P ionization limit. The corresponding level in Sr IV was estimated to be 460,000 cm^{-1} with respect to the ^3P states of Sr V.

In the data for strontium, the most intense pair of lines having the separation of the ground levels, yielded a level nearest to normal state. Since the $4s4p^6\ ^2S_{1/2}$ level is expected to lie closest to the ground state, these lines were thought to be the transitions

$$4s^24p^5\ ^2P^0_{3/2,\ 1/2}-4s4p^6\ ^2S_{1/2}.$$

Since these transitions would have to follow the

TABLE IV. *Term values for* Rb III.

TERM SYMBOL		APPROXIMATE ABSOLUTE TERM VALUE (cm^{-1})
$4s^24p^5$	$^2P^0_{3/2}$	320,000
"	$^2P^0_{1/2}$	312,620
$4s\ 4p^6$	$^2S_{1/2}$	189,964
$4s^24p^4(^3P)4d$	$^4D_{3/2}$	167,647
"	$^4D_{1/2}$	165,597
$4s^24p^4(^3P)5s$	$^4P_{3/2}$	155,493
"	$^4P_{1/2}$	151,915
$4s^24p^4(^3P)4d$	$^4P_{1/2}$	149,577
"	$^4P_{3/2}$	149,153
$4s^24p^4(^3P)5s$	$^2P_{3/2}$	147,955
$4s^24p^4(^3P)4d$	$^2D_{3/2}$	146,525
$4s^24p^4(^3P)5s$	$^2P_{1/2}$	144,604
$4s^24p^4(^3P)4d$	$^2P_{3/2}$	142,956
$4s^24p^4(^1D)5s$	$^2D_{3/2}$	137,037
$4s^24p^4(^1D)4d$	$^2D_{3/2}$	119,117
"	$^2P_{3/2}$	115,896
$4s^24p^4(^1S)5s$	$^2S_{1/2}$	112,723

TABLE V. *Term values for* Sr IV.

TERM SYMBOL		APPROXIMATE ABSOLUTE TERM VALUES (cm^{-1})
$4s^24p^5$	$^2P^0_{3/2}$	460,000
"	$^2P^0_{1/2}$	450,269
$4s\ 4p^6$	$^2S_{1/2}$	309,495
$4s^24p^4(^3P)4d$	$^4D_{3/2}$	276,695
"	$^4D_{1/2}$	273,935
$4s^24p^4(^3P)4d$	$^4P_{1/2}$	250,786
"	$^4P_{3/2}$	250,471
"	$^2D_{3/2}$	245,655
"	$^2P_{3/2}$	241,061
$4s^24p^4(^3P)5s$	$^4P_{3/2}$	238,851
"	$^4P_{1/2}$	234,147
"	$^2P_{3/2}$	227,030
"	$^2P_{1/2}$	221,797
$4s^24p^4(^1D)5s$	$^2D_{3/2}$	212,384
$4s^24p^4(^1D)4d$	$^2D_{3/2}$	210,354
"	$^2P_{3/2}$	206,767
$4s^24p^4(^1S)5s$	$^2S_{1/2}$	188,226

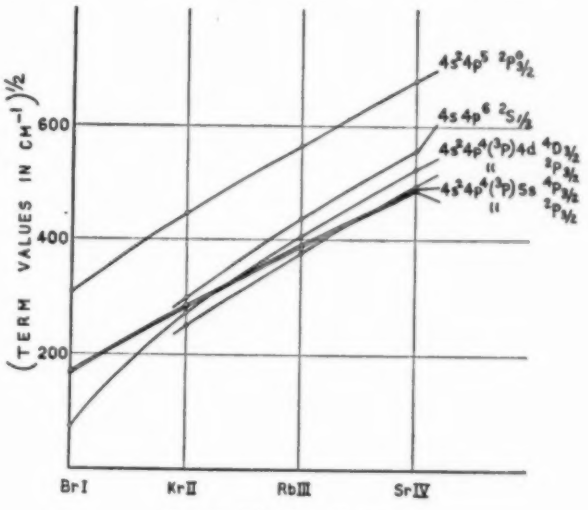

FIG. 3. Moseley diagram.

TABLE VI. *Classified lines of* Rb III.

INT.	λ/ν (VAC.)	λ/ν CM⁻¹	CLASSIFICATION	INT.	λ/ν (VAC.)	λ/ν CM⁻¹	CLASSIFICATION
18	815.27	122,658	$4s^24p^5\ ^2P^o_{1/2}$ — $4s4p^6\ ^2S_{1/2}$	25	589.42	169,658	$4s^24p^5\ ^2P^o_{1/2}$ — $4s^24p^4(^3P)4d\ ^2P_{3/2}$
25	769.03	130,034	" $^2P^o_{3/2}$ — "	20	586.78	170,422	" $^2P^o_{3/2}$ — " $4d\ ^4P_{1/2}$
12	689.80	144,969	$4s^24p^5\ ^2P^o_{1/2}$ — $4s^24p^4(^3P)4d\ ^4D_{3/2}$	d8	585.29	170,855	" $^2P^o_{3/2}$ — " $4d\ ^4P_{3/2}$
10	680.16	147,024	" $^2P^o_{1/2}$ — " $4d\ ^4D_{1/2}$	30	581.26	172,040	" $^2P^o_{3/2}$ — " $5s\ ^2P_{3/2}$
15	656.34	152,360	" $^2P^o_{3/2}$ — " $4d\ ^4D_{3/2}$	25	576.43	173,482	" $^2P^o_{3/2}$ — " $4d\ ^2D_{3/2}$
15	647.66	154,402	" $^2P^o_{3/2}$ — " $4d\ ^4D_{1/2}$	20	570.14	175,396	" $^2P^o_{3/2}$ — " $5s\ ^2P_{1/2}$
3	636.42	157,129	" $^2P^o_{1/2}$ — " $5s\ ^4P_{3/2}$	5	569.53	175,583	$4s^24p^5\ ^2P^o_{1/2}$ — $4s^24p^4(^1D)5s\ ^2D_{3/2}$
18	622.26	160,704	" $^2P^o_{1/2}$ — " $5s\ ^4P_{1/2}$	10	564.81	177,051	" $^2P^o_{3/2}$ — $4s^24p^4(^3P)4d\ ^2P_{3/2}$
6	613.33	163,044	" $^2P^o_{1/2}$ — " $4d\ ^4P_{1/2}$	25	546.56	182,963	" $^2P^o_{3/2}$ — $4s^24p^4(^1D)5s\ ^2D_{3/2}$
30	611.77	163,460	" $^2P^o_{1/2}$ — " $4d\ ^4P_{3/2}$	30	516.78	193,506	" $^2P^o_{1/2}$ — " $4d\ ^2D_{3/2}$
15	607.88	164,506	" $^2P^o_{3/2}$ — " $5s\ ^4P_{3/2}$	8	508.33	196,723	" $^2P^o_{1/2}$ — " $4d\ ^2P_{3/2}$
15	607.28	164,669	" $^2P^o_{1/2}$ — " $5s\ ^2P_{3/2}$	30	500.25	199,900	" $^2P^o_{1/2}$ — $4s^24p^4(^1S)5s\ ^2S_{1/2}$
40	602.09	166,088	" $^2P^o_{1/2}$ — " $4d\ ^2D_{3/2}$	20	497.81	200,880	" $^2P^o_{3/2}$ — $4s^24p^4(^1D)4d\ ^2D_{3/2}$
15	595.18	168,016	" $^2P^o_{1/2}$ — " $5s\ ^2P_{1/2}$	25	489.95	204,103	" $^2P^o_{3/2}$ — " $4d\ ^2P_{3/2}$
25	594.93	168,087	" $^2P^o_{3/2}$ — " $5s\ ^4P_{1/2}$	30	482.45	207,275	" $^2P^o_{3/2}$ — $4s^24p^4(^1S)5s\ ^2S_{1/2}$

TABLE VII. *Classified lines of* Sr IV.

INT.	λ/ν (VAC.)	λ/ν CM⁻¹	CLASSIFICATION	INT.	λ/ν (VAC.)	λ/ν CM⁻¹	CLASSIFICATION
45	710.35	140,776	$4s^24p^5\ ^2P^o_{1/2}$ — $4s4p^6\ ^2S_{1/2}$	20	456.76	218,933	$4s^24p^5\ ^2P^o_{3/2}$ — $4s^24p^4(^3P)4d\ ^2P_{3/2}$
70	664.43	150,504	" $^2P^o_{3/2}$ — " $^2S_{1/2}$	12	452.18	221,151	" $^2P^o_{3/2}$ — " $5s\ ^4P_{3/2}$
25	576.10	173,580	" $^2P^o_{1/2}$ — $4s^24p^4(^3P)4d\ ^4D_{3/2}$	6	447.95	223,239	" $^2P^o_{1/2}$ — " $5s\ ^2P_{3/2}$
30	567.11	176,333	" $^2P^o_{1/2}$ — " $4d\ ^4D_{1/2}$	25	442.77	225,851	" $^2P^o_{3/2}$ — " $5s\ ^4P_{1/2}$
35	545.55	183,301	" $^2P^o_{3/2}$ — " $4d\ ^4D_{3/2}$	8	437.69	228,472	" $^2P^o_{1/2}$ — " $5s\ ^2P_{1/2}$
15	537.44	186,067	" $^2P^o_{3/2}$ — " $4d\ ^4D_{1/2}$	15	429.24	232,970	" $^2P^o_{3/2}$ — " $5s\ ^2P_{3/2}$
d2	501.29	199,485	" $^2P^o_{1/2}$ — " $4d\ ^4P_{1/2}$	3	420.37	237,886	" $^2P^o_{1/2}$ — $4s^24p^4(^1D)5s\ ^2D_{3/2}$
50	500.51	199,796	" $^2P^o_{1/2}$ — " $4d\ ^4P_{3/2}$	25	419.81	238,203	$4s^24p^5\ ^2P^o_{3/2}$ — $4s^24p^4(^3P)5s\ ^2P_{1/2}$
30	488.74	204,608	" $^2P^o_{1/2}$ — " $4d\ ^2D_{3/2}$	1	416.82	239,912	" $^2P^o_{1/2}$ — $4s^24p^4(^1D)4d\ ^2D_{3/2}$
5	477.98	209,214	" $^2P^o_{1/2}$ — " $4d\ ^2P_{3/2}$	8	410.67	243,505	" $^2P^o_{1/2}$ — " $4d\ ^2P_{3/2}$
			" $^2P^o_{3/2}$ — " $4d\ ^4P_{1/2}$	25	403.85	247,616	" $^2P^o_{3/2}$ — " $5s\ ^2D_{3/2}$
20	477.26	209,530	" $^2P^o_{3/2}$ — " $4d\ ^4P_{3/2}$	d3	400.56	249,651	" $^2P^o_{3/2}$ — " $4d\ ^2D_{3/2}$
8	473.00	211,416	" $^2P^o_{1/2}$ — " $5s\ ^4P_{3/2}$	20	394.90	253,229	" $^2P^o_{3/2}$ — " $4d\ ^2P_{3/2}$
20	466.52	214,353	" $^2P^o_{3/2}$ — " $4d\ ^2D_{3/2}$	12	381.62	262,041	" $^2P^o_{1/2}$ — $4s^24p^4(^1S)5s\ ^2S_{1/2}$
25	462.70	216,123	" $^2P^o_{1/2}$ — " $5s\ ^4P_{1/2}$	10	367.95	271,776	" $^2P^o_{3/2}$ — " $5s\ ^2S_{1/2}$

irregular doublet law, a corresponding pair of lines in Rb III were located readily by extrapolating backwards from Sr IV to Kr II. The $4s4p^6\ ^2S$ level is not known in Br I.

The intermediate term structure presented here is of necessity incomplete. Since the analysis is based on transitions to the ground doublet, it has been possible to establish only even levels with J values equal to $\frac{3}{2}$ to $\frac{1}{2}$. The assignments are therefore considered subject to correction until the important odd $5p$ levels are located. It is hoped that with new data the analysis can be extended to the classification of the $5s-5p$ transitions. The term values and the classified lines of Rb III and Sr IV are included in Tables IV to VII.

The author wishes to express his gratitude to Professor R. C. Gibbs for helpful advice and criticism given during the course of this investigation.

Optical Activity of Crystalline Nickel Sulfate α-Hexahydrate[1]

N. Underwood, F. G. Slack and E. B. Nelson
Vanderbilt University, Nashville, Tennessee

(Received June 13, 1938)

The optical activity of crystalline nickel sulfate α-hexahydrate has been measured throughout the visible portion of the spectrum. The observations are extended near to absorption regions by an adaptation of the method of Fizeau and Foucault. Both right- and left-hand crystals are found and the rotatory dispersion curves show anomalous rotatory dispersion. By application of Drude's equation, in which two terms are used, the observed anomaly is predicted as due to absorption bands lying at 3954A and 7187A, respectively. Transmission data for the crystal show the presence of these two bands, in agreement with previous absorption data for solutions of the material.

IN the course of some magneto-optic measurements it was found that the α-hexahydrate form of nickel sulfate is optically active. Beevers and Lipson[2] have investigated the crystal structure of this form of nickel sulfate with x-rays. Their data lead to the prediction of right and left crystals which should possess right and left rotatory power. They confirmed their predictions and discovered that the rotatory power was anomalous. However, their work was largely qualitative in this respect, so that it was thought worth while to investigate the optical activity of α-hexahydrate nickel sulfate quantitatively. The crystal is of the tetragonal form and cleaves readily along the (001) planes whose surfaces are perpendicular to the optic axis of the crystal.

The relative abundance of right and left crystals was determined by making a random selection of 104 crystals which were carefully cleaved and examined in the polarimeter with light from a sodium arc. It so happened that 52 gave a positive rotation and 52 a negative rotation at this wave-length. The rotation per mm thickness was numerically the same for the right and left specimens.

Two solutions were made, one from only right crystals, and one from only left crystals. Since no activity was observed in these solutions it is to be concluded that the optical activity is due to the crystal structure. This is in agreement with the work of Longchambon[3] who found that solutions made from nickel sulfate 7 H_2O were not optically active.

Visual and photographic measurements of the rotatory dispersion of the crystals were obtained in the region 4200A to 6500A. A Lippich half-shade polarimeter was used for the visual work. The photographic observations were made by a modification of the method used by Fizeau and Foucault.[4] The essential parts of the apparatus and their arrangement are shown in Fig. 1: (1) a Pointolite lamp, (2), (3), and (4) the Lippich half-shade polarizer, analyzer and the telescope of the polarimeter, (5) a glass prism spectrograph, and (6) a mercury arc. The Pointolite lamp which was used as a source of white light was placed directly before the polarizer and adjusted so that the two halves of the field received equal illumination. The polarimeter was placed on its side so that the dividing line of the field of view was horizontal instead of vertical. The spectrograph was placed behind the telescope of the polarimeter and the image of the fields focused on the vertical spectrograph slit so that a sharp image of the line of demarcation between the two half-fields was formed on the photographic plate. Light from the mercury arc was reflected by a right angled prism upon the slit for use as a comparison spectrum. The specimen was oriented so that its axis coincided with the optical axis of the system and was placed as indicated by (7) in Fig. 1.

When the Lippich double field polarimeter is used with a continuous spectrum, two spectra

[1] Edward B. Nelson, Phys. Rev. **53**, 849A (1938).
[2] C. A. Beevers and H. Lipson, Zeits. f. Krist. **83**, 134 (1932).
[3] Longchambon, Comptes rendus **173**, 89 (1921).
[4] T. M. Lowry, *Optical Rotatory Power* (Longmans Green Co., 1935), p. 199.

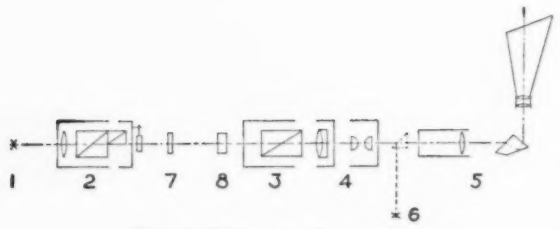

FIG. 1. Diagram of apparatus.

are observed on the ground glass of the spectrograph due to the illumination of the slit by the image of the double field polarizer. In the absence of an optically active medium there is a certain position of the analyzer for which the two spectra are equally but feebly illuminated throughout their entire length. This is the zero position. On introducing an optically active medium possessing rotatory dispersion and turning the analyzer, a dark extinction band appears in each spectrum, but the bands are slightly displaced relative to one another by an amount which is dependent on the value of the half-shade angle. At a point between the two bands the spectra are equally illuminated. The reading of the analyzer circle gives the rotation of the plane of polarization for the wave-length at this point of equal illumination. This wave-length is obtained by measurement of the photographic plate. When the dispersion is small this method of Fizeau and Foucault[4] is not very satisfactory because the dark extinction bands are broad and diffuse and the general illumination is so low that long exposures are required. However, this difficulty was surmounted by introducing a large rotatory dispersion through the addition of a quartz plate, cut with its axis perpendicular to its faces, into the optical system between the crystal specimen and the analyzer. (See 8, Fig. 1.) The thickness of the quartz plate is 7.92 mm and is such that the rotatory dispersion spreads the plane of polarization of the light of the visible spectrum through an angular dispersion of approximately 360°. The total rotation of the plane of polarization is equal to the algebraic sum of the rotations by the crystal and the quartz. The use of the quartz results in a sharp narrow extinction band in each spectrum and it is not particularly difficult to pick the point of equal illumination between them. First a series of spectrograms was taken for various settings of the analyzer with only the quartz in the optical system. Then another series of spectrograms was taken for the same angular settings of the analyzer, but in this case both the quartz and the specimen were in position. The differences between these two sets of photographs are obviously those introduced by the specimen. In order to make accurate comparisons, the photographs were taken adjacent to one another on the same photographic plate; first the quartz alone and then the quartz plus the specimen. The use of the quartz plate increased the light intensity so much that a three hour exposure was adequate in a spectral region only slightly removed from the absorption bands of the nickel sulfate crystal.

The results of all these measurements both visual and photographic are shown in the graph of Fig. 2. The experimental points indicated by circles were determined by visual observations and those indicated by crosses were obtained photographically. Observations by the two methods were made to overlap as a check. All measurements were made at room temperature. These dispersion curves (1) and (2) are a composite of all the data secured, having been plotted on the basis that the crystals are mirror-images of each other. Wave-lengths in Angstrom units have been plotted as abscissae; rotations of the plane of polarization, in degrees per mm light path, have been plotted as ordinates. The crystals are optically inactive to light of 5030A. The rotation of the plane of polarization is opposite in sign on either side of this wave-length, i.e., if red light is rotated positively by a particular crystal, then that crystal will rotate blue light negatively. The curves are almost straight lines

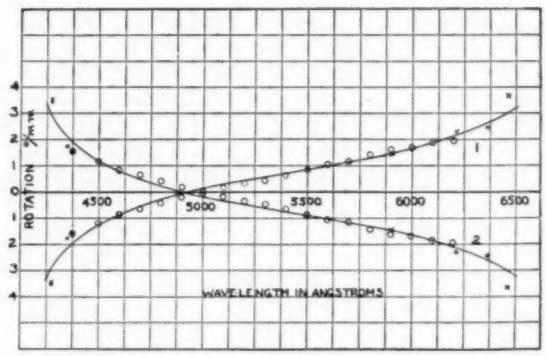

FIG. 2. Rotatory dispersion of α-$NiSO_4 \cdot 6H_2O$.

within the region 4600A to 6000A. However, beyond this region the dispersion begins to increase rapidly.

According to Drude the rotation of the plane of polarization is given by $\alpha_\lambda = \Sigma K_i/(\lambda^2 - \lambda_i^2)$, where α_λ is the rotation of the plane of polarization at the particular wave-length λ, λ_i's are the wave-lengths corresponding to the natural frequencies of the optically active groups, and the K_i's are constants for each term of the series. For the sake of simplicity it is assumed that the observed dispersion curve can be computed from a two term equation. Because of the long straight portions of the curves and the fairly abrupt changes in slope at the ends, it is not to be expected that a two term equation will fit over the entire range. Since the wave-lengths of the active absorption bands are of chief interest, the points for the computations were chosen so as to obtain a good fit in the curved regions, and yet not cause too great a departure in other portions. The points used for computation are

rotation (°/mm)	+2.95	+1.0	−1.0	−2.4
wave-length (microns)	0.428	0.455	0.560	0.630

The resulting equation is

$$\alpha_\lambda = \pm[0.33750/(\lambda^2 - 0.51661) + 0.10485/(\lambda^2 - 0.15634)].$$

This equation is plotted as the full line in Fig. 2. The agreement with the experimental points is reasonably close, but not within experimental error.

The constants of Drude's equation computed from our data predict absorption bands at 3954A and at 7187A. The transmission characteristics of the nickel sulfate crystals were measured from 4300 to 6300A by means of a spectrophotometer. The results are shown in the graph of Fig. 3. The absorption spectrum was also photographed with a quartz spectrograph. This photograph shows an absorption band whose center is located at 3890A. An absorption

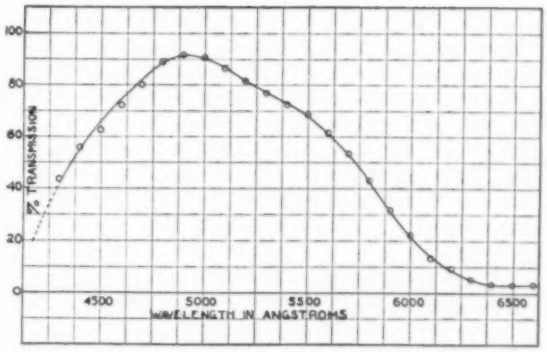

FIG. 3. Transmission curve for α-$NiSO_4 \cdot 6H_2O$. (1 mm thick.)

spectrogram of the aqueous solution does not show an appreciable shift of this absorption band, which is in accord with the work of Brewster, H. Becquerel[5] and others who have made observations on the absorption spectra of aqueous solutions of the nickel salts. Davis[6] reports a strong absorption band at 7200A for an aqueous solution of nickel sulfate.

CONCLUSIONS

The observations of Beevers and Lipson[2] in regard to the optical activity of α-hexahydrate nickel sulfate have been confirmed and extended quantitatively. Drude's equation has been fitted to the experimental data. The absorption bands computed on the basis of this equation are 3954A which is to be compared with the observed band at 3890A, and 7187A which may be compared with the 7200A band observed by Davis[6] in aqueous solutions of nickel sulfate.

An experimental technique has been devised on the basis of the method of Fizeau and Foucault[4] which greatly increases the light intensity available for photographic measurements.

[5] D. Brewster, H. Becquerel, Mellor, *A Comprehensive Treatise on Inorganic and Theoretical Chemistry*, Vol. 15 (1936), p. 74.

[6] Davis, *Studies on Solution in its Relation to Light Absorption, Conductivity, Viscosity, and Hydrolysis* (Carnegie Institution of Washington, 1918), p. 60.

Magneto-Optical Activity of Crystalline Nickel Sulfate, α-Hexahydrate[1]

F. G. Slack, R. T. Lageman* and N. Underwood
Vanderbilt University, Nashville, Tennessee

(Received June 13, 1938)

The dispersion of the Verdet constant of crystalline nickel sulfate, α-hexahydrate, has been measured through the visible spectrum. Temperature effect has also been investigated over a narrow range of temperatures. All measurements are made with the light path parallel to the optic axis of the crystal. The magnetic rotatory dispersion curve may be fitted by a single term electronic dispersion equation as suggested by Drude. Calculation on this basis indicates an active absorption band at 964A. The Verdet constant is found to be inversely proportional to the absolute temperature, throughout the range measured. The Verdet constant for the sodium D line is 0.0221 min./oersted-cm.

IT has seemed desirable to investigate the Faraday effect in comparatively simple paramagnetic crystals. Considerable work has been done by Becquerel[2] and his co-workers on some rather complex rare earth crystals, and Van Vleck[3] has shown these results to be of considerable theoretical interest. Of the paramagnetic crystals available in stable form few are satisfactory for optical work due to their opaque character or to difficulty in preparing optical surfaces. After some investigation it was found that the α-hexahydrate form of nickel sulfate is quite satisfactory for such measurements. This form occurs as blue tetragonal crystals with ready cleavage in the (001) plane. Fortunately also the optic axis of the crystal is perpendicular to this cleavage plane. No reports of previous observations of the magneto-optic activity of this form of the material have been found. The β-hexahydrate occurs as green monoclinic crystals but efforts to obtain or to prepare suitable specimens have been unsuccessful. Longchambon[4] has reported the optical activity of the heptahydrate. Efforts to obtain suitable specimens of this hydrate either in the pure form (unstable green rhombic crystals) or as the naturally occurring Morenosite were unsuccessful. Solutions of nickel sulfate have been found to be optically inactive[5] and the magneto-optic activity has been investigated by W. Koenig, by R. W. Roberts and by L. Longchambon.[6]

In this paper we desire to present the results of observations made on the tetragonal α-hexahydrate crystals of nickel sulfate with polarized light passing accurately parallel to the optic axis of the crystal that is perpendicular to the (001) cleavage face. A considerable number of crystals of different thicknesses (1.0–5.0 mm) were used. They were made by cleaving, with a specially mounted razor blade, large selected crystals from "Baker's analyzed" $NiSO_4 \cdot 6H_2O$. Samples of both right- and left-hand optically active crystals were used. They were mounted on a goniometer head which in turn was mounted on a spectrometer table so that proper orientation with respect to the direction of the magnetic field and the light path could easily be effected.

The observations were mostly made directly with a Schmidt and Haensch Lippich half-shade polarimeter. A special Leybold-Lange[7] drilled core electromagnet was suspended between the polarizer and analyzer of the polarimeter. With this arrangement magnetic fields up to 16,000 oersteds could easily be obtained for the small pole piece separations required. In order to prevent heating of the magnet, however, and for convenience in orienting the specimens and to make it possible to use only a portion of the field which is reasonably uniform, smaller currents

* Now at Ohio State University.

[1] F. G. Slack, R. T. Lageman and N. Underwood, Phys. Rev. **51**, 685A (1937).

[2] J. Becquerel, see W. Schütz, *Magneto-optik*, pp. 160–173.

[3] J. H. Van Vleck and M. H. Hebb, Phys. Rev. **46**, 17 (1934).

[4] M. L. Longchambon, Comptes rendus **173**, 89 (1921).

[5] N. Underwood, F. G. Slack and E. B. Nelson, Phys. Rev. **54**, 351 (1938).

[6] J. W. Mellor, *A Comprehensive Treatise on Inorganic and Theoretical Chemistry*, Vol. 15, p. 459.

[7] E. Leybold's Nachfolger A.-G. Special List No. 5, p. 26.

and greater pole piece separations were used so that the field ordinarily used was around 8000 oersteds. This field strength was determined by measuring the rotation of the plane of polarization in the field by samples of temperature-controlled water and carbon disulphide and by quartz and calibrated glass specimens. While the agreement among these calibration materials was excellent the values of the Verdet constants given in this paper are not considered absolute determinations. In all cases rotations were taken as one-half the net rotation obtained upon reversal of the magnet field current. The light source consisted of (1) a Pointolite source used with a monochromator placed in front of the polarimeter or (2) mercury and sodium arc line spectra used with appropriate filters. Some points on the curve were also checked by use of the set up described in the preceding paper[5] for photographic measurements though taken visually with the spectrometer telescope replacing the camera. Since agreement within experimental error was obtained in all cases no differentiation is made among the data taken in the different manners.

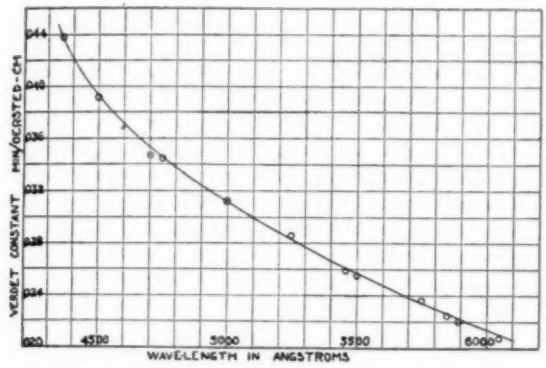

FIG. 1. Magneto-optic dispersion of α-$NiSO_4 \cdot 6H_2O$.

In order to make observations at reduced temperatures an asbestos paper jacket was fitted around the pole pieces and dry air was circulated through this and out through the pole piece borings. The air was cooled by passage through a copper coil immersed in solid carbon dioxide; the temperature was controlled by the depth of immersion of the coils and the quantity of air which passed through the coils. The temperature was read on a mercury thermometer extending from the jacket. The lowest temperature attained by this method was -15°C.

The results of the measurements are given in Figs. 1 and 2. Fig. 1 shows the magnetic rotatory dispersion for the nickel sulfate α-hexahydrate within the visible spectrum. Absorption bands[5] prevent further extension of the observations at both ends of the spectrum. Contrary to the anomalous natural rotatory dispersion[5] displayed by this material this curve shows a normal mag-

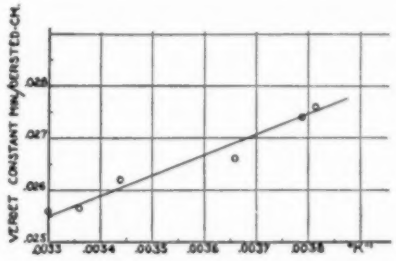

FIG. 2. Verdet constant of $\alpha \cdot NiSO_4 \cdot 6H_2O$ at λ5500 *vs.* reciprocal of absolute temperature.

netic rotatory dispersion. Wave-lengths of light in A are plotted as abscissae and Verdet constants in minutes per oersted centimeter as ordinates. These data are for room temperature. Fig. 2 shows the result at one wave-length (λ5500A) of temperature variation measurements. The reciprocal of absolute temperature is plotted as abscissae with Verdet constants as ordinates. This curve shows a linear relation between these factors to within the precision of measurement which is not high since actual crystal temperature was uncertain. Recent tests have indicated that it will be possible to make observations at much lower temperatures without damage to this crystal and it is hoped that this work may be continued in the near future.

The magnetic rotatory dispersion curve indicates the possibility of applying a simple electronic dispersion equation of the form suggested by Drude, Richardson and others.[6] The equation is used in the form

$$n_\lambda \delta_\lambda = K\lambda^2/[\lambda^2 - \lambda_1^2]^2 \qquad (1)$$

on the assumption of a single active absorption band. δ_λ is Verdet's constant as given in Fig. 1 n_λ is the index of refraction taken for this com-

[6] T. M. Lowry, *Optical Rotatory Power* (Longmans Green Co., 1935), p. 462–464.

putation from the work of Töpsoe and Christiansen as given by Mellor.[6] λ is the wave-length for which n_λ and δ_λ are measured. λ_1 is the equivalent absorption wave-length and K is a constant[9] such that:

$$K=(eb_1/2mC^2)\times 3437, \qquad (2)$$

where e/m is the ratio of effective charge to mass of the dispersing electrons, C is the velocity of light and b_1 the constant given in the Ketteler-Helmholtz dispersion equation[9]

$$n^2-1=b_0+b_1/(\lambda^2-\lambda_1^2). \qquad (3)$$

By substituting for various combinations of n_λ, δ_λ and λ in Eq. (1) average values of the constants were found to be $K=1.099\times10^{-10}$ and $\lambda_1=964\times10^{-8}$ cm. With this value of λ_1 in (3) the constants b_0 and b_1 were found to be $b_0=1.244$ and $b_1=1.324\times10^{-10}$. By substituting these values of K and b_1 in (2) e/m for the dispersing electrons is found to be 4.35×10^{17} e.s.u./g or 82 percent of the accepted value for the free electron. The wave-length of this absorption and the anomalous value of e/m are of the usual order of magnitude[10] for a substance showing normal diamagnetic magnetic rotatory dispersion. The equations representing this may thus be written

$$n_\lambda\delta_\lambda=1.099\times10^{-10}\lambda^2/[\lambda^2-(964\times10^{-8})^2]^2 \qquad (1a)$$

and

$$n^2-1=1.244+\frac{1.324\times10^{-10}}{\lambda^2-(964\times10^{-8})^2}. \qquad (3a)$$

These results indicate that the magnetic rotatory power found at normal temperatures and in the visible region of the spectrum is not affected by the absorption bands adjacent to each end of the visible region[5] but that an ultraviolet band at λ964A is effective. Nor does the paramagnetic character of the crystal (it is magnetic enough to support its own weight when placed in contact with the magnet pole piece) appear to introduce a paramagnetic term of sufficient magnitude to be observed within the range of observations. As stated above further work over an increased range of temperature and also at wave-lengths extending into the ultraviolet are contemplated. The Verdet constant of the nickel sulfate α-hexahydrate for the sodium D line was found to be $\delta_{5893}=0.0221$ min./oersted-cm.

The authors wish to express thanks to the National Research Council for a grant-in-aid during the summer of 1936 which made possible the beginning of this work.

[9] R. T. Lageman and F. G. Slack, Phys. Rev. **49**, 807 (1936).

[10] G. G. Darwin and W. H. Watson, Proc. Roy. Soc. **A114**, 474 (1927).

The Angular Distribution of Resonance Disintegration Products*

R. D. MYERS
Purdue University, Lafayette, Indiana
(Received June 2, 1938)

For resonance symmetry considerations alone are found to give definite results on the angular distribution of the products of nuclear reactions. Formulae are developed for general coupling and Russell-Saunders coupling. It is found that the distribution is axially symmetric about the direction of the incident particle. It is also symmetric about the equatorial plane. The expression for the distribution is usually restricted to a small number of terms in an expression in spherical harmonics. These results are applied to the reactions: $D^2+D^2\rightarrow H^3+H^1$; $B^{11}+H^1\rightarrow Be^8+He^4$, $Li^7+H^1\rightarrow 2He^4$, and $Li^6+H^2\rightarrow Li^7+H^1$. For Russell-Saunders coupling the distribution for these reactions is uniquely determined by the assignment of the quantum number to the states involved.

§1. INTRODUCTION

THE spatial distribution of the products of a nuclear disintegration has already been investigated experimentally for several reactions. The results were in some cases unexpected, e.g., for $H^2+H^2=H^3+H^1$ and for $B^{11}+H^1=3He^4$ large deviations from spherical symmetry were found. From these angular distributions important conclusions can be drawn about the mechanism of the nuclear reaction concerned. E.g., the symmetry of all observed distributions about the "equatorial plane" (plane perpendicular to the motion of the incident particle) gives strong evidence for the validity of the Bohr mechanism in the reactions studied (§3). It seems worth while to investigate theoretically, in a more quantitative way, how the angular distribution is connected with the angular momenta of the particles involved in the reaction.[1] To give a general treatment of this problem would require a specific nuclear model. However, the symmetry about the equatorial plane mentioned above shows that in all probability we are dealing with resonance disintegrations, and that only one level of the compound nucleus is important (§3). Under this assumption significant conclusions can be reached without detailed assumptions. In this paper we shall restrict our considerations to resonance disintegrations.

The state of the compound nucleus is characterized by its total angular momentum J and its parity. There are strict selection rules for both of these quantities. In particular the parity rule determines the permissible values of the relative orbital momentum l of the initial particles causing the reaction. We shall designate in the following by S the spin of the incident particle P and by i the spin of the initial nucleus A, although the theory is, of course, symmetrical in the two. In all practical cases the incident particle is very light (proton, neutron, deuteron, α-particle) and therefore has even parity. The rule for the parity can thus be formulated as:

I. The relative orbital momentum l of the initial particles must be even if the initial and compound nucleus have the same parity, and l must be odd, if they have opposite parity.

The angular momentum selection rule is:

II. $|\mathbf{i}+\mathbf{s}+\mathbf{l}|_{\min}\leqq J\leqq i+s+l$,

where $|\mathbf{i}+\mathbf{s}+\mathbf{l}|_{\min}$ is the smallest value which the resultant of the three vectors $\mathbf{i}$, $\mathbf{s}$, $\mathbf{l}$ can take. Corresponding rules hold for the final particles. Ordinarily, the knowledge of J and the parity alone does not determine the angular distribution completely. Additional assumptions must be made about the coupling of the various angular momenta. For light nuclei it is probably a good approximation to assume Russell-Saunders coupling.[2] Orbital momentum and spin are separately conserved. The compound nucleus has then definite values of L (total orbital momentum) and S (total spin). Similarly the

* Parts of this paper were submitted in a thesis for a doctor's degree at Cornell University.

[1] Reinsberg (Zeits. f. Physik **108**, 189 (1938)) has published a paper on this subject. His results are, however, based on incorrect selection rules.

[2] Oppenheimer and Serber, Phys. Rev. **53**, 636 (1938).

total momentum i of the initial nucleus is composed of an orbital part λ and a spin part σ. The spin s of the incident particle forms a resultant S with σ, and the intrinsic orbital momentum λ is coupled with the orbital momentum of relative motion l to form L. Then L and S are coupled to give J. In "allowed" transitions the total orbital momentum and total spin of the final nuclei, L' and S' are equal to L and S, respectively. The calculation becomes somewhat complicated since, for initial particles alone, four pairs of vectors must be considered, *viz.* $(\lambda\sigma)i$, $(\lambda l)L$, $(s\sigma)S$, $(L\,S)J$ (cf. §2). There is considerable simplification if the intrinsic momentum i of the initial nucleus is due entirely to spin,[3] as is probably the case for all nuclei up to Li^6. In this case, i and s form a resultant S, and S and l are compounded to give J. This case will be treated in detail in §2 of the present paper.

If Russell-Saunders coupling cannot be assumed, we have to sum the result over all possible values of S, taking interference into account. A particularly simple case arises again when there is no trace of the Russell-Saunders coupling left, i.e., when the probability of each value of S is proportional to its statistical weight. The quantitative results will then, in general, be different from Russell-Saunders coupling or intermediate coupling. Most of the qualitative results are, however, independent of the coupling assumed.

§2. Calculations

As already mentioned we shall assume that only one resonance level of the compound nucleus is involved. Then the cross section per unit solid angle for scattering through the angle θ, φ is given by:[4]

$$I(\theta,\varphi)=\frac{\pi^2\lambda_p}{(W-W_c)^2+\frac{1}{4}\Gamma_c^2}\left|\sum_{ll'm_{l'}M} e^{i(\delta_l+\delta_{l'})}(2l+1)^{\frac{1}{2}} \times \mathrm{H}^{JM}_{los m_s i m_i}\mathrm{H}^{*JM}_{l'm_{l'}s'm_{s'}i'm_{i'}} P_{l'm_{l'}}(\theta,\varphi)\right|^2, \quad (1)$$

where λ_p is the wave-length of the incident particle divided by 2π, l, l' the relative orbital momental of the initial and final particles, $m_{l'}$ the projection of l' on the direction of motion of the incident particle, i, s, m_i, m_s, the spins and their projectors for the initial particles, i', s', $m_{i'}$, $m_{s'}$ the same for the final particles, J, M the total angular momentum of the compound state and its projection, H the matrix element between the states as shown by the indices, δ_l the phase shift introduced by the potential between the particles, W, W_c the energy of the system and compound level, respectively, Γ_c the width of the compound level, P_{lm} the normalized spherical harmonic.

The angular distribution is most conveniently discussed if the intensity is expanded in spherical harmonics:

$$I(\theta,\varphi)=\frac{\pi^2\lambda_p{}^2}{(W-W_c)^2+\frac{1}{4}\Gamma_c^2}\sum_{pq}A_{pq}P_{pq}(\theta,\varphi). \quad (2)$$

By the customary Fourier method we find:

$$A_{pq}^{m_i m_s m_{i'} m_{s'}}=(2i+1)(2s+1)\int\left|\sum_{ll'm_{l'}M} e^{i(\delta_l+\delta_{l'})} \times(2l+1)^{\frac{1}{2}}\mathrm{H}^{JM}_{los m_s i m_i}\mathrm{H}^{*JM}_{l'm_{l'}s'm_{s'}i'm_{i'}} P_{l'm_{l'}}(\theta,\varphi)\right|^2 \times P^*_{pq}(\theta,\varphi)\sin\theta\,d\theta\,d\varphi. \quad (3)$$

Since in experiments one is not interested in the result for specific orientations of the spins of the particles, we only need the above expression averaged over the magnetic quantum numbers, *viz.*:

$$A_{pq}=\frac{1}{(2i+1)(2s+1)}\sum_{m_i m_s m_{i'} m_{s'}}A_{pq}^{m_i m_s m_{i'} m_{s'}}. \quad (3a)$$

Bethe and Placzek[5] have shown that this is facilitated by expressing the matrix elements as given above, as linear combinations of matrix elements between states of such symmetry that the matrix elements are independent of the magnetic quantum numbers. This is accomplished by expressing the wave functions describing the initial and final states as a linear combination of wave functions characterized by a definite resultant angular momentum. In accord with our considerations in §1, we consider the resultant J to be formed in two stages, *viz.*:

[3] A momentum entirely due to orbital motion would also give simple results.

[4] Bethe, Rev. Mod. Phys. **9**, 105 (1937).

[5] Bethe and Placzek, Phys. Rev. **51**, 450 (1937).

$i+s=j$, $j+l=J$, and $i'+s'=j'$, $j'+l'=J$. We have:

$$H^{JM}_{l'm_l's'm_s'i'm_i'}=\sum_{j'm'} C^{JM}_{l'm_l'j'm'}C^{j'm'}_{s'm_s'i'm_i'}\mathrm{H}^{J}_{l's'i'j'}, \quad (4)$$

where the C's are the coefficient common to all problems in which two angular momenta are combined to form a resultant and are defined:

$$C^{jm}_{lm_lsm_s}=\int\psi^*(lsjm)\psi(l_{m_l}sm_s)d\tau. \quad (5)$$

When (4) is introduced (3a), the summations over the spin orientations m_i m_s m_i' m_s' can be carried out at once by virtue of the orthogonality relations for the C's:

$$\sum_{m_sm_i} C^{jm}_{sm_sim_i}C^{j^*m^*}_{sm_sim_i}=\delta_{jj^*}\delta_{mm^*}. \quad (6)$$

We obtain

$$A_{pq}=\sum_{ll^*l'l^{*\prime}} e^{i(\delta_l+\delta_{l'}-\delta_{l^*}-\delta_{l^{*\prime}})}\mathrm{H}^{J}_{lsij}\mathrm{H}^{*J}_{l^*sij}\mathrm{H}^{*J}_{l's'i'j'}$$

$$\times H^{J}_{l^{*\prime}s'i'j'}(2l+1)^{\frac{1}{2}}(2l^*+1)^{\frac{1}{2}}\sum_{mMm'm_{l'}} C^{JM}_{lojm}C^{JM}_{l^*ojm}$$

$$\times C^{JM}_{l'm_l'j'm'}C^{JM}_{l^{*\prime}m_{l'}j'm'}A^{l'}_{l^{*\prime},\,p}C^{l'm_{l'}}_{l^{*\prime}m_{l'}pq}. \quad (7)$$

Here we have used the relation

$$\int P^{*}_{pq}P^{*}_{l^{*\prime}m_{l^{*\prime}}}P_{l'm_{l'}}=A^{l'}_{l^{*\prime},\,p}C^{l'm_{l'}}_{l^{*\prime}m_{l^{*\prime}}pq}. \quad (8)$$

The summation over the remaining magnetic quantum numbers is effected with the aid of the theorem (cf. Appendix):

$$\sum_{m_l,\,m} C^{JM}_{lm_ljm}C^{J^*M^*}_{l^*m_{l^*}jm}C^{l^*m_{l^*}}_{lm_lpq}=B^{l^*J^*}_{lJ,\,jp}C^{J^*M^*}_{JMpq}, \quad (9)$$

giving

$$A_{pq}=\sum_{ll^*l'l^{*\prime}jj'} [\text{part independent of } p \text{ and } q]$$

$$\times A^{l^{*\prime}}_{l',\,p}\mathrm{B}^{l^{*\prime}J}_{l'J,\,j'p}B^{Jl^*}_{Jl,\,jp}C^{l^*o}_{lopq}. \quad (10)$$

This formula is independent of the coupling and will be used in §3 for discussing qualitative results. Since, however, it involves summations over j, j', and the matrix elements will depend on specific nuclear properties, it can in general not be explicitly evaluated. This difficulty is removed if the intrinsic orbital momenta of the initial and final nuclei λ and λ' are both zero, in which case $j=j'=S-$the intrinsic spin of the compound state.

If Russell-Saunders coupling holds this difficulty can be circumvented if instead of (4) one uses the following:

$$H^{JM}_{lm_lsm_sim_i}=\sum_{m_\lambda m_\sigma M_LM_S} C^{im_i}_{\lambda m_\lambda\sigma m_\sigma}C^{LM_L}_{lm_l\lambda m_\lambda}$$

$$\times C^{SM_S}_{sm_s\sigma m_\sigma}C^{JM}_{LM_LSM_S}H^{J}_{lLS}. \quad (11)$$

If (11) is substituted into (3), although no formal summation over the magnetic quantum numbers has been obtained, one can write the results of the averaging in the form

$$A_{pq}=\sum_{l,\,l'l^*l^{*\prime}} F(H)\times f(p,q), \quad (12)$$

where f is determined only by the spatial symmetry and may be calculated by direct summation over the magnetic quantum numbers, and F depends upon the specific nuclear properties but is independent of p, q.

Equations (10), (12) determine the angular distribution completely if JLS and l are known. The first three are determined by the compound level concerned. l is usually fairly restricted by selection rules; at least for all reactions to which the theory will be applied in §4, the selection rules restrict the sum in (12) to one term. Except for the special case $\lambda=\lambda'=0$, the summation over j, j' makes (10) the less useful, although it is slightly more general.

§3. Discussion

We shall base the discussion of the result on Eq. (10). First of all, we note that the distribution is axially symmetric, since the coefficient $C^{l^*b}_{lopq}$ vanishes if $q\neq 0$. This result also follows from more general considerations since after averaging over the spins, the direction of the incident beam is the only characteristic direction.

Second, the distribution must be symmetric about the equatorial plane. This results from the

parity selection rule (I in §1). According to this rule, the outgoing wave can contain either only even or only odd orbital momenta l'. Therefore, l' and $l^{*\prime}$ are either both odd or both even, and from the definition of A in (8) it follows that p must be even, i.e., the angular distribution of the outgoing particles contain only even spherical harmonics, which means symmetry about the equatorial plane.

The condition for the validity of this rule is obvious. Either only one compound level must be involved (resonance disintegration) or, if several levels contribute, they must all have the same parity.

The number of terms in the expression in spherical harmonics (2) is very limited for any given nuclear process. The maximum value of p is determined by the fact that all the coefficients A, B, and C in (10) will vanish if p is greater than the sum of the corresponding upper and lower indices. For example if the particles are incident on s waves, the products are spherically symmetric even though p waves or even higher are present in the outgoing waves. Similarly disintegrations produced by p waves can have only $p=0$ and 2 in the intensity.[6]

Even with an incident wave of nonvanishing l, the angular distribution will be spherically symmetrical if $J=0$, and generally p must be $\leqslant 2J$. In the case of Russell-Saunders coupling (Eq. (12)) it follows in a similar way that $p \leqslant 2L$.

The interference between terms of different l, l^* (or $l', l^{*\prime}$) is similarly restricted by the fact that $|l-l^*| \leqslant p, |l'-l^{*\prime}| \leqslant p$.

One of the applications of the angular distributions will be the determination of the quantum numbers of compound states. In discussing actual reactions, it should of course be remembered that slow incident particles will in general only reach the nucleus when they have small orbital momentum l, i.e., $H^J{}_{lLS}$ is small for large l. On the other hand there is no such restriction for the outgoing particles which are usually fast.

§4. Discussion of Experimental Results

The distribution has been investigated experimentally by Neuert[7] for the α-particles of the reactions:

$$(1)\mathrm{Li}^7+\mathrm{H}^1\rightarrow\mathrm{Be}^8\rightarrow 2\mathrm{He}^4,$$
$$(2)\quad \mathrm{B}^{11}+\mathrm{H}^1\rightarrow\mathrm{C}^{12}\rightarrow\mathrm{Be}^8+\mathrm{He}^4,$$

and for the protons of the reactions:

$$(3)\quad \mathrm{H}^2+\mathrm{H}^2\rightarrow\mathrm{He}^4\rightarrow\mathrm{H}^3+\mathrm{H}^1,$$
$$(4)\quad \mathrm{Li}^6+\mathrm{H}^2\rightarrow\mathrm{Be}^8\rightarrow\mathrm{Li}^7+\mathrm{H}^1.$$

In the reactions (1) and (4) the distributions were isotropic, and in (2) and (3) the distributions are equatorially symmetric as is predicted for resonance disintegrations and have distinct minima at 90°. Bethe[8] has shown qualitatively how one may interpret these results. We shall summarize his arguments.

Reaction (4) is dismissed by noting that at low energies of the incident deuterons only s waves are effective in producing the disintegration and we have already noted this results in isotropy.

Reaction (1) is somewhat more complex. Since the α-particles obey Bose statistics and have no spin their relative motion must be symmetric, hence the parity of the final state is even, since the internal parity of an α-particle is even. Therefore, the initial state must also be even. But the internal parity of Li^7 is probably odd so that the relative motion must be odd and $l=1$. (This relation of $l=1$ may be connected with the observed low probability of this reaction.[9]) We would therefore expect anisotropy unless for the state of the Be^8 we have $J=0$. This value of J is therefore assumed.

The second reaction has been studied by Williams *et al.*,[10] and the excitation function of the homogeneous group of long range alphas, which are the ones for which the angular distribution has been investigated, showed a maximum at 180 Kev with a width of about 10 Kev. This corresponds to an excited level of C^{12} at about 16 Mev. This same level is associated with γ-ray emission, and was tentatively assigned $J=1$, odd parity.[11] Because of the rapidly decreasing penetration into the nucleus of the waves with increasing l, one expects that $l=0$ will be the dominant factor and one would find an isotropic distribution, unless some selection rule prevents

[6] I wish to thank Professor E. Teller for pointing out these restrictions for the special cases and suggesting their generality.

[7] Neuert, Physik. Zeits. **38**, 122 (1937).

[8] Bethe, Rev. Mod. Phys. **9**, 215 (1937).

[9] Goldhaber, Proc. Camb. Phil. Soc. **30**, 561 (1934).

[10] J. H. Williams, W. H. Wells, J. T. Tate, and E. L. Hill, Phys. Rev. **51**, 434 (1937).

[11] Bethe and Livingston, Rev. Mod. Phys. **9**, 276 (1937).

$l=0$ from giving rise to reaction. Since the distribution has been found anisotropic, we shall assume this to be the case. The simplest assumption is that the excited level of C^{12} is even. Then since the parity of the ground state of B^{11} is odd, only odd relative momenta will cause the reaction. Similarly since the parities of both Be^8 and He^4 are even, the relative momenta will be even. Further since both particles have zero spin, the relative momentum will be the same as the total angular momentum of the excited state. $J=0$ would lead to spherical symmetry so we must take $J=2$. We shall then classify the excited state of C^{12} as $^1D_2$ even. This assignment is not contradictory to the γ-transition since for nuclei dipole and quadripole transitions are almost equally probable. This assignment is also in agreement with the fact that the product particles must form a singlet state, since both Be^8 and He^4 have zero spin. The ground state of B^{11} is thought to be $^2P_{3/2}$, odd. With these assignments and supposing that L-S coupling holds rigorously, we find that the angular distribution is given by

$$I(\theta)=1+3\cos^2\theta. \tag{13}$$

This gives a greater anisotropy than that observed experimentally by Neuert. His results seem to be best represented by

$$I(\theta)=1+1.8\cos^2\theta. \tag{14}$$

If we return to expression (11) we find that when the spin and orbital momenta are not conserved separately the same assignments would lead to the more general result,

$$I(\theta)=A(1+3\cos^2\theta)+B\sin^2\theta, \tag{15}$$

where A and B are both positive constants whose relative values depend upon the strength of the interaction between spin and orbital momenta. We see, however, that the assumption of L-S coupling gives rise to the greatest anisotropy so that a partial relaxation of the spin selection rule would tend to bring the predicted and experimental results into agreement. After the completion of these calculations, Oppenheimer and Serber[12] have investigated the reaction $B^{11}+H'=Be^8+He^4$ much more thoroughly. They conclude, with the same arguments as given here, that the C^{12} level is even and has probably $J=2$, but they consider 5 different possibilities for this state ($^1D_2$, $^3P_2$, $^3D_2$, $^3F_2$, $^3F_4$) and 6 possibilities for the ground state of B^{11} ($^2P_{1/2,\ 3/2}$, $^2D_{3/2,\ 5/2}$, $^2F_{5/2,\ 7/2}$). Of these, only very few give an angular distribution compatible with Neuert's experiments, and none of these permits an explanation of the selection rule forbidding the production of long range alphas by protons with $s=0$ and of the occurrence of capture γ-rays along with the long range alphas.

The third reaction is probably not of the type to which our theory can be applied. Its excitation function has been studied and there is little evidence that it is of resonance type, but is well fitted by the Gamow function. Then too for such light nuclei the Bohr scheme is questionable. Calculations by Schiff[13] show that direct interaction between the initial and final wave functions already gives a larger cross section than observed. At the same time he has found a much smaller departure from a spherical distribution than is reported experimentally. If, however, one ignores these facts one can carry out the calculations on the basis of this theory. First the action of $l=0$ is excluded by supposing that the excited state has odd parity. Feenberg predicts such a state near the disintegration energy of the alpha-particle. Since the parities of all particles are even, the relative orbital momentum is most probably 1. Because the deuterons obey Bose statistics the odd orbital momentum necessitates a total spin 1 (triplet state). This is compatible with the spins of the outgoing particle ($\frac{1}{2}$ each). The compound state must therefore be a $^3P_1$ or $^3P_2$ state ($J=0$ is excluded because of the anisotropy). Since the ground state of all particles considered are S states $\lambda=\lambda'=0$, and Eq. (10) may be used with $j=1$, $S'=1$, and we obtain for

$$\begin{aligned} J&=1: \quad I(\theta)=1+\cos^2\theta, \\ J&=2: \quad I(\theta)=21\cos^2\theta+13. \end{aligned} \tag{16}$$

The experimental results of Neuert are represented by

$$I(\theta)=1+0.7\cos^2\theta. \tag{17}$$

This agreement would be satisfactory if it were not for the questionable assumptions which underlie the application of a resonance theory to

[12] Oppenheimer and Serber, Phys. Rev. **53**, 636 (1938).

[13] Schiff, Phys. Rev. **51**, 783 (1937).

this reaction. This reaction also proceeds in an alternate manner to give neutrons and He^3. One would perhaps expect the distribution of neutrons to be the same as that for the protons. This point does not seem to be settled experimentally, for although Kempton, Maasdorf, and Brown report it as such, more recently Oliphant at a conference reported a spherical distribution of the neutrons. If this latter should be the case one must suppose that mechanism of the reaction to be quite different. Two possibilities suggest themselves—that the s waves are responsible, or that the state of the compound nucleus has total angular momentum zero, either of which would lead, according to our results, to a spherical distribution. Since the yields of neutrons and protons are about the same and low, one is inclined to believe that p waves are primarily responsible—hence the intermediate state, one of total momentum zero.

It might finally be noted that only those reactions which have low yields would be expected to have an anisotropic distribution, since to have anisotropy p waves or those with larger orbital momentum must be primarily responsible. One should therefore investigate the distribution of the products of low yield reactions to find other distributions of interest.

In conclusion I wish to acknowledge the aid and valuable suggestions which Professor H. A. Bethe has given me in connection with this problem.

Appendix

In order to carry out the summation we utilized several theorems which will now be established.

The product of two angular functions can, because of the completeness of the system of such functions, be expressed:

$$\psi_{lm_l}(\theta_1)\psi_{sm_s}(\theta_2)=\sum_{jm}A^{jm}_{lm_lsm_s}\psi_{lsjm}(\theta), \tag{18}$$

where Θ_1, Θ_2 refer to all the angle variables of ψ_l, ψ_s, respectively, and Θ contains all the variables in both. If we operate on both sides of the expression (18) with the momentum operator[14] $(J_x+iJ_y)\hbar$ we get:

$$[(l-m_l)(l+m_l+1)]^{\frac{1}{2}}\psi_{lm_l+1}(\theta_1)\psi_{sm_s}(\theta_2)+[(s-m_s)(s+m_s+1)]^{\frac{1}{2}}\psi_{lm_l}(\theta_1)\psi_{sm_s+1}(\theta_2)$$

$$=\sum_{jm-1}[(j+m)(j-m+1)]^{\frac{1}{2}}A^{jm-1}_{lm_lsm_s}\psi_{jm}(\theta).$$

If we express the terms on the left in the manner of (18) and equate coefficients we find:

$$[(l-m_l)(l+m_l+1)]^{\frac{1}{2}}A^{jm}_{lm_l+1sm_s}+[(s-m_s)(s+m_s+1)]^{\frac{1}{2}}A^{jm}_{lm_lsm_s+1}=[(j+m)(j-m+1)]^{\frac{1}{2}}A^{jm-1}_{lm_lsm_s}.$$

If this is compared with the recursion relation for the m dependence of the C[15] we find that it is the same so that one may write

$$A^{jm}_{lm_lsm_s}=a^{j}_{ls}C^{jm}_{lm_lsm_s}.$$

In particular:

$$P_{lm}(\theta,\varphi)P_{l^*m^*}(\theta,\varphi)=\sum_{LM}A^{L}_{ll^*}C^{LM}_{lml^*m^*}P_{LM}(\theta,\varphi)$$

so that

$$\int P^{*}_{LM}P_{lm}P_{l^*m^*}=A^{L}_{ll^*}C^{LM}_{lml^*m^*}.$$

[14] Condon and Shortley, *Theory of Atomic Spectra*, p. 43.
[15] Reference 14, p. 74.

If we multiply $\psi_{ls jm}(\theta_1, \theta_2) = \sum_{m_s m_l} C^{jm}_{lm_l sm_s} \psi_{lm_l}(\theta_1)\psi_{sm_s}(\theta_2)$ by $\psi_{pq}(\theta_1)$.

By using the multiplication theorem, we get:

$$\sum_{l'j'm'} a^{l'j'}_{lj,\,sp} C^{j'm'}_{jmpq} \psi_{l'sj'm'}(\theta_1, \theta_2) = \sum_{l'm_{l'}m_l m_s} C^{jm}_{lm_l sm_s} b^{l'}_{lp} C^{l'm_{l'}}_{lm_l pq} \psi_{l'm_{l'}}(\theta_1)\psi_{sm_s}(\theta_2).$$

If now we multiply by

$$\psi_{l^*sj^*m^*}(\theta_1, \theta_2) = \sum_{m_l m_s} C^{j^*m^*}_{l^*m_l sm_s} \psi_{l^*m_l}(\theta_1)\psi_{sm_s}(\theta_2)$$

we get because of orthogonality

$$a^{l^*j^*}_{lj,\,sp} C^{j^*m^*}_{jmpq} = \sum_{m_l m_s} b^{l^*}_{lp} C^{jm}_{lm_l sm_s} C^{j^*m^*}_{l^*m_{l^*}sm_s} C^{l^*m_{l^*}}_{lm_l pq}.$$

By combining the b and a we get

$$B^{l^*j^*}_{lj,\,sp} C^{j^*m^*}_{jmpq} = \sum_{m_l m_s} C^{jm}_{lm_l sm_s} C^{j^*m^*}_{l^*m_{l^*}sm_s} C^{l^*m_{l^*}}_{lm_l pq}.$$

SEPTEMBER 1, 1938 PHYSICAL REVIEW VOLUME 54

The Static Interaction of Charged Particles

CHARLES D. THOMAS
West Virginia University, Morgantown, West Virginia
(Received May 16, 1938)

The energy of the field due to two charges as described by the field equations of the unquantized Born-Infeld theory is calculated to the first approximation in the case of stationary charges not subject to other external fields. The method of representing the field as the superposition of plane waves in a very large cavity is applied to the field equations expanded in a power series in the constant $1/b^2$ of the Born theory. For the first term this leads to the usual Coulomb energy. The process is then extended to calculate the second term from insertion of the coefficients arising in the first term evaluation. In this case it is found necessary to perform threefold averages in place of the previous single averages, since three of the radiation oscillators describing the field enter into combination. The resulting energy is $e_1e_2/r[1-(1/b^2)(e_1^2+e_2^2)/8r^4]$. The nature of the series expansion makes the method invalid in the region near 10^{-13} cm since there the series becomes divergent.

THE derivation of the energy of the field due to point charges from Maxwell's equations suggests that a somewhat similar procedure might be applied to arrive at the corresponding relation for field equations which are slightly different from those of Maxwell. Despite the persistent difficulties arising in the nonclassical, as well as in the classical theories, the belief that some such departure is necessary seems to be well founded. Whether the alteration should be introduced as a semi-classical concept before quantization, or arise in the process of quantization is not yet clear. In any case, it seems probable that for large fields or small distances the classical equations of Maxwell must be modified by the addition of a small nonlinear part. It is the purpose of the present discussion to calculate the interaction

of charged particles on the basis of the Born-Infeld equations in the simplest case, i.e., two stationary charges. The restriction to two particles is imposed only to simplify the index notation and facilitate the integration operations arising in a more complex system. The restriction to stationary charges is a more serious limitation, since in the region of validity of these calculations it is doubtful that any corresponding natural state would be appreciably influenced by the added terms. It seems advisable, however, to view first the simplest consideration, and thus to attempt to prescribe a means of reducing the averaging to a simple set of quadratures. Since the departure must be slight in the classical region (small charges and large inter-particle distances), the energy must closely approximate the Coulomb value in that region. The Coulomb part will, in fact, be taken as the first term of the series representing the total energy.

For the case treated here, Born-Infeld equations reduce to

$$\operatorname{div}\mathbf{D}=4\pi\Sigma e_i\delta(\mathbf{r}-\mathbf{r}_i),\quad \operatorname{curl}\mathbf{E}=0,$$
$$\mathbf{D}=\mathbf{E}(1-E^2/b^2)^{-\frac{1}{2}},\quad (1)$$

where δ is the Dirac δ function. These would, of course be the usual expressions in free space if $1/b^2$ were zero, hence this quantity will be used as the expansion parameter in the power series. The regions of convergence of such expansions are evidently limited by the relative magnitudes of the field strength and the value of the constant $1/b^2$. Eq. (1) may be written as

$$\operatorname{div}\mathbf{E}(1-E^2/b^2)^{-\frac{1}{2}}=\operatorname{div}(\mathbf{E}+\mathbf{E}E^2/2b^2+\cdots)$$
$$=4\pi\Sigma e_i\delta(\mathbf{r}-\mathbf{r}_i),\quad \mathbf{E}=-\operatorname{grad}\Phi.\quad (2)$$

When the quantities entering into (2), $\mathbf{E}$ and Φ, are expressed as a power series in $1/b^2$ as mentioned, e.g. $\mathbf{E}=\mathbf{E}^{(0)}+\mathbf{E}^{(1)}/b^2+\cdots$, and substituted into (2), one obtains a set of equations by equating coefficients:

$$\operatorname{div}\mathbf{E}^{(0)}=4\pi\Sigma e_i\delta(\mathbf{r}-\mathbf{r}_i),\quad \mathbf{E}^{(0)}=-\operatorname{grad}\Phi^{(0)},$$
$$\operatorname{div}\mathbf{E}^{(1)}=-\operatorname{div}\mathbf{E}^{(0)3}/2,\quad \mathbf{E}^{(1)}=-\operatorname{grad}\Phi^{(1)},\quad (3)$$
$$\cdots\cdots\cdots\cdots$$

The zero-order term is seen at once to have a solution possessing singularities, whereas $\mathbf{E}$ should remain finite. This inconsistency may be seen in a clearer light by returning for a moment to Eq. (1). The $\mathbf{E}$ value resulting from the distribution of charges e_i may be expressed in terms of $\mathbf{D}$ in a fashion similar to that in the spherically symmetric case. Here $\Sigma e_i/r_i^2$ replaces the single term e/r^2 of the spherically symmetric field. This will show $\mathbf{E}$ to remain finite even at one of the points r_i. However, if one makes use of the expansion of the sort under consideration,

$$\mathbf{E}=\mathbf{D}(1+D^2/b^2)^{-\frac{1}{2}}=\mathbf{D}(1-\tfrac{1}{2}D^2/b^2+\cdots),\quad (4)$$

it is seen that the first term, as well as each of the following, is singular. Actually such an expansion is not convergent for $D^2/b^2\geq 1$, and hence this apparent infinity of the separate terms of $\mathbf{E}$ is not of a troublesome nature.

The solution for the energy from the first-order term follows a procedure somewhat similar to one that has been applied to the equation here designated as the zero order,[1] and the latter will therefore be briefly outlined here in the restricted static case. The calculation cited, being applicable to a quantized non-static case, is more general than the one given below which is changed only in details that make it more adaptable to calculation of the higher order terms in the present consideration.

The Zero-Order Equation

The "hohlraum" method of treating the field as the superposition of plane waves is employed. For convenience, the unit of volume will be chosen so that the space is unity, which space must be very large in comparison to the distance between particles. The frequency density can easily be shown to equal $\nu^2 d\nu/(2\pi c)^3$ per solid angle $d\Omega$. This description of the field gives the zero order potential as

$$\Phi^{(0)}=N\Sigma a_\delta^{(0)}\cos(\mathbf{k}_\delta\mathbf{r}),\quad (5)$$

where $N=(8\pi c^2)^{\frac{1}{2}}$ is inserted for ease in handling the numerical factors. Poisson's equation now becomes

$$N\Sigma a_\delta^{(0)}k_\delta^2\cos(\mathbf{k}_\delta\mathbf{r}_\delta)=4\pi\Sigma e_i\delta(\mathbf{r}-\mathbf{r}_i).\quad (6)$$

If this is multipled by $\cos(\mathbf{k}_\delta\mathbf{r})$ and integrated

[1] E. Fermi, Rev. Mod. Phys. **4**, 87 (1932).

over the whole space,

$$a_\delta^{(0)} k_\delta^2 N = 8\pi \Sigma e_i \cos(\mathbf{k}_\delta \mathbf{r}_i). \quad (7)$$

It may be shown that for this case the Hamiltonian is $\Sigma \frac{1}{2} a_\delta^{(0)2} \nu_\delta^2$. This must be averaged over a finite region of space as well as summed over all directions of $\mathbf{k}_\delta$ and over all values of k (or ν). In the latter case the integration is performed after multiplying by the density function for ν_δ. Upon carrying out these averaging processes for the energy in a finite space, one finds the result to be $\Sigma(e_i e_j)/(2r_{ij})$ where $r_{ij} = r_i - r_j$ (the term involving $r_i + r_j$ has vanished because of its periodicity with respect to the radius vector). Thus, this equation leads to the ordinary Coulomb energy, but is not valid too near the center of charge.

The First-Order Equation

The method considered above will now be extended to the first-order equation of (3). This time three of the radiation oscillators enter into combination to give a pseudo-charge on the right-hand side. Consequently the averages must be taken simultaneously over three of the oscillators, and the integrations as well as the algebraic manipulation become correspondingly more tedious. In the outline of the procedure given below it is found more convenient to designate the negative of a wave number vector by an index different from that applied to the positive direction.

Since $\mathbf{E}^{(0)}$ is defined by $-\text{grad}\ \Phi^{(0)}$, the right-hand side of the equation for $\mathbf{E}^{(1)}$ may be expressed in terms of the $a^{(0)}$ of Eq. (7) This along with the introduction of the new set of ϕ's such that

$$\phi^{(1)} = N \Sigma a_\delta^{(1)} \cos(\mathbf{k}_\delta \mathbf{r})$$

reduces it to

$$\Sigma a_\delta^{(1)} k_\delta^2 \cos(\mathbf{k}_\delta \mathbf{r}) = -(N^2/2) \sum_{\sigma\lambda\mu} a_\sigma^{(0)} a_\lambda^{(0)} a_\mu^{(0)} \times (\mathbf{k}_\sigma \mathbf{k}_\lambda) \mathbf{k}_\mu \cdot (\mathbf{k}_\sigma + \mathbf{k}_\lambda + \mathbf{k}_\mu) \cos[(\mathbf{k}_\sigma + \mathbf{k}_\lambda + \mathbf{k}_\mu)\mathbf{r}]. \quad (8)$$

As before, this is multiplied by $\cos(\mathbf{k}_\delta r)$ and integrated over all space. Because of its periodicity in space, the right-hand side vanishes except for $\mathbf{k}_\delta$ equal to one of the sums $\mathbf{k}_\sigma + \mathbf{k}_\lambda + \mathbf{k}_\mu$. Hence (8) becomes

$$a_\delta^{(1)} k_\delta^2 = -(N^2/2) \Sigma a_\sigma^{(0)} a_\lambda^{(0)} a_\mu^{(0)} (\mathbf{k}_\sigma \mathbf{k}_\lambda)(\mathbf{k}_\mu \mathbf{k}_\delta). \quad (9)$$

The summation is to take place only over values such that $\mathbf{k}_\sigma + \mathbf{k}_\lambda + \mathbf{k}_\mu = \mathbf{k}_\delta$, therefore, in any on the averaging processes the average or summation need be taken only over three of the four k's as the fourth is thereby determined.

It is now necessary to find an expression for the energy in terms of the coefficients "a." Again successive approximations are resorted to and we find

$$4\pi U = b^2[(1 - E^2/b^2)^{-\frac{1}{2}} - 1] = \tfrac{1}{2} E^{(0)2} + 1/b^2 (\mathbf{E}^{(0)} \mathbf{E}^{(1)} + \tfrac{3}{8} E^{(0)4}) + \cdots. \quad (10)$$

When the $\mathbf{E}$'s are replaced and the space averaging performed, it is found that

$$U = \Sigma \tfrac{1}{2} a_\delta^{(0)2} \nu_\delta^2 + 1/b^2 [\Sigma a_\delta^{(0)} a_\delta^{(1)} \nu_\delta^2 + 3\pi c^4 \Sigma a_\sigma^{(0)} a_\lambda^{(0)} a_\mu^{(0)} a_\delta^{(0)} (\mathbf{k}_\sigma \mathbf{k}_\lambda)(\mathbf{k}_\mu \mathbf{k}_\delta)]. \quad (11)$$

The first term the zero-order energy is that already considered in the first part of the discussion. The next two terms, the first-order energy, exhibit a dissymmetry because one of them is written in terms of $a^{(1)}$). By substitution of (9) they may be combined into

$$-\pi c^4 \Sigma a_\sigma^{(0)} a_\lambda^{(0)} a_\mu^{(0)} a_\delta^{(0)} (\mathbf{k}_\sigma \mathbf{k}_\lambda)(\mathbf{k}_\mu \mathbf{k}_\delta). \quad (12)$$

Or by the introduction of the value of the $a^{(0)}$'s they are further reduced to

$$-N^2 \frac{\pi}{C^4} \Sigma e_i e_j e_m e_n \frac{(\mathbf{k}_\sigma \mathbf{k}_\lambda)(\mathbf{k}_\mu \mathbf{k}_\delta)}{(k_\sigma k_\lambda k_\mu k_\delta)^2} \cos(\mathbf{k}_\sigma \mathbf{r}_i) \times \cos(\mathbf{k}_\lambda \mathbf{r}_j) \cos(\mathbf{k}_\mu \mathbf{r}_m) \cos(\mathbf{k}_\delta \mathbf{r}_n). \quad (13)$$

Up to this point the discussion for both the zero and for the first orders in applicable to any number of singularities. The argument will henceforth be restricted to the simplest case, i.e. two charges only. There are three possibilities: (a) two of the subscripts of the r's (or of the e's) are identical, and belong to one of the particles, and the other two are identical, and belong to the second of the particles; (b) three of the subscripts belong to one particle; (c) all of the subscripts belong to one particle.

For case (a), one takes all combinations of equal subscript pairs and performs the space averaging on Eq. (13). The nonvanishing terms must have $\mathbf{k}_\sigma+\mathbf{k}_\lambda+\mathbf{k}_\mu=\mathbf{k}_\delta$, which terms may be shown to vanish[2] upon summing over all directions of $\mathbf{k}$ and integrating over all of its values. The physical meaning of the disappearance of these terms is at once evident if it is noted that the terms would involve $e_1^2e_2^2$ which would appear with the same sign whether the signs of the charges e_1 and e_2 were alike or opposite.

For case (*b*), however, there will be found to be a nonvanishing part. Here let $i=j=m\neq n$, which, upon taking the space average and making use of the fact that $\mathbf{k}_\sigma+\mathbf{k}_\lambda+\mathbf{k}_\mu=\mathbf{k}_\delta$, one finds that (13) reduces to

$$8\pi^3\Sigma e_i^3e_n\frac{(\mathbf{k}_\sigma\mathbf{k}_\lambda)(\mathbf{k}_\mu\mathbf{k}_\delta)}{(k_\sigma k_\lambda k_\mu k_\delta)^2}\cos(\mathbf{k}_\delta\mathbf{r}_{in}). \tag{14}$$

The scalar product part of this may be written as

$$(\mathbf{k}_\sigma\mathbf{k}_\lambda)(k_\delta^2-\mathbf{k}_\delta\mathbf{k}_\sigma-\mathbf{k}_\delta\mathbf{k}_\lambda). \tag{15}$$

For the direction and magnitude integrations of the first term of this, $\mathbf{k}_\sigma$, $\mathbf{k}_\lambda$, $\mathbf{k}_\mu$ are chosen as the variables since k_δ does not occur and it may also be eliminated from $\cos(\mathbf{k}_\delta\mathbf{r}_{in})$ by expanding it in terms of the other $\mathbf{k}$'s. After multiplication by the three density functions, for k_σ, k_λ, k_μ, the first term may now be summed over direction and magnitude for each separately. The final result for this part is, then,

$$-\Sigma e_i^3e_n/8r_{in}^5. \tag{16}$$

In considering the second part of (15) it is more convenient to choose $\mathbf{k}_\lambda$, $\mathbf{k}_\mu$, $\mathbf{k}_\delta$ as the wave number variables. Upon averaging as in the first part, it is found that this part vanishes.

The third part of (15) is exactly the same as the second except that the indices σ and λ are interchanged, hence this part also vanishes.

In case (*c*), one is dealing with the action of the charge on itself and, as pointed out in the first part of the discussion, the arguments used here are not valid when the distances are too small. Case (*c*) may, in fact, be considered as a special case of (*b*) where $i=j=m=n$, and an infinite part is obtained.

Thus for the first-order equation the only term remaining is (16). Combined with the zero order result, the interaction between two stationary particles is therefore given by this calculation to be

$$U=\frac{e_1e_2}{r}\left(1-\frac{1}{b^2}\frac{(e_1^2+e_2^2)}{8r^4}+\cdots\right).$$

The approximation is valid only so long as the value of $1/b^2$ is small enough with respect to the values of e and r that the series converges. In practical considerations, one would generally be concerned with charges in motion, the resulting terms of which may differ considerably from that for the static case.

[2] Except for the self-energy part.

The Process of Diffusion in a Centrifugal Field of Force. II

WILLIAM J. ARCHIBALD
Rouss Physical Laboratory, University of Virginia, Charlottesville, Virginia

(Received June 13, 1938)

The general equation for the settling of particles and molecules in a liquid suspension or ideal solution has been solved for the case of a cell with radial sides and two bounding cylindrical ends. A set of curves is given which shows the concentration at all points in the cell for different values of the time.

IN a previous article[1] the equation for the settling of particles and molecules in a liquid suspension or ideal solution in a centrifugal field of force was solved for the case of a sector shaped cell extending to the center of the centrifuge. It is the object of the present paper to find a solution of this equation for the case of a cell with radial sides and two bounding cylindrical ends. It is of great practical importance to obtain the solution for a cell of this type since this is the kind most commonly used in experimental determinations of molecular weights by the use of the ultracentrifuge. A solution based on a perturbation method has recently been given,[2] but the perturbation imposes such severe restrictions upon the quantities involved that the results are of mathematical interest only and are of little importance for comparison with experimental results.

The equation to be considered is[3]

$$\frac{1}{r}\frac{\partial}{\partial r}\left\{\left(D\frac{\partial c}{\partial r}-\omega^2 rsc\right)r\right\}=\frac{\partial c}{\partial t}, \tag{1}$$

in which c is the concentration of the solution, s the sedimentation constant, D the diffusion constant, ω the angular velocity of the rotor, and r the distance from the center of rotation to any point in the cell. (For a more precise definition of the quantities involved the reader is referred to the previous article[1] mentioned above.) The solution of (1) will give the concentration c as a function of r and t.

An acceptable solution, $c(r, t)$, must satisfy the following boundary conditions; (i) the net flow of dissolved substance through each cylindrical bounding surface is zero. This condition may be expressed mathematically by saying that

$$\frac{\partial c}{\partial r}-\delta rc=0 \quad \text{for } r=\begin{cases} r_1 \\ r_2 \end{cases}, \tag{2}$$

where r_1 and r_2 are the coordinates of the inner and outer bounding surfaces, respectively, and where $\delta=\omega^2 s/D$. (ii) When $t=0$ the function $c(r, t)$ represents an arbitrary initial distribution of concentration which is assumed to be known.

It can be shown[1] that a particular solution, $c(r, t)$, of (1) is

$$c(r, t)=M(\alpha; 1; z)e^{(\alpha-1)\tau} \quad (\tau=2\omega^2 st), \tag{3}$$

where α is a constant which is to be determined from the boundary conditions, and where $M(\alpha; \gamma; z)$ is a solution of the differential equation

$$\frac{d^2M}{dz^2}+\left(\frac{\gamma}{z}-1\right)\frac{dM}{dz}-\frac{\alpha}{z}M=0 \quad \left(z=\frac{\delta r^2}{2}\right). \tag{4}$$

In the case of the cell extending to the center of the rotor only that solution of (4) which is bounded at the origin was required. However, for the type of cell under discussion here, the relation (2) must be satisfied for two different values of r. Consequently it will be necessary to use the complete solution of (4), and the usefulness of the final result will depend in great measure upon how successful we are in our search for a solution which possesses simple and convenient properties.

In terms of the new variable z the first boundary condition becomes

$$\frac{d}{dz}M(\alpha; 1; z)-M(\alpha; 1; z)=0 \quad \text{for } z=\begin{cases} \delta r_1^2/2=a \\ \delta r_2^2/2=b. \end{cases} \tag{5}$$

[1] Archibald, Phys. Rev. **53**, 746 (1938).
[2] S. Oka, Proc. Physico-Mat. Soc., Japan **19**, 1094 (1937).
[3] Lamm, Arkiv. Mat., Astron., Fysik **21B**, No. 2 (1929).

From the theory of differential equations

$$M(\alpha;\gamma;z)=AF(\alpha;\gamma;z)+BW(\alpha;\gamma;z), \quad (6)$$

where A and B are constants and where $F(\alpha;\gamma;z)$ and $W(\alpha;\gamma;z)$ are two independent solutions of Eq. (4). The solution, bounded at the origin, is the confluent hypergeometric series; *viz.*

$$F(\alpha;\gamma;z)=1+\frac{\alpha}{1\cdot\gamma}z+\frac{\alpha(\alpha+1)}{1\cdot 2\cdot\gamma(\gamma+1)}z^2+\cdots.$$

A list of recurrence formulae for this function have been given by Webb and Airey.[4]

Several methods are available for determining a second solution $W(\alpha;\gamma;z)$ but not all of them lead to forms which are useful. If possible we should like the function $W(\alpha;\gamma;z)$ to possess the same recurrence formulae as $F(\alpha;\gamma;z)$. Such a function may be found in the following manner:

$F(\alpha;\gamma;z)$ can be expressed as the sum of two contour integrals as follows[5] (γ is assumed to be a positive integer):

$$F(\alpha;\gamma;z)=W_1(\alpha;\gamma;z)+W_2(\alpha;\gamma;z),$$

where

$$W_1(\alpha;\gamma;z)=\frac{\Gamma(\gamma)}{2\pi i}\int_C\left(1-\frac{z}{t}\right)^{-\alpha}e^t t^{-\gamma}dt,$$

and the contour C is a path in the t plane which comes from $-\infty$, encircles the point $t=0$ once in a counter-clockwise direction and returns to $-\infty$. W_2 is given by the same integrand, and a path that comes from $-\infty$, encircles the point $t=z$ once in a counter-clockwise direction and returns to $-\infty$.

It can be shown[6] that W_1 and W_2 are two independent solutions of Eq. (4). Consequently we are at liberty to choose for our function $W(\alpha;\gamma;z)$ either W_1 or W_2 or a linear combination of them both. However, for the purpose in hand, we are restricted to a choice which will give a real value for $W(\alpha;\gamma;z)$ whenever z is real. Such a choice is the following:

$$W(\alpha;\gamma;z)=\pi\cot\pi\alpha W_1(\alpha;\gamma;z)-i\pi W_2(\alpha;\gamma;z). \quad (7)$$

It can be shown that $W(\alpha;\gamma;z)$ as defined in (7) shares with $F(\alpha;\gamma;z)$ the three properties listed below, the first two of which will be needed subsequently. The third has been very useful for purposes of computation.

$$(d/dz)F(\alpha;\gamma;z)=(\alpha/\gamma)F(\alpha+1;\gamma+1;z), \quad (8a)$$

$$\alpha F(\alpha+1;\gamma+1;z)=(\alpha-\gamma)F(\alpha;\gamma+1;z)+\gamma F(\alpha;\gamma;z), \quad (8b)$$

$$\alpha F(\alpha+1;\gamma;z)=(z+2\alpha-\gamma)F(\alpha;\gamma;z)+(\gamma-\alpha)F(\alpha-1;\gamma;z). \quad (8c)$$

The expression for $W(\alpha;\gamma;z)$ is[7]

$$W(\alpha;\gamma;z)=F(\alpha;\gamma;z)\{\log z+\psi(1-\alpha)-\psi(\gamma)+C\}+\sum_{n=0}^{\gamma-2}\frac{\Gamma(\gamma)\Gamma(n+\alpha-\gamma+1)\Gamma(\gamma-n-1)(-1)^{n+\gamma}}{\Gamma(\alpha)n!z^{\gamma-n-1}}+\sum_{n=1}^{\infty}P_nQ_nz^n,$$

where

$$P_n=\frac{\Gamma(n+\alpha)}{\Gamma(\alpha)}\cdot\frac{\Gamma(\gamma)}{\Gamma(n+\gamma)}\cdot\frac{1}{n!},$$

$$Q_n=\left(\frac{1}{\alpha}+\frac{1}{\alpha+1}+\cdots+\frac{1}{\alpha+n-1}\right)-\left(\frac{1}{\gamma}+\frac{1}{\gamma+1}+\cdots+\frac{1}{\gamma+n-1}\right)-(1+\tfrac{1}{2}+\cdots+1/n),$$

$$\psi(a)=\Gamma'(a)/\Gamma(a),$$

$C=$ Euler's constant $=0.5772\cdots$.

(Extensive tables of the ψ function are available.[8]) It is the presence of the ψ functions in the expression for $W(\alpha;\gamma;z)$ which renders this solution a particularly suitable one. If they are omitted the expression is still a solution of Eq. (4) but the recurrence formulae (8) are no longer satisfied.

Consequently we choose (6) as the general solution of Eq. (4) where the functions F and W

[4] Webb and Airey, Phil. Mag. **36**, 129 (1919).
[5] Mott and Massey, *Atomic Collisions* (1933), p. 36.
[6] Whittaker and Watson, *Modern Analysis* (1927), p. 343.
[7] Cf. an article by the author to appear in a subsequent issue of Phil. Mag.
[8] Davis, *Tables of the Higher Mathematical Functions* (1933).

are defined above. If the expression for $c(r, t)$ given by Eq. (3) be substituted in the boundary condition (5) the following relations must hold:

$$\begin{aligned} &A\{F'(\alpha;1;a)-F(\alpha;1;a)\} \\ &\quad +B\{W'(\alpha;1;a)-W(\alpha;1;a)\}=0, \\ &A\{F'(\alpha;1;b)-F(\alpha;1;b)\} \\ &\quad +B\{W'(\alpha;1;b)-W(\alpha;1;b)\}=0. \end{aligned} \tag{9}$$

However, by virtue of (8a) and (8b)

$$F'(\alpha;1;a)-F(\alpha;1;a)=(\alpha-1)F(\alpha;2;a),$$

and

$$W'(\alpha;1;a)-W(\alpha;1;a)=(\alpha-1)W(\alpha;2;a).$$

These two equations enable (9) to be expressed in the simple form,

$$\begin{aligned} &(\alpha-1)\{AF(\alpha;2;a)+BW(\alpha;2;a)\}=0, \\ &(\alpha-1)\{AF(\alpha;2;b)+BW(\alpha;2;b)\}=0. \end{aligned} \tag{10}$$

Thus one permissible value of α is $\alpha=1$.

The system of Eqs (10) can have roots other than the trivial ones $A=0$, $B=0$ only if the determinant

$$\begin{vmatrix} F(\alpha;2;a), & W(\alpha;2;a) \\ F(\alpha;2;b), & W(\alpha;2;b) \end{vmatrix}$$

is equal to zero. Thus the permissible values of α (in addition to $\alpha=1$) are those values of α which satisfy the equation

$$\begin{aligned} &F(\alpha;2;a)W(\alpha;2;b) \\ &\quad -F(\alpha;2;b)W(\alpha;2;a)=f(\alpha)=0. \end{aligned} \tag{11}$$

Consequently we may take as the complete solution of Eq. (1)

$$\begin{aligned} c(z,t)=\sum_{n=0}^{\infty}\{&A_nF(\alpha_n;1;z) \\ &+B_nW(\alpha_n;1;z)\}e^{(\alpha_n-1)\tau}, \end{aligned} \tag{12}$$

where the α_n's are the roots of the equation

$$(\alpha-1)f(\alpha)=0.$$

From Eq. (10) we have

$$B_n=-\frac{F(\alpha_n;2;a)}{W(\alpha_n;2;a)}A_n=-K_nA_n.$$

Thus (12) may be written as

$$c(z,t)=\sum_{n=0}^{\infty}A_nM(\alpha_n;1;z)e^{(\alpha_n-1)\tau}, \tag{13}$$

where $M(\alpha_n;1;z)=F(\alpha_n;1;z)-K_nW(\alpha_n;1;z)$.

The coefficients A_n are determined by the application of the second boundary condition. For $t=0$ we have

$$c(z,o)=\sum_{n=0}^{\infty}A_nM(\alpha_n;1;z),$$

where $c(z, 0)$ is the initial distribution of concentration which will be taken to be constant and equal to c_0. It can be shown[1] that the functions $M(\alpha;1;z)$ are orthogonal in the range $a\leqslant z\leqslant b$ with the weight factor e^{-z}. Thus the coefficient A_n is given by

$$A_n=\frac{c_0\int_a^b e^{-z}M(\alpha_n;1;z)dz}{\int_a^b e^{-z}\{M(\alpha_n;1;z)\}^2dz}.$$

The two integrals occurring in the above expression may be integrated by methods outlined in the previous article by the author.[1] However, only for the case of the integral occurring in the numerator does a simplification result from so doing. The other integral can be more easily evaluated by numerical integration. For the first integral we get

$$\begin{aligned} &\int_a^b e^{-z}M(\alpha_n;1;z)dz \\ &\quad =(1/\alpha_n)\{be^{-b}M(\alpha_n;1;b)-ae^{-a}M(\alpha_n;1;a)\}. \end{aligned}$$

Thus the complete solution of Eq. (1) which satisfies the boundary conditions is

$$\begin{aligned} \frac{c}{c_0}=\sum_{n=0}^{\infty}\Bigg[&\frac{be^{-b}M(\alpha_n;1;b)-ae^{-a}M(\alpha_n;1;a)}{\alpha_n\int_a^b e^{-z}\{M(\alpha_n;1;z)\}^2dz} \\ &\times M(\alpha_n;1;z)\exp((\alpha_n-1)\tau)\Bigg]=\sum_{n=0}^{\infty}T_{\alpha_n}. \end{aligned} \tag{14}$$

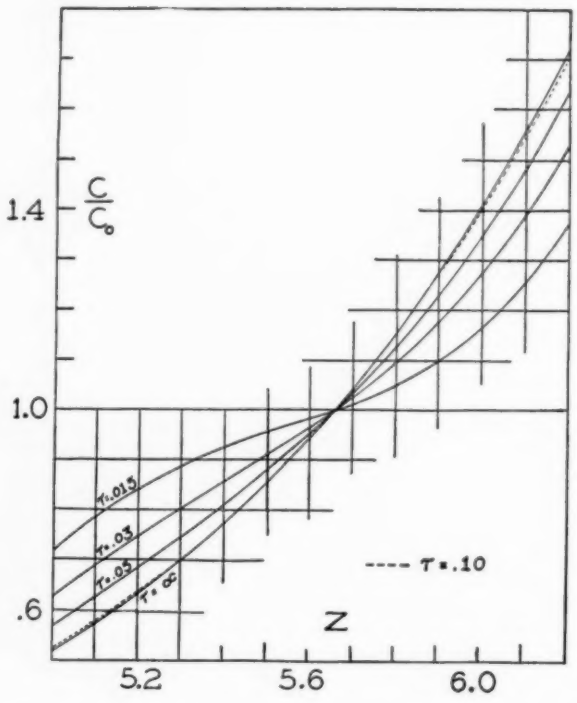

FIG. 1. Values of concentration change c/c_0 (c_0=initial constant concentration) as a function of position $z(=\omega^2 sr^2/2D)$ for various values of $\tau(=2\omega^2 st)$ when $a=5.0$ and $b=6.2$.

The term for which $\alpha=1$ can be greatly simplified. We have

$$M(1;1;z)=F(1;1;z)-\frac{F(1;2;a)}{W(1;2;a)}W(1;1;z)=e^z$$

since $W(1;2;a)=\infty$ and $F(1;1;z)=e^z$. Thus we may write (14) in the form

$$\frac{c}{c_0}=\frac{b-a}{e^b-e^a}e^z+\sum_{n=1}^{\infty}T_{\alpha_n}, \qquad (15)$$

where the α_n's are the roots of Eq. (11).

In actual problems the constants a and b are rather large and z which lies between them is also large. Hence it would be advantageous to have asymptotic expansions for the functions $F(\alpha;\gamma;z)$ and $W(\alpha;\gamma;z)$. These expansions are available since it can be shown that[9]

$$W_1(\alpha;\gamma;z)\sim\frac{\Gamma(\gamma)}{\Gamma(\gamma-\alpha)}(-z)^{-\alpha}G(\alpha,\alpha-\gamma+1;-z),$$

$$W_2(\alpha;\gamma;z)\sim\frac{\Gamma(\gamma)}{\Gamma(\alpha)}e^z z^{\alpha-\gamma}G(1-\alpha,\gamma-\alpha;z),$$

where G denotes the semi-convergent series

$$G(p,q;z)=1+\frac{pq}{z1!}+\frac{p(p+1)q(q+1)}{z^2 2!}+\cdots.$$

The recurrence formula (8c) and the asymptotic expansions for the functions involved enable computations to be made from Eq. (15) in a straightforward and relatively simple manner. The series (15) converges so rapidly that two or three terms give good accuracy.

The curves in Fig. 1 were calculated from Eq. (15). The constants were chosen to correspond to an actual experiment described by Svedberg,[10] in which the dissolved substance was carbon-monoxide hemoglobin which has a molecular weight $M=68{,}000$ and a partial specific volume $V=0.749$ cm³/g. For the cell used $r_1=4.16$ cm and $r_2=4.61$ cm. Also $\omega=290\pi$ and $T=293°$K. These data are sufficient to determine the two constants a and b. We have[1]

$$\begin{Bmatrix} a \\ b \end{Bmatrix}=\frac{M(1-Vp)\omega^2}{2RT}\begin{Bmatrix} r_1^2 \\ r_2^2 \end{Bmatrix}.$$

The numerical values are $a=5.0$ and $b=6.2$. The curves show that the concentration has reached its equilibrium value to a high degree of approximation when $\tau(=2\omega^2 st)$ has the value 0.10. Since $s=5\times10^{-13}$ for carbon-monoxide hemoglobin this corresponds to a time of 33 hours. In the actual experiment an exponential distribution of concentration had been reached after a period of 39 hours. This indicates an excellent agreement between theory and experiment.

The author wishes to express his appreciation to Dr. Beams who suggested the importance of this problem and to the School of Physics of the University of Virginia for the facilities provided.

[9] Mott and Massey, reference 5, p. 38.

[10] Svedberg, article in *Colloidal Chemistry, Theoretical and Applied*, edited by Alexander, Vol. 1, p. 851.

A Lower Limit for the Theoretical Energy of the Normal State of Helium

A. F. STEVENSON, *Department of Applied Mathematics, University of Toronto, Canada*
AND
M. F. CRAWFORD, *McLennan Physical Laboratory, University of Toronto, Canada*

(Received July 2, 1938)

The method of using a modification of Weinstein's lower limit for the energy, as given recently by one of the authors, has been applied to the normal state of helium, with the same sequence of functions as was employed by Hylleraas in his upper limit calculations. The ninth approximation leads to the lower limit -1.45508 Hylleraas units, which can very probably be increased to -1.45446, whereas the upper limit found by Hylleraas is -1.45187. The bearing of the results found on the probable location of the true eigenvalue is discussed, as is also the applicability of the method in general.

1. INTRODUCTION

IT is well known that the variational method, as ordinarily used in quantum mechanics, gives an upper limit to the energy. It is evidently desirable to be able to obtain also a lower limit, since in no other way can the accuracy of the result be judged with *certainty*, although the apparent convergence of the sequence of values obtained with the Ritz method may be a strong indication. An expression for a lower limit has been given by Weinstein,[1] although doubts have been expressed concerning its trustworthiness.[2] In a recent note by one of us,[3] however, it was shown that a rigorous proof of a modification of Weinstein's result can be given under assumptions which, though not rigorously proved, are nevertheless of the type made implicitly in many quantum-mechanical calculations, and are almost certainly true. At the same time, a method of applying this result was suggested. In this paper, the method is used to find a lower limit for the normal state of helium. This problem is, perhaps, of especial interest, since the well-known calculations of Hylleraas[4] have furnished an upper limit which is in very close agreement with the experimental value—a fact which is often cited as one of the striking successes of quantum mechanics.

[1] D. H. Weinstein, Proc. Nat. Acad. Sci. **20**, 529 (1934).
[2] See, for instance, J. H. Bartlett, Phys. Rev. **51**, 661 (1937), or W. Romberg, Physik. Zeits. Sowjetunion **8**, 516 (1935).
[3] A. F. Stevenson, Phys. Rev. **53**, 199 (1938).
[4] E. A. Hylleraas, Zeits. f. Physik **54**, 347 (1929); **65**, 209 (1930). We shall refer to these two papers as H I and H II, respectively.

2. THE LOWER LIMIT FOR EIGENVALUES

We shall first discuss the applicability of the method in general. The result already proved[3] is that if E_0 is the lowest eigenvalue, then $E_0 \geq L$, where the lower limit L is given in terms of a normalized trial function ψ by

$$L=\alpha-(I_2-2\alpha I_1+\alpha^2)^{\frac{1}{2}}, \tag{1}$$

where

$$I_1=\int \psi H\psi d\tau, \quad I_2=\int (H\psi)^2 d\tau,$$

and α is any number $\leq (E_0+E_1)/2$, where E_1 is that eigenvalue nearest to E_0 (and below the continuous spectrum) which has the same symmetry characteristics (with respect to permutation, rotation of axes, etc.) as the eigenfunction corresponding to E_0 (and which are supposed to have been correctly reproduced in the trial function).

A somewhat more general result, proved in an analogous manner, is the following: let the equation be $H\psi=E\rho\psi$ where H is self-adjoint in the complex sense

$$\left(\int f_1 H f_2 d\tau=\int f_2 H^* f_1 d\tau\right),$$

and let $E_0, E_1, \cdots$ be the eigenvalues, arranged in ascending order of magnitude, whose eigenfunctions $\psi_0, \psi_1, \cdots$ have all the same symmetry characteristics. Then if ψ is a trial function, normalized in the sense

$$\int |\psi|^2 \rho d\tau=1,$$

and which is *accurately* orthogonal to $\psi_0, \cdots, \psi_{n-1}$ the expression (1) furnishes a lower limit for the eigenvalue E_n, where now

$$I_1=\int \psi^* H\psi d\tau, \quad I_2=\int |H\psi|^2/\rho \cdot d\tau,$$

$$\alpha \leq (E_n+E_{n+1})/2.$$

We assume that E_{n+1} lies below the continuous spectrum, if there is any.[5]

For the remainder of this section, we shall confine ourselves to the lowest eigenvalue for simplicity. The expression (1), for given ψ, increases steadily[6] with α, so that the best value of α is its greatest allowable one, namely $(E_0+E_1)/2$. In order to apply (1), we therefore first fix α, choosing the greatest value for which the inequality $\alpha \leq (E_0+E_1)/2$ is safely satisfied, and then determine ψ so that L is a maximum, i.e., so that

$$I_2-2\alpha I_1=\text{minimum}. \tag{2}$$

The condition (2) lends itself to the Ritz method in the same way as the more usual upper limit method. Weinstein's original expression corresponds to the value $\alpha=I_1$, which is justified if $I_1 \leq (E_0+E_1)/2$.[7] Romberg[8] has proposed the empirical expression $-I_2^{\frac{1}{2}}$ as a lower limit, which is obtained from (1) with $\alpha=0$. As already pointed out,[3] Romberg's expression depends on the zero of energy; it can, in fact, always be made to fail by proper choice of this zero. Ordinarily, it is true, the zero is chosen to be at some stage of ionization, but examples can be given where it fails even when this "natural" choice is made.[9] Thus although Romberg's expression may well be correct in particular cases, it is clear that no reliance can be placed on it in general. We may here mention that Romberg's[8] example purporting to show that Weinstein's expression (with $\alpha=I_1$) may fail, is not valid, for the restriction $I_1 \leq (E_0+E_1)/2$ has not been taken into account; when this is done, no contradiction is obtained.

The lower limit (1) will usually only be a good approximation to the eigenvalue E_0 if the "mean square deviation"

$$\left(I_2-I_1^2=\int [(H-I_1)\psi]^2 d\tau\right)$$

is small. It is clear that this is a more stringent requirement on ψ than is necessary to make the "mean energy" I_1 a good approximation, so that we may expect that, with any given trial function, the upper limit will give a better result than the lower limit. It is possible that an exception to this statement might occur if E_1 lies far above E_0, so that a large value of α could be taken. Moreover, the lower limit is more laborious to calculate than the upper, so that the present method cannot compete with the more usual one if it is merely desired to find an approximation to the energy, but is only of value when limits to the error are required. It is possible, also, that the function obtained by the lower limit method may be a better approximation to the true eigenfunction for some purposes, since it probably yields a function whose derivatives represent more closely the actual derivatives.[10]

3. Application to the Normal State of Helium

We shall use the notation and units of Hylleraas, namely: unit of length $=a_0/4$, unit of energy $=4$ rydbergs; and for coordinates: $s=r_1+r_2$, $t=r_1-r_2$, $u=r_{12}$. The Hamiltonian is $H=T+V$, where the kinetic and potential energy operators are given by[11]

[5] The result $E_n \leq \alpha+(I_2-2\alpha I_1+\alpha^2)^{\frac{1}{2}}$ provided $\alpha<E_n$, may be proved analogously (cf. Weinstein, reference 1). But this upper limit increases steadily with α, so that the best value is reached for $\alpha=-\infty$, which gives $E_n \leq I_1$, which is the usual upper limit expression.

[6] The geometrical picture is useful: L, plotted against α, is a branch of a hyperbola which has the lines $L=I_1$, $L=I_1+2(\alpha-I_1)$ as asymptotes. The smaller the quantity $I_2-I_1^2$, the closer the hyperbola approaches its asymptotes. In the limiting case of $I_2=I_1^2$ (exact solution), the hyperbola degenerates into its asymptotes, and $L=E_0$ for any $\alpha \geq E_0$.

[7] This restriction was mentioned by Weinstein, Phys. Rev. **41**, 839 (1932).

[8] W. Romberg, reference 2.

[9] Thus consider the lowest state of the hydrogen atom, with the trial function $\psi=r^3e^{-kr}$. Then not only does Romberg's expression fail for sufficiently small k (this is *always* so when a scale factor is used), but it even fails for the value of k which is "best" from the point of view of minimizing the upper limit.

[10] Cf. the discussion by James and Coolidge, Phys. Rev. **51**, 860 (1937).

[11] These results follow, e.g., from the variational principle given in H I.

$$-\tfrac{1}{8}T\psi=\frac{\partial^2\psi}{\partial s^2}+\frac{\partial^2\psi}{\partial t^2}+\frac{\partial^2\psi}{\partial u^2}+2\frac{s(u^2-t^2)}{u(s^2-t^2)}\frac{\partial^2\psi}{\partial s\partial u}$$
$$+2\frac{t(s^2-u^2)}{u(s^2-t^2)}\frac{\partial^2\psi}{\partial t\partial u}+\frac{4s}{s^2-t^2}\frac{\partial\psi}{\partial s}$$
$$-\frac{4t}{s^2-t^2}\frac{\partial\psi}{\partial t}+\frac{2}{u}\frac{\partial\psi}{\partial u},$$

$$V\psi=\left[-\frac{16s}{s^2-t^2}+\frac{2}{u}\right]\psi.$$

For the trial function, we choose, with Hylleraas,[12]

$$\psi=\phi(ks, kt, ku), \tag{3}$$

where $\phi(s, t, u)=e^{-s/2}\times$(polynomial in s, t^2, u)

$$=\sum_{n=0}^{\infty}c_n\phi_n(s, t, u), \text{ for example.} \tag{4}$$

The following nine functions were used:

$$\phi_0=(1/2)e^{-s/2}, \qquad \phi_1=(1/6)se^{-s/2},$$
$$\phi_2=(1/6)ue^{-s/2}, \qquad \phi_3=(1/24)t^2e^{-s/2},$$
$$\phi_4=(1/24)s^2e^{-s/2}, \qquad \phi_5=(1/24)u^2e^{-s/2},$$
$$\phi_6=(1/24)sue^{-s/2}, \qquad \phi_7=(1/120)t^2ue^{-s/2},$$
$$\phi_8=(1/120)u^3e^{-s/2},$$

the numerical factors being inserted for convenience and to accord with H II.

Substituting (3) and (4) in the variational principle (2), and minimizing with respect to the c's, we obtain, in the usual way, the determinantal equation

$$|k^4A_{ij}+k^3B_{ij}+k^2C_{ij}$$
$$-2\alpha(k^2M_{ij}+kP_{ij})-\lambda N_{ij}|=0, \tag{5}$$

where $\lambda=I_2-2\alpha I_1$, $A_{ij}=\int T\phi_iT\phi_j d\tau$,

$$B_{ij}=\int(T\phi_iV\phi_j+T\phi_jV\phi_i)d\tau,$$

$$C_{ij}=\int V\phi_iV\phi_j d\tau, \quad M_{ij}=\int\phi_iT\phi_j d\tau, \tag{6}$$

$$P_{ij}=\int\phi_iV\phi_j d\tau, \qquad N_{ij}=\int\phi_i\phi_j d\tau.$$

The symbol $\int d\tau$ in (6) denotes

$$\int d\tau=\tfrac{1}{8}\int_0^{\infty}ds\int_0^{s}du\int_0^{u}dt\cdot u(s^2-t^2),$$

the factor $\frac{1}{8}$ being introduced for convenience and to accord with H II.

The integrals M, P, N are given at once from the tables in H II[13] (though the integrals M, P were calculated independently as a check). The somewhat laborious integrals A, B, C were not previously available, and were calculated and carefully checked. The results are given in Table I.[14]

Equation (5) must be solved for λ and the lowest root minimized with respect to k. The lower limit is then immediately given by $L=\alpha-(\lambda+\alpha^2)^{\frac{1}{2}}$. The constant α must first be fixed. As regards the ground state, the results of the present paper justify *a posteriori* the assumption that $E_0>-1.455$, while for the level E_1—in this case the $1s2s\,^1S$ level—the experimental value is about -1.073, while the theoretical calculation of Hylleraas and Undheim gave -1.07245, which is known to be too high.[15] Thus the value $\alpha=-1.3$ is seen to allow an ample margin for safety, while the value $\alpha=-1.27$ is in all probability also allowable. The detailed calculations were all made with the value $\alpha=-1.3$, but in the final

[12] The Hylleraas function is such that $H\psi$ has singularities which are not, of course, present for the correct eigenfunction, and it might be thought that this would affect the lower limit more adversely than the upper. It could be avoided, for instance, by multiplying the function by the factor $u^2(s^2-t^2)^2$. But this would introduce nodes into the function which should not be there and would also make the calculations more laborious. It was decided, therefore, to use the original Hylleraas functions.

[13] Our M, N are precisely the same as those of H II, while our $P_{ij}=L'_{ij}/2-L_{ij}$ in the notation of that paper.

[14] The integrals are all either rational numbers or else linear functions of the quantities log 2 or π^2 with rational coefficients. As some of the expressions are quite complicated, however, they have all been given in decimal form to 8 places. The last figure is uncertain in some cases.

[15] See, for instance, H. Bethe, *Handbuch der Physik*, second edition, Vol. 24, p. 366.

TABLE I. *Values of integrals A, B and C.*

ij	A_{ij}	B_{ij}	C_{ij}	ij	A_{ij}	B_{ij}	C_{ij}
00	12.00000000	−28.50000000	18.66666667	28	21.33333333	− 57.33333333	48.44444444
01	8.00000000	−28.50000000	24.88888889	33	46.22222222	− 64.58333333	25.75238095
02	9.83333333	−27.67602874	20.53713985	34	15.11111111	− 56.91666667	41.14444444
03	12.66666667	−23.25000000	11.75555556	35	30.66666667	− 60.75000000	33.61111111
04	3.33333333	−26.25000000	31.11111111	36	24.34722222	− 59.68380873	36.91248685
05	8.00000000	−25.41666667	22.00000000	37	59.37222222	− 89.51131767	38.19609000
06	6.20833333	−26.26170260	25.67142482	38	40.31666667	− 84.22564774	49.51987627
07	11.90000000	−22.87404311	12.65570978	44	19.55555556	− 82.50000000	108.88888889
08	6.50000000	−22.90842587	23.20009254	45	17.33333333	− 71.69444444	77.00000000
11	11.55555556	−41.00000000	41.48148148	46	18.19444444	− 77.05922055	89.84998685
12	11.38888889	−38.78713985	34.22856642	47	24.49444444	− 80.57276727	59.05997890
13	15.11111111	−38.75000000	23.51111111	48	24.08333333	− 96.91966036	108.26709849
14	11.55555556	−51.25000000	62.22222222	55	32.88888889	− 78.69444444	60.55555556
15	13.33333333	−46.25000000	44.00000000	56	27.17618296	− 77.08933885	67.66693655
16	12.66666667	−49.01560346	51.34284963	57	43.90641921	− 87.29687209	49.51987627
17	18.63333333	−46.30118296	29.52998949	58	44.97246898	−110.62808623	87.90308623
18	14.16666667	−51.78070978	54.13354925	66	25.38383498	− 78.30555556	77.00000000
22	17.49127392	−39.88888889	29.33333333	67	35.57442380	− 85.08888889	53.77777778
23	21.38888889	−40.25011976	21.09284963	68	36.26666667	−106.40000000	96.88888889
24	10.11111111	−47.95224618	51.34284963	77	90.85444620	−143.73111111	64.24000000
25	20.18539082	−49.73626534	38.66682089	78	68.37333333	−140.58000000	82.80000000
26	17.49127392	−49.86111111	44.00000000	88	76.16000000	−184.06000000	145.09333333
27	25.08120397	−48.62222222	26.88888889				

approximation the value $\alpha=-1.27$ was also considered.

As regards the scale factor k, the upper limit calculation (H I and H II) gives $k=0.844$ in first approximation (i.e., with one function), and $k\leqq 0.9$ for the higher approximations. In our case, the first approximation gave $k=0.907$, and trials with different values of k for the third approximation gave a minimum for λ at $k\leqq 0.935$. The value $k=0.93$ was therefore adopted for the sixth and ninth approximations.

The results obtained, from 1, 3, 6, and 9 functions are given in Table II, where the upper limits found by Hylleraas are also given for comparison. We also give (except for the final approximation) the lower limit obtained by using the Hylleraas "upper limit" function; the value for the sixth approximation is obtained by using the value of I_2 calculated by Bartlett, Gibbons, and Dunn[16] for this particular case. The improvement obtained by maximizing L directly is seen to be significant.

Our results, combined with those of Hylleraas, enable us to say with certainty that the lowest eigenvalue lies between the limits

$$-1.45508<E_0<-1.45187, \qquad (7)$$

the "spread" between these values being 0.174 ev. We can improve our value slightly by using the value $\alpha=-1.27$ (cf. above). The new value of L was estimated approximately from the first order formula

$$\delta L=[1-(\alpha-I_1)/(I_2-2\alpha I_1+\alpha^2)^{\frac{1}{2}}]\delta\alpha$$

and utilization of the Hylleraas value -1.45187 for I_1. (Actually it can be seen that a complete recalculation of L with the new value of α would yield a slightly better value for L). We thus obtain the limits

$$-1.45446<E_0<-1.45187. \qquad (8)$$

The spread is then 0.140 ev.

It has been shown by Coolidge and James[17] that the use of the Ritz method with the Hyl-

TABLE II. *Upper and lower bounds for the energy of the normal state of helium. Unit of energy=4 Rydbergs.*

FUNCTIONS USED	UPPER LIMIT (HYLLERAAS)	LOWER LIMIT	LOWER LIMIT, WITH "UPPER LIMIT" FUNCTION
ϕ_0	−1.42188	−1.77015	−1.7896
ϕ_0, ϕ_2, ϕ_3	−1.45122	−1.47407	−1.4864
$\phi_0-\phi_5$	−1.45162	−1.46073	−1.46519
$\phi_0-\phi_8$	−1.45187	−1.45508	

[16] J. H. Bartlett, J. J. Gibbons, and C. G. Dunn, Phys. Rev. **47**, 679 (1935).

[17] A. S. Coolidge and H. M. James, Phys. Rev. **51**, 855 (1937).

leraas functions yields an upper limit which converges to the true eigenvalue E_0, and their proof can easily be extended to show that the lower limit must also converge to E_0 provided $E_0<\alpha\leqq(E_0+E_1)/2$. The spread between the limits in either (7) or (8) is, however, much greater than the experimental error, so that it cannot be said that complete finality in the helium problem has yet been reached. To carry the approximation farther would be very laborious. Nevertheless, it is probable that E_0 lies close to the Hylleraas value -1.45187, for, as mentioned above, the upper limit is almost certainly a better approximation than the lower limit at any stage of the process, and further, the trend of the values in Table II indicates that the upper limit sequence has converged much more nearly to its limiting value than has the lower limit sequence. However, the fact that the convergence of the latter has also slowed up considerably in going from the sixth to the ninth approximation indicates that possibly E_0 does not lie quite so close to the Hylleraas value as has been generally supposed. On the other hand, the Hylleraas value agrees very closely with the experimental value when the small corrections due to relativity and nuclear motion are included.[18]

[18] H. Bethe, reference 15, 359.

SEPTEMBER 1, 1938 PHYSICAL REVIEW VOLUME 54

The Effect of a Direct Electric Field on the Laue Diffraction Photograms

A. Němejcová and J. Brož
Institute of Spectroscopy of Charles University, Prague, Czechoslovakia

(Received April 20, 1938)

The effect of a direct electric field (d.e.f.) on the Laue photograms of silica, mica and gypsum crystals has been investigated. It was found that under the action of a d.e.f. (1) the intensity of the Laue reflections is increased, (2) the central spot (which is caused by the rays passing directly through the crystal and the rays reflected backward) is made narrower. If the d.e.f. was applied to the crystals through Al coatings deposited by evaporation on both surfaces of the crystals, the narrowing of the central spot increased only up to a certain intensity of the d.e.f. used. In this case also a time influence was observed. That is to say, if the d.e.f. was applied for a longer time or if sufficiently aged Al coatings were used, the difference in the central spot with and without the d.e.f. disappeared. It was proved that the observed narrowing of the central spot is caused by the alternations provoked in the crystal lattice itself by the d.e.f. and not by the specific properties of the Al coatings. This was done by using instead of the Al coatings obtained by evaporation thin foils of Al pressed on both crystal surfaces for the application of the d.e.f. In this case also the narrowing of the central spot was observed but no time influence was found. The observed phenomena are explained partly by the perfection of the crystal lattice, partly by the shift of the positive and negative ions of the crystal and the positive metallic ions of the deposited Al coatings, which take place in a d.e.f.

MANY authors have studied the influence of electric oscillations, generated in piezoelectric crystals by means of an alternating electric field, on the intensities and the structure of the Laue reflections.[1] It has been found that under the action of electric oscillations the intensity of the Laue spots increases in their intermediate parts, which are due to the reflection of the interior part of the oscillating crystal plate under investigation. Besides this, Fox and Fraser[2] have ascertained that at the same time a widening of the central spot mainly due to the primary x-ray beam takes place. An explanation of these observed phenomena was given[3] by assuming that the perfection of the crystal lattice is disturbed by electric oscillations not only on both surfaces of the crystal plate but also in its interior part which thus contributes to the increase of the intensity of the Laue reflections.

[1] E.g., Fox and Carr, Phys. Rev. **37**, 1622 (1931); Colby and Harris, Phys. Rev. **43**, 562 (1933); Fox and Cork, Phys. Rev. **38**, 1420 (1931); Barrett and Howe, Phys. Rev. **39**, 889 (1932); Nishikawa, Sakisaka, Sumoto, Phys. Rev. **43**, 363 (1933); Jauncey and Deming, Phys. Rev. **48**, 462 (1935).

[2] Fox and Fraser, Phys. Rev. **47**, 15 (1935).

[3] Langer, Phys. Rev. **38**, 573 (1931); **49**, 206 (1936).

In this case the width of the wave-length range ($\Delta\lambda'$) reflected from the continuous incident x-radiation is greater than that ($\Delta\lambda$) of a crystal at rest. The central spot is formed not only by rays passing directly through the crystal but also by rays reflected backward. Dispersion of these rays is greater, the greater is $\Delta\varphi'$ as calculated on the basis of $\Delta\lambda'$, from the Bragg equation. As a result of this, a widening of the central spot in the case of an oscillating crystal takes place. The influence of the imperfection of the crystal lattice on the structure of Laue reflections was then affirmed by results obtained both for crystals with a perfect lattice (silica) as compared with those for crystals with imperfect lattice (rock-salt). This was further proved with crystals whose lattices were intentionally disturbed to a depth of 0.1 mm by polishing[4] the crystal with emerald, and finally with crystals whose lattices were disturbed as the result of an uneven drop of temperature or uneven mechanical strains.[5] Conversely the effect of the perfection of the crystal lattice was investigated by gradually etching away the imperfect surface layers.[2]

As for the influence of a d.e.f. on the crystal lattice, Német[6] found by the Bragg method differences in the intensities of the lines only in the case of Rochelle salt and ice, whereas the differences for the majority of other crystals lay within the limits of experimental errors. The differences in intensity obtained by Hengstenberg[7] and Bennett[8] for crystals with and without the action of a d.e.f. are similarly not of such magnitude as to be compared with the results obtained in the present investigation. Dolejšek and Jahoda[9] also did not observe any appreciable change in the intensity of reflection when they studied the changes of the value of the grating constant under the influence of a direct electric field.

The aim of this work is to show the results obtained when we investigated the influence of a d.e.f. on the structure of Laue reflections and of the central spot for the case of piezoelectric (silica) and apiezoelectric (mica, gypsum) crystals.

The direct electric field was applied to the plates of the crystals by means of aluminum coatings which were deposited directly on both surfaces of the crystal plates by the evaporation of aluminum in high vacuum. These aluminum coatings were deposited so thinly, that on exposure they showed practically no Debye-Sherrer interferences corresponding to the characteristic radiation of the anode of the x-ray tube. As the source of x-rays, a Roentgen tube with Cu anode and Lindemann windows was used; at a voltage of 40 kv and a current of 10 ma the time exposures were 15 minutes.

Experimental Results

(1) Silica

The influence of the d.e.f. was studied on two silica plates cut vertically to the electric axis. Their thickness was 0.4 and 0.1 mm, respectively. The potential differences applied amounted to 400, 600, and 1000 volts, which correspond to an intensity variation of the electric field of 1×10^4 to 1×10^5 volts/cm.

It was found that the lattice of silica gives in the d.e.f. Laue reflections which are more sharp and intense than when no electric field is applied. The corresponding microphotometric curves obtained for a plate 0.4 mm thick with a potential difference of 400 and 600 v are shown on Figs. 1 and 2. It can be seen from Fig. 1 (potential difference of 400 volts; Laue reflection corresponding to such a large value of φ that reflections from both surfaces can be discerned) that on applying a d.e.f. not only the intensity of Laue reflections is increased but also the ratio between the intensities reflected from both surfaces is slightly. changed. From the microphotometric curve *a* of the spot obtained without the action of the d.e.f. is to be seen that the rocking curve has two maxima of which the right one is higher than the left, as a result of the fact that at larger values of φ the rays reflected from the surface of the crystal opposite to the film have to pass a longer way through the crystal and thus are more absorbed than the rays which go directly through the crystal and are reflected from the face of the crystal turned toward the film. On the other hand

[4] Barrett, Phys. Rev. **38**, 832 (1931).
[5] Nishikawa, Sakisaka, Sumoto, Phys. Rev. **38**, 1078 (1931).
[6] Német, Helv. phys. Acta **8**, 97 (1935).
[7] Hengstenberg, Zeits. f. Physik **58**, 345 (1928).
[8] Bennett, Phys. Rev. **36**, 65 (1930).
[9] Dolejšek and Jahoda, Comptes rendus (in print).

(b) (a)

FIG. 1. Microphotometric curves of Laue reflection in silica plate 0.4 mm thick. (a) Without electric field; (b) under action of electric field, 400 volts.

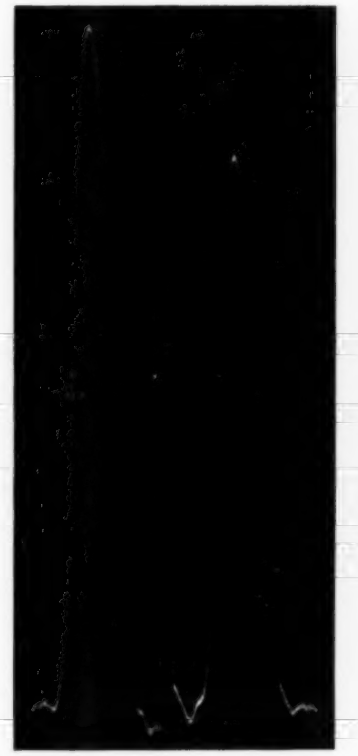

(b) (a)

FIG. 2. Microphotometric curves of Laue reflection in silica plate 0.4 mm thick. (a) Without electric field; (b) under action of electric field, 600 volts.

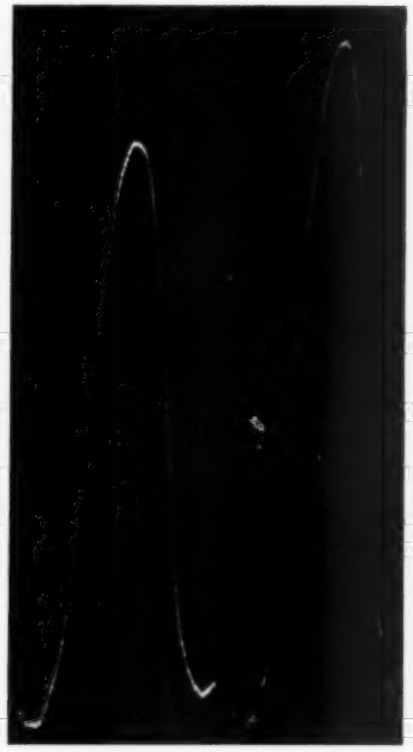

(a) (b)

FIG. 3. Microphotometric curves of Laue reflection in mica. (a) Without field; (b) under action of field.

the photometric curve of the same spot under the action of the d.e.f. *b* shows a total increase of the intensity and a change in the ratio between the intensities of both maxima. Under the electric field the left and right maxima of the spot are of equal height. Thus the left maximum corresponding to the reflection from the crystal surface connected with the positive pole of the electric source was slightly increased in relation to the maximum due to reflection from the crystal surface connected with the negative pole of the electric source. As mentioned above, the application of an alternating electric field to silica plates effects on the contrary an increase of the intensity mainly in the intermediate part of the Laue spot which lies between both maxima; i.e., an increase of the reflection power of the inner part of the crystal plate takes place.

Besides this we investigated the influence of etching on the sharpness and intensity of the Laue reflections. In agreement on the whole with Fox and Fraser we ascertained that after etching the crystal plate with 40 percent HF for 15–30 minutes neither the sharpness nor the intensity of Laue reflections is appreciably changed and that after more prolonged etching a sharpening and a simultaneous decrease of the intensity takes place. There is however no appreciable difference between the photograms obtained by means of a plate etched with 40 percent HF for long time as, e.g., for 3 or 20 hours.

(2) Mica

For the experiments analogous to those performed with silica, mica plates 0.07 mm thick were used. The potential difference varied within the limits of 400 to 1000 volts which correspond to an intensity of the electric field of 6×10^4 to 1.4×10^5 volts/cm. For mica similarly as for silica an increase of the intensity and sharpness of

the Laue spots under the action of a d.e.f. was observed as is evident from the microphotometric curve in Fig. 3 which shows the rocking curve of a Laue spot when tension is (b) or is not applied (a). In this case the microphotometric curve indicates (cf. silica) not only the increase of both maxima corresponding to the reflections from both surfaces of the plate but also the change of the ratio of both maximum intensities. The maximum due to the reflection from the crystal surface connected with the positive pole of the electric source is increased more than that due to reflection from the surface connected with the negative pole when the d.e.f. is applied.

We observed also for mica crystals an influence of the d.e.f. on the width of the central spot. Under the influence of a d.e.f. on mica crystals this spot diminished as can be seen from Fig. 4(a) and (b); however this diminution continued only to a certain potential difference applied. The magnitude of the diminution of the central spot was dependent on the direction of the rays in respect to the direction of the electric field. The central spot was appreciably narrowed when the rays entered the crystal through the coating connected to the negative pole and left it through the coating connected to the positive pole. However, if the crystal of mica used had been coated with metal a long time before the experiment, or if the electric field was applied to the crystal for a longer time, the difference between the central spot with and without the application of d.e.f. disapeared.[10]

(3) Gypsum

Phenomena analogous to those observed in mica were also found for gypsum but they were much less distinct and thus nothing definite can be said about them.

(4) The influence of aluminum coatings in general on all crystals

It was ascertained that the deposition of aluminum coatings on the surfaces of all three mentioned minerals, i.e., silica, mica, and gypsum effects an appreciable increase in the intensity of that part of the spots which corresponds to reflections from both surfaces of the crystal plates. Because the intensity of reflection increases from both crystal faces whereas the intensity of reflection from the inner layers of the crystal remains unchanged, the spots appear much more in contrast than in the case when the

[10] In the case of silica the influence of the d.e.f. on the narrowing of the central spot could not be studied. We worked with silica earlier than with mica, and arranged our experiments in such a manner that the rays entered the crystal through the metal coating connected with the positive pole of the source. With this arrangement the influence of the d.e.f. on the central spot is insignificant as we proved later in the case of mica. When later with opposite connections and with mica, a marked narrowing of the central spot as a result of the application of a d.e.f. was observed, we could not undertake analogous experiments with silica since all coatings were already aged and other silica plates were not available.

(a) (b)

FIG. 4. Laue pattern for mica. (a) Without field; (b) under action of field.

Al coating is washed off. From the microphotometric curves of the Laue spot corresponding to the mica plate coated and uncoated with aluminum in Fig. 5(a) and (b), respectively, it can be seen that both maxima of blackening corresponding to the reflections from both surfaces of the crystal plate are increased when the coated plate is used (Fig. 5a), and further that the ratio of these maxima has been quite changed by coating the plate. At the same time it was determined that coating mica with Al has the effect of widening the central spot (the respective photograms are not reproduced here since they are similar to those in Fig. 4).

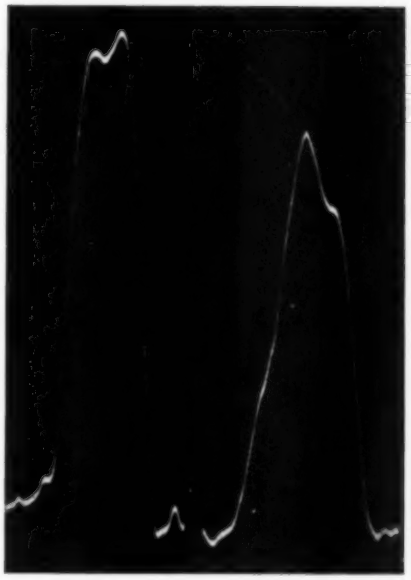

(a) (b)

FIG. 5. Microphotometric curves of Laue spot from mica. (a) Coated with aluminum; (b) uncoated.

DISCUSSION OF THE RESULTS

In order to explain our findings occurring when a d.e.f. is applied to certain crystals it is necessary to presuppose that under the influence of a d.e.f.:

(1) A perfection of the lattice, in the inner part of the crystal takes place,[11]

(2) That on the crystal-aluminum interface the positive and negative ions of the crystal penetrate into both Al coatings connected with the negative and positive poles of the electric source, respectively,

(3) That the metallic ions of Al penetrate into the crystal from the coating connected with the positive pole of the electric source.

The perfection of the crystal lattice caused by the influence of a d.e.f. explains the observed sharpening of Laue spots and the narrowing of the central spot. In order to confirm that the central spot under the action of the d.e.f. is really affected by the perfection of the crystal lattice and not by some specific properties of the Al coatings, we used thin leaves of aluminum pressed to both surfaces of the crystal plate in place of these coatings. Also in this case when the d.e.f. was applied, the central spot became narrower. This can serve as a proof that the narrowing of the central spot in a d.e.f. is caused by a perfection of the lattice itself and not by the nature of the coatings themselves.

The observed increase of the intensity of Laue reflections from both crystal faces under the influence of an electric field can be explained by the penetration of positive and negative ions from the crystal lattice into both aluminum coatings. When a d.e.f. is applied, negative ions from the crystal lattice on the aluminum-crystal border are shifted towards the Al coatings connected with the positive pole and the positive ions towards the coatings connected with the negative pole of the electric source; thus at both faces of the crystal plate a layer of a very imperfect lattice is formed.

As long as the intensity of the applied d.e.f. does not exceed a certain value, the ions remain shifted from their normal positions while the d.e.f. is acting and when the d.e.f. is removed they go back to their original positions. This formation of layers with disturbed lattices when a

[11] Such an arrangement of the "lattice" of fluids in a d.e.f. was observed by R. L. McFarlan (Phys. Rev. **35**, 1469–75 (1930)) and F. C. Todd (Phys. Rev. **44**, 787–793 (1933)) who found an increase in the intensity of the main maximum for nitrobenzene under the influence of a d.e.f. This effect is explained as caused by the more regular arrangement of the molecules. Német, reference 6, however, did observe by means of the Bragg method a decrease of the intensity of the reflection lines when a d.e.f. was applied to the crystal of Rochelle salt. He explains this fact by a disarrangement of the lattice. But it has to be taken into account that his observations (made by the Bragg method) concern only the surface of the crystal where the regularity of the lattice and the equilibrium of the lattice forces are mostly disturbed. Thus under the influence of the d.e.f. changes of a very different nature from those in the inner part of the crystal with which we are dealing can occur. Besides this, in the case of ice, he used an artificial reflecting surface.

d.e.f. is applied explains the increase in the intensity of Laue reflections from both surfaces as it was observed.

The formation of layers with imperfect crystal lattice should oppose to a certain degree the narrowing of the central spot provoked by the total perfection of the crystal lattice. According to the experiments the narrowing of the spot provoked under the influence of the d.e.f. by the perfection of the inner crystal lattice prevails, however, over the broadening of the spot caused by the penetration of ions into the thin surface layers.

Finally the third assumption, i.e., the penetration of positive metallic Al ions from the coating connected with the positive pole of the electric source into the crystal lattice explains the increase of the intensity of Laue reflections from the crystal face connected with the positive pole, and the dependence of the narrowing of the central spot on the direction of the incident x-rays in respect to the orientation of the electric field. This is due to the circumstance that under the influence of the d.e.f. the shift of the positive Al ions from the coating connected with the positive pole towards the crystal lattice forms on the respective Al crystal border a layer with greatly disturbed lattice. As a result of this, at the Al crystal border close to the positively charged coating there will be a thicker layer with a disturbed lattice than on the face connected with the negative pole, where on the contrary the disturbance of the lattice is produced only by the penetration of positive ions from the crystal into the Al coating, since the Al ions from the coating cannot penetrate into the crystal. Therefore it is to be expected that those parts of the Laue spots which correspond to the reflections from the crystal face connected with the positive pole should be more intense than those which correspond to the reflections from the face connected with the negative pole. This was observed.

By means of the penetration of metallic Al ions into the crystal lattice the dependence of the narrowing of the central spot on the direction of incident rays with respect to the orientation of the d.e.f. can be also explained. If the rays enter the crystal through the coating connected with the negative pole then the rays reflected from the strongly disturbed part of the lattice ($\Delta\varphi'$) situated on the opposite face of the crystal are practically inefficacious as to the back reflection. Thus the narrowing of the central spot under the influence of the d.e.f. which was distinctly determined for mica, is much more pronounced than in the case where the rays enter the crystal through the coating connected with the positive pole, in which case on the contrary more rays reflected from the strongly disturbed part of the lattice contribute to the back reflection, so that the influence of the perfection of the lattice is to a great extent counteracted. This confirms our experimental results.

If, however, the intensity of the d.e.f. applied exceeds a certain value or if it is applied long enough, the ions leave their normal positions permanently and the difference between photograms taken with or without the application of the d.e.f. disappears, as was observed. The same result is obtained if the coatings on the crystal are sufficiently aged. In such cases atoms of aluminum penetrate permanently into the crystal lattice by their own diffusion.

Finally the observed increase of the intensity of Laue reflections and the broadening of the central spot for crystals coated with aluminum in respect to those with the aluminum coating washed off, can be explained in the following way: atoms of aluminum deposited from aluminum vapors in high vacuum on both surfaces of the crystal plate arrange themselves in sufficiently thin layers according to the lattice of the crystal. In this way, on both surfaces of the crystal whose lattices already are almost ideally imperfect—as is known—thin layers of aluminum are formed whose lattices are still more imperfect and which therefore show on a Lauegram very intense reflections and a widening of the central spot.

In conclusion the authors wish to express their indebtedness to Professor V. Dolejšek, Director of the Institute of Spectroscopy of Charles University for valuable suggestions and criticisms of this work.

A Note on the Nature of the Primary Cosmic Radiation

THOMAS H. JOHNSON
Bartol Research Foundation of the Franklin Institute, Swarthmore, Pennsylvania
(Received July 22, 1938)

THE existence of an east-west asymmetry in the cosmic radiation showing that almost all of the field-sensitive part of the intensity in the lower half of the atmosphere is produced by positive primaries,[1] raises some interesting points regarding the possible nature of the primary radiation. Swann[2] has pointed out what enormous potential differences would exist between relatively close points in interstellar space if any appreciable fraction of the radiation were unneutralized in the statistical sense. These potentials go up as the square of the distance and the calculation shows that if all of the primary rays are positive, potential differences between points at a distance of one light year would amount to as much as 7×10^{18} volts. It appears essential, therefore, that any theory must provide for a statistically neutral primary radiation. In a theory of the origin of auroral particles from the sun, Gunn[3] has presented a rather special mechanism by means of which a beam of charged particles could keep itself neutralized by drawing out charges of the opposite sign from the surrounding ionized atmosphere. It is unnecessary to consider the details of the process to the extent of Gunn's postulates, but merely assume that some means exists within the atmosphere of a star or nebulum by means of which charges of either sign acquire an energy E of the order of cosmic-ray energies. After the emission has been going on for some time the source becomes charged with the opposite sign to a potential V determined by the condition that the initial particles when slowed down by loss of energy eV shall have the *same velocity* at infinity as the particles of opposite sign after the latter have acquired an equal energy eV. This is the necessary and sufficient condition for an equilibrium in which there is no space charge at infinity and a steady potential on the star.

Since the energies of positives and negatives whose velocities are equal are in proportion to their respective rest masses, a beam of heavy positives, such as protons, neutralized by negative electrons would constitute an apparently positive radiation at the earth's surface where the lower energy negatives are excluded by the magnetic field. It is not necessary to make any special assumption as to the sign of the charge which receives the original impulse for on this view the positive character of the radiation is a consequence only of the fact that more mass is associated with positive charge.

Whereas this interpretation of the primary radiation satisfies the asymmetry requirement and avoids the objectionable interstellar space charge, it does not account for the variation of the intensity with depth in the first layers of the atmosphere, for this is in agreement, as the balloon flights of Bowen, Millikan and Neher[4] have shown, with the quantum theoretical multiplication and absorption of a primary electron component of the energies dictated by the observed latitude effect. Ruling out the fantastic possibility of a positive electron radiation neutralized by a still lighter, and as yet undiscovered, negative particle, and accepting the premise that the first part of the ionization depth curve demands a primary electron component, the situation can be reconciled only by assuming the existence of two components of the primary radiation, the one consisting of positive and negative electrons in equal numbers and with similar distributions of energy, and the other composed of heavy positives, let us say protons, neutralized by negative electrons. Although the requirements would also be satisfied if the latter component contained positive barytrons (heavy electrons) neutralized by negative electrons, this

[1] The most recent estimates of the composition of the primary radiation based upon the asymmetry and the latitude effect leave but a small margin for negatives and the most probable result is that all of the field-sensitive intensity at sea level is due to positives. Defining $\beta\equiv(j^+-j^-)/(j^++j^-)$, from the latitude effect we find $\beta=1.16\pm0.50$ and from the north-south asymmetry $\beta=0.8\pm0.30$. For first estimates see T. H. Johnson, Phys. Rev. **45**, 569 (1934); **48**, 287 (1935); Terr. Mag. **43**, 1 (1938).

[2] W. F. G. Swann, Phys. Rev. **44**, 124 (1933).

[3] R. Gunn, Terr. Mag. **38**, 247 (1933).

[4] I. S. Bowen, R. A. Millikan, and H. V. Neher, Phys. Rev. **53**, 855 (1938).

hypothesis is not required since the barytrons in the atmosphere are already recognized as secondaries, and it does not seem likely that conditions exist in the universe where such a radiation could find its origin. In either case the east-west asymmetry must arise from a heavy positive primary radiation.

It is well known that studies of the absorption of cosmic rays near sea level have led to the identification of two types of secondaries, the hard component consisting of barytrons, and the soft component of positrons, negatrons and photons in equilibrium with one another. Our primary electron component has been invoked to give legitimate parentage to the soft component; it remains to establish the identity of the heavy positive primaries as the progenitors of the hard component secondaries. The fact that the asymmetry occurs at sea level demonstrates that the lowest energies of the heavy primaries contribute appreciably to the intensity in the lower half of the atmosphere. Indeed the asymmetry persists to a depth of at least two atmospheres, as is known from sea level measurements at zenith angles of 60°. While this is cogent evidence that the asymmetrical radiation comes down from the top of the atmosphere in the form of barytrons perhaps the strongest argument to this effect is found in the experiments[5] which showed that lead absorbing screens up to 30 cm thick placed between the coincidence counters reduced the relative east-west difference by only a few percent and the first layers of the lead actually increased the asymmetry. Thus it was shown that the asymmetrical rays in spite of having been produced by primaries of the lowest energies actually belong to the more penetrating part of the radiation at sea level. Other experiments[6] made at a depth of six meters have shown that the soft component, which at that depth produces the major part of the showers, is almost completely symmetric, and while this does not necessarily point to an equality in the numbers of positives and negatives in the primary electron component, it does place the burden of the geomagnetic effects in the lower part of the atmosphere entirely upon the penetrating rays.

As for the showers at sea level it is reasonable to suppose that many are produced by progeny of the penetrating rays, and it is not difficult to explain an asymmetry of the same order as that of the total radiation, such as was found[7] in shower experiments at the equator.

This identification of the asymmetry with the penetrating rays allows us to explain the fact that practically all of the sea level field-sensitive intensity in the lower part of the atmosphere is produced by primary positives by invoking the well-recognized fact that most of the intensity there is produced by the penetrating component, and it leaves the way clear for the soft component primaries to be made up of equal numbers of positrons and negatrons. Even though some small fraction of the intensity below six meters is produced by soft primaries, their energies required to reach to that depth would place them above the field-sensitive range.

Thus far our picture of the primary radiation has been built around the asymmetry, the transition effect at the top of the atmosphere and the demands for neutral interstellar space. If we now consider the fact brought out by Bowen, Millikan and Neher's balloon flights that by far the greater part of the primary radiation is electrically charged, the absence of an equilibrium intensity of photons seems to contradict the stellar origin introduced to provide a source of neutralizing particles, for but a few water-equivalent centimeters of absorbing matter would be required in the outer atmosphere of the star to give rise to as many photons as there are electrons. Their results have led the above authors to conclude that the rays are generated in vacuous interstellar space and that they have never passed through as much as a few centimeters of water equivalent matter before their arrival at the top of our atmosphere. Another alternative to this conclusion has been proposed by Alvén[8] and it is more in harmony with the view developed here. He postulates a source of cosmic rays within our galaxy in which an equilibrium intensity of all types of radiation is generated. The photons, however, pass freely away from the galaxy and are lost in intergalactic space while

[5] Experiments by S. A. Korff, B. Rossi and the writer have been summarized by the writer; see Phys. Rev. **48**, 287 (1935).

[6] T. H. Johnson, Phys. Rev. **47**, 318 (1935).

[7] T. H. Johnson, Phys. Rev. **45**, 569 (1934).

[8] H. Alfvén, Zeits. f. Physik **107**, 579 (1937); Phys. Rev. **54**, 97 (1938).

the charged rays are retained and their intensity allowed to grow through the action of a galactic magnetic field. This view, although having to postulate a magnetic field, has the advantage that no unusual process need be envisaged for the generation of the energy of the cosmic radiation, since this would be quite small, nor for realizing the actual composition of the radiation. Thus the positron-negatron component would most naturally be regarded as a secondary product of the electrons or protons, whichever received the original impulse, having been generated as the latter were passing out through the atmosphere of the stellar source.

Summarizing, we suppose the existence of some unspecified process within the atmospheres of stars in which either electrons or positive ions are given an original impulse. As these pass outwards through the stellar atmosphere secondary positron-negatron pairs and an equilibrium intensity of photons are generated. The charge of the primary particles, being of one sign, raises the potential of the star to the point where opposite charges are repelled and both types of particles move along with equal velocities, the heavier particles having most of the energy. The secondary photons pass out into intergalactic space and are lost while the charged particles are retained by a galactic magnetic field. When these encounter the earth's field the positrons and negatrons pass through in equal proportion and constitute the soft component primaries. Of the other rays, only the heavy positives have sufficient energy to reach the earth's surface. There they constitute the positive primary radiation whose penetrating secondaries produce most of the intensity at sea level and below and account for the east-west asymmetry.

LETTERS TO THE EDITOR

Prompt publication of brief reports of important discoveries in physics may be secured by addressing them to this department. Closing dates for this department are, for the first issue of the month, the eighteenth of the preceding month, for the second issue, the third of the month. Because of the late closing dates for the section no proof can be shown to authors. The Board of Editors does not hold itself responsible for the opinions expressed by the correspondents.

Communications should not in general exceed 600 words in length.

On the Existence of H^3

Several attempts have been made in the last few years to find a stable isotope of hydrogen of mass three in the natural state. The only experiments[1, 2, 3] which gave some positive evidence for H^3 were not very conclusive. The work of Smith[4] showed that a primary ion made up of three hydrogen atoms may be produced in hydrocarbons by single electron impact. This discovery offers a possible, though somewhat improbable, interpretation of the results[1] of the mass spectrograph.

Some months ago the problem was reexamined. The purest heavy water available[5] was decomposed on hot tungsten filaments in an evacuated system consisting of twenty-nine glass diffusion pumps[5] of the Hertz type. Samples were taken of the gas before the pumps were operated and also samples were withdrawn from the light and heavy ends after equilibrium had been established. Analyses, made with the same instrument and by the same method previously used,[1] of the untreated gas confirmed in general the earlier results, namely the production of a primary ion of mass 5. Gas extracted from the light reservoir contained about ten percent protium and ninety percent deuterium but other impurities were extremely minute. This pure sample gave a peak at mass 5 whose relative size vanished when extrapolated to zero pressure. This result, we believe, shows that the mass spectrograph was working properly. The gas from the heavy end contained many impurities and gave a much larger peak at mass 5 although light hydrogen molecules were presumably eliminated.

Another sample was collected at the heavy reservoir after some of the heavy gas had been discarded. Since the pumps separate other gases from hydrogen very efficiently this procedure practically eliminated all heavier compounds. Calculations supported by measurements on various hydrogen gases convinced us that if mass 5 molecules were present at all there would still be a considerable enrichment in this sample over the untreated gas. The analysis showed this sample to be one of the purest of deuterium we have ever tested. The ratio of mass 5 to mass 4 was 3×10^{-7}, too small to make the regular pressure run. From this result we conclude that we have no evidence for H^3 and that the former interpretation of similar data was in error. The occurrence of the primary mass 5 ion in unpurified samples is not understood at present.

Estimating the total enrichment to be expected both from electrolysis and diffusion our results indicate that the abundance of H^3 in ordinary hydrogen is less than 1 in 10^{12}. We believe this test is a more drastic one than that reported by Rutherford[6] and it is in line with the suggestion of Bonner[7] that H^3 may be unstable. In the light of these results it may be of interest to repeat the experiment of Tuve, Hafstad and Dahl.[2]

RUBBY SHERR
LINCOLN G. SMITH
WALKER BLEAKNEY

Palmer Physical Laboratory,
Princeton University,
Princeton, New Jersey,
August 12, 1938.

[1] Lozier, Smith and Bleakney, Phys. Rev. **45**, 655 (1934).
[2] Tuve, Hafstad and Dahl, Phys. Rev. **45**, 840 (1934).
[3] Selwood, Taylor, Lozier and Bleakney, J. Am. Chem. Soc. **57**, 780 (1935).
[4] L. G. Smith, Phys. Rev. **51**, 263 (1937).
[5] Sherr, J. Chem. Phys. **6**, 251 (1938).
[6] Rutherford, Nature **140**, 303 (1937).
[7] Bonner, Phys. Rev. **53**, 711 (1938).

The Atomic Vibrations of a Zinc-Copper Alloy

A paper of the above title by Robert A. Howard[1] has led to the preparation of this note. Howard has proposed and experimentally verified the idea that in hexagonal close-packed crystals the atomic vibrations are greatest along the C axis of the crystal in case the axial ratio is greater than 1.633 and least when the axial ratio is less than 1.633. The axial ratio 1.633 is the ratio which would obtain in the hexagonal close-packing of spheres. The literature is cited for the cases of zinc and cadmium with axial ratios greater than 1.633 and the epsilon phase of the copper-zinc alloy system is the experimental basis for the case of an axial ratio less than 1.633.

It has occurred to the writer that the change in crystal lattice dimensions accompanying the variation of the composition of the eta and epsilon copper-zinc phases is in experimental support, or at least, experimental analogy to the work of Howard. The eta phase is the solid solution of copper in zinc, having at all compositions axial ratios greater than 1.633. The epsilon phase is an intermediate phase, also hexagonal close-packed, but with axial ratios less than 1.633. Fig. 1 portrays the rate of change of atomic spacings with change of composition for these two phases.

An increase in copper content of eta causes an increase in atomic spacing in a direction perpendicular to the C axis and a very large decrease parallel thereto; whereas in epsilon, the spacing perpendicular to the C axis undergoes a decrease while the direction parallel to the C axis changes very little. The increase in copper content (or the decrease

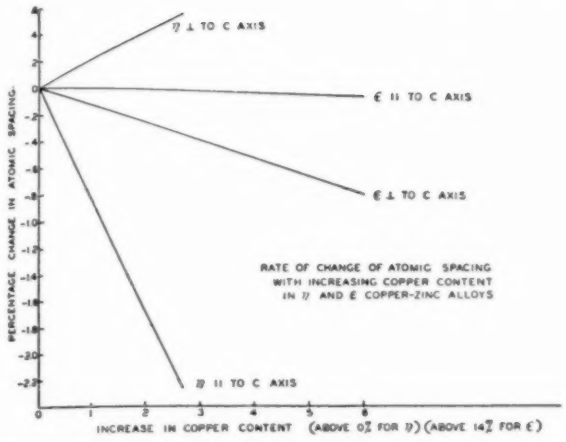
η ⊥ TO C AXIS
ε ∥ TO C AXIS
ε ⊥ TO C AXIS
RATE OF CHANGE OF ATOMIC SPACING WITH INCREASING COPPER CONTENT IN η AND ε COPPER-ZINC ALLOYS
η ∥ TO C AXIS
PERCENTAGE CHANGE IN ATOMIC SPACING
INCREASE IN COPPER CONTENT (ABOVE 0% FOR η) (ABOVE 14% FOR ε)

FIG. 1. Rate of change of atomic spacing with increasing copper content in eta and epsilon copper-zinc alloys.

in zinc content) causes a large decrease in atomic spacing in the directions of greatest atomic vibration in each of the two crystal lattices.

The pronounced anisotropy of zinc is demonstrated by these two alloy phases. Although both phases are hexagonal close-packed with the same coordination number, a complete series of solid solutions is not formed. There exists a gap in axial ratio and in composition between eta and epsilon within which no hexagonal close-packed copper-zinc phase exists. In eta the influence of the zinc atom is evidently in the shape of a prolate spheroid and in epsilon, in the shape of an oblate spheroid, without the intermediate spherical condition at axial ratio 1.633.

M. L. FULLER

The New Jersey Zinc Co.,
Research Division,
Palmerton, Pa.,
August 3, 1938.

[1] Robert A. Howard, Phys. Rev. **53**, 966 (1938).

The Internal Friction of Metallic Crystals

Several investigators have studied the internal friction of polycrystalline metals,[1] but as far as the writer is aware the only observations on single metal crystals are those of Zacharias on nickel,[2] and these deal entirely with the ferromagnetic contribution. Accordingly the following results, obtained in the course of a systematic investigation of internal friction in single and polycrystalline metals, seem worth reporting at this time. The experimental method is that devised by Cooke and Brown.[3]

Observations have been made on single crystals of copper, lead and tin. The vibration frequency is 38.9 kilocycles in each case, and the temperature is about 25°C. The observed longitudinal decrements of the crystals are 3.6×10^{-5}, 2.8×10^{-4}, and 6.9×10^{-5}, respectively. These values may be compared with those of the corresponding polycrystalline substances obtained by Forster and Korster,[1] namely, 3.5×10^{-3}, 4.6×10^{-3}, and 5.4×10^{-3}. It thus appears that the internal friction of a single metal crystal is substantially less than that of the polycrystalline material. The decrement of crystalline quartz is 3×10^{-6}, and it is suggested that the decrement of a pure and strain free metal crystal might approach this value.

The effect of internal strain on the internal friction of crystalline copper is noteworthy. The decrement of a crystal, on removal from the furnace in which it is grown, is of the same order as that of the polycrystalline material. The low value here reported is obtained by annealing the crystal in a vacuum. Lead and tin crystals, on the other hand, remain unaffected by annealing.

The writer is indebted to Dr. Clarence Zener for helpful suggestions made during the course of the present work.

T. A. READ

Pupin Physics Laboratories,
Columbia University,
New York, N. Y.,
August 15, 1938.

[1] See for example, Wegel and Walther, Physics **6**, 141 (1935); Forster and Korster, Zeits. f. Metallkunde **29**, 116 (1937).
[2] Zacharias, Phys. Rev. **44**, 116 (1933).
[3] Cooke and Brown, Phys. Rev. **50**, 1158 (1936).

Ignition Potential in a Low Pressure Neon Tube

In an article by Lindenhovius[1] an expression is derived and experimentally verified for the relation between the voltage at which ignition of a low pressure irradiated neon glow occurs and the frequency of the applied sinusoidal voltage. The expression was based on the determination of the time constant of an assumed exponential current rise,[2] and this time constant was shown to depend upon the magnitude of the overvoltage applied to the discharge. The time required for ignition can be computed from the relation

$$\log\frac{i_1}{i_0}=a\int_{t_0}^{t_1}(v-V_0)dt, \qquad (1)$$

where v is the instantaneous electrode voltage, V_0 is the minimum ignition voltage, i_0 and t_0 are the current and time when $v=V_0$, i_1 is the current at time t_1 when ignition takes place and a is a constant depending upon the ionization coefficient, mobility of the ions, and number of electrons ejected from the cathode per ion pair formed. It is assumed that space charge does not distort the electric field.

If an exponentially increasing voltage, obtained from the plates of a condenser C charged through a resistance R by a battery V_m, is placed across the electrodes Eq. (1) may be conveniently tested. The term $[V_m(1-\epsilon^{t/RC})-V_0]$ may be substituted for $(v-V_0)$ in Eq. (1) and the solution of the resulting equation may be written

$$\log\frac{i_1}{i_0}=a\left[(V_m-V_0)(t_1-t_0)+RCV_m\left\{\exp\left(-\frac{t_1}{RC}\right)-\exp\left(-\frac{t_0}{RC}\right)\right\}\right]. \qquad (2)$$

A neon discharge tube with parallel-plane iron electrodes was used. The transient visualizer[3] was used to apply the exponential voltage to the electrodes at a very low frequency, and at the same time to sweep the beam of a

TABLE I. *Calculated and observed values of ignition voltage in a neon tube as a function of the time constant of an exponentially increasing voltage.*

RC (SEC.)	V_m (VOLTS)	V_{calc} (VOLTS)	V_{obs} (VOLTS)
2.37×10^{-2}	250	195	197
	295	204	205
	340	209	206
	385	222	219
	420	236	231
1.33×10^{-2}	250	209	202
	295	211	210
	340	213	212
	385	228	223
	420	245	250
0.59×10^{-2}	250	218	217
	295	219	218
	340	222	222
	385	232	231

cathode-ray oscillograph. The voltage across the discharge was measured by the oscillograph, the persistence of vision providing a means of determining the maximum tube voltage. The time for discharge was measured as a check on the voltage measurement. As a criterion for ignition, it was assumed that ignition occurred at the maximum discharge voltage and that immediately after ignition the voltage dropped. This assumption is reasonable from the appearance of oscillograms obtained by Reich and Depp.[4] The condenser discharge current was made large compared with the pre-ignition current of the discharge so that the latter current did not distort the applied voltage shape. The frequency of application of voltage was so low that de-ionization was judged to be complete. The condenser voltage was short-circuited after each discharge to hasten de-ionization.

Table I shows the experimentally determined ignition voltage compared with the value computed from Eq. (2). It is seen that the results are within the experimental error of about 2 percent. Divergences are expected at the higher values of V_m, since in arriving at Eq. (1) only the first term of a Taylor's expansion for a was used.

It is proposed to use the method described with that described by Reich and Depp,[4] with a modification to control time of de-ionization, to study the effect of the application of various voltage wave shapes on the ignition voltage, not only as a check on Eq. (1) for the initial breakdown, but also to determine the effects of change of de-ionizing time.

G. H. FETT

Department of Electrical Engineering,
University of Illinois,
Urbana, Illinois,
July 28, 1938.

[1] H. J. Lindenhovius, Physica **4**, 1212 (1937).
[2] M. Steenbeck, Veröff. a.d. Siemens-Konz. **9**, 83 (1930); A. V. Engel, and M. Steenbeck, *Elektrische Gasentladungen* (Julius Springer, 1934), Vol. II, p. 178.
[3] H. J. Reich, Rev. Sci. Inst. **2**, 164 and 234 (1931).
[4] H. J. Reich, and W. A. Depp, J. App. Phys. **9**, 421 (1938).